

CHAPTER 18

Deep Foundations

18.1 DIFFERENT TYPES OF DEEP FOUNDATIONS

Shallow foundations are typically less expensive than deep foundations. Therefore, it is economically prudent in most cases to start by investigating whether a shallow foundation can be used. Only if it is shown to be insufficient should the design proceed with deep foundations. It is nearly always possible to use a shallow foundation to carry a vertical load, but the area required may be excessive or unavailable. For example, a building with a column spacing equal to s has a limited amount of room between columns to place the footing. Typically, if the area B^2 required for the footing is more than one-half of the area available (s^2), then it is better to use a mat foundation or a deep foundation (Figure 18.1). In other words:

$$B \leq 0.707s \quad (18.1)$$

where B is the footing width and s is the column spacing.

A typical deep foundation consists of a cluster of piles installed down to a certain depth in order to transfer the load to a more competent bearing layer or to distribute the load over a larger depth. Piles come in many different shapes and are made of many different materials. The cross section can be circular and full, tubular, square, or hexagonal. The diameter varies from 0.15 m for micropiles to 3 m for some of the bored piles and offshore pipe piles. The length may be as short as a few meters (bored piles for a house foundation) to more than 100 m for offshore piles (pipe piles to anchor offshore platforms). The material may be steel for pipe piles and H piles, concrete for bored piles or driven concrete piles, wood for timber piles, or even plastic (more recent installations). These piles may be prefabricated in a factory or cast in place. The installation process may consist of driving the piles into the soil with either impact hammers or vibratory hammers (driven piles), or the installers may proceed drilling a hole in the ground, lowering a reinforcing cage, and filling the hole with concrete (*bored piles*, also known as *drilled shafts* or *drilled piers*). There are many variations of these two basic installation techniques, but driven piles and bored piles remain the two major installation categories. The names *end-bearing*

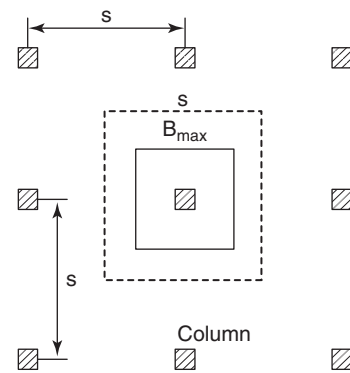


Figure 18.1 Maximum area for shallow foundation.

piles and *friction piles* are used to refer to the load distribution in the pile. End-bearing piles carry the load mostly at the pile point, whereas friction piles carry the load mostly in friction along the pile shaft. *Battered piles* are piles installed at an inclined angle in order to better resist horizontal loads.

18.2 DESIGN STRATEGY

The design of a deep foundation consists of selecting the type of piles and calculating the length, size, and number of piles necessary to carry the load safely and within a tolerable settlement. The design also includes the planning of the installation process. Much like in the case of shallow foundations, deep foundations are now designed on the basis of the LRFD approach (see section 17.4). Here again two limit states are considered: the ultimate or strength limit state and the service limit state (section 17.4). In the LRFD approach, the limit state is written as:

$$\sum_{i=1}^n \gamma_i L_i \leq \sum_{j=1}^m \varphi_j R_j \quad (18.2)$$

where γ_i is the load factors for the loads L_i , and φ_j is the resistance factors for the resistances R_j . The load factors γ

are the same for shallow and deep foundations (Chapter 17, Table 17.1), but the resistance factors ϕ are different, as they are tied to specific design methods for calculating the pile capacity. These resistance factors for the ultimate limit state vary between 0.2 and 0.5 (AASHTO 2010) and will be discussed in sections 18.5.1 and 18.6.4. The ultimate limit state or strength limit state might look like this:

$$\gamma_1 DL + \gamma_2 LL \leq \phi_1 R_{uf} + \phi_2 R_{up} \quad (18.3)$$

where DL is the dead load, LL is the live load, R_{uf} is the pile ultimate friction resistance, and R_{up} is the pile ultimate point resistance. The service limit state can be presented as:

$$\gamma_3 DL + \gamma_4 LL \leq \phi_3 R(s_{all}) \quad (18.4)$$

where s_{all} is the allowable settlement of the foundation, and $R(s_{all})$ is the pile load that generates the allowable settlement. For the service limit state, the load factors and the resistance factors are usually taken equal to 1. Furthermore, if the settlement will take place over a long period of time, the live load is not included in the settlement calculations except for the permanent live load.

Prior to the development of the load and resistance factor design approach (LRFD; also called limit state design or LSD), the working stress design (WSD; also called allowable stress design or ASD) approach was used. WSD consists of applying a global factor of safety against the ultimate bearing capacity of the soil in order to obtain the safe load. The equation is:

$$L < R_u/F \quad (18.5)$$

where L is the applied load to be safely carried, R_u is the ultimate resistance, and F is the global factor of safety. The factor of safety varied from 2.5 to 3 when R_u was based on calculations down to 2 when R_u was based on an appropriate number of load tests.

The type and size of piles selected for a project are often influenced by what is available locally; for example, in Hawaii steel pipe piles are rare, but concrete piles are common. Also, in given stratigraphies, some piles are easier to install than others; for example, in stiff clay with a water table at a large depth, bored piles drilled dry are very economical. In very soft soils, it is very difficult to drill and keep open a clean hole, so driven piles are preferred because they are easy to drive. Sometimes the size of the load to be carried dictates the pile type; for example, large, heavy loads can be carried more readily by a single large-diameter bored pile than by an equally large driven pile because it is easier to drill a large hole in the ground than to drive a large-diameter pile unless the soil is very soft.

The pile length can be determined by calculations. This is the case with offshore piles, where a required ultimate pile capacity is determined by using the load and resistance factors; then an ultimate pile capacity profile is generated as a

function of depth, and the pile length is chosen to correspond to the depth where that ultimate capacity is first reached. In many instances, however, the pile length is chosen by inspecting the stratigraphy of the site. If a hard layer exists at some reasonable depth below the ground surface, the piles will be founded in that bearing layer and the pile length is fixed. If the stratigraphy is uniform and does not have a strong layer, or if the strong layer is too thin to support the pile group, the pile length may be dictated by the maximum length that can be transported without special permits, or the maximum length available; for example, timber piles are typically no longer than 20 m. In onshore practice and for driven piles, the length of the pile is often dictated by the pile blow count that is written into the specifications: this is called driving to a blow count. In simple terms, onshore you drive until you reach a set blow count; offshore you drive until you reach a set penetration.

If the pile size, type, and length are determined, then the design consists of finding the number of piles required to carry the load safely and within a tolerable settlement. Note that this load may be a vertical load, a horizontal load with or without overturning moment, or a combination of all of these. Combination loading is handled by considering the two load types separately and ignoring the interaction effect. The reason for this choice is that the resistance to vertical load tends to be mobilized at depth, whereas the resistance to horizontal loads tends to be mobilized close to the ground surface. The design strategy for either load case proceeds according to the following steps:

1. Choose the pile size, type, and length.
2. Calculate the ultimate bearing capacity of one pile (and maximum bending moment for horizontal loads).
3. Calculate the number of piles required to satisfy the ultimate limit state criterion under the given load.
4. Check the group effect.
5. Reiterate steps 1 through 4 until the ultimate limit state criterion is satisfied.
6. Under the foundation load, calculate the movement of the pile group and check that the service limit state is satisfied.
7. If the calculated movement is larger than the acceptable movement, the foundation must be modified (increase pile depth, pile size, use different pile type) and step 6 repeated.
8. If the movement is acceptable, the design is complete, as the ultimate limit state and the service limit state will have been satisfied.

Design methods for deep foundations can be classified into three categories: design by theory, design by empiricism, and design by analogy. Design methods by theory rely on theoretical derivations for recommending the design equations. Design methods by empiricism rely on experimental data and correlations for recommending the design equations. Design methods by analogy rely on the close analogy between the

mode of deformation in the soil test and in the foundation case. Generally speaking, the best methods are those that combine the advantages of all three methods by including a close analogy, experimental data, and appropriate theoretical background.

18.3 PILE INSTALLATION

18.3.1 Installation of Bored Piles

Bored piles are also known as drilled shafts or drilled piers. Bored piles are installed by drilling a hole in the ground, removing the drilling tool, inserting the reinforcement cage, and filling the hole with concrete. In more detail, the sequence is as follows: First the hole is drilled with a drill rig. The diameter of the hole varies from 0.3 m all the way to 3 m. If the soil is free standing over the depth drilled, the hole is drilled dry. If not, slurry is placed into the hole to help prevent caving of the hole. The level of the slurry in the drilling hole must always be higher than the groundwater level, to ensure a positive flow from the drill hole to the soil through the borehole wall. Slurries can be mineral slurries or polymers. The most common type of mineral slurry is bentonite slurry, prepared by mixing bentonite particles with water. The consistency of this slurry is very liquid. When the slurry stands in the open hole, the slurry starts flowing horizontally into the soil; during this process, the bentonite particles accumulate on the wall and form a thin cake that seals the hole from incoming or outgoing water. This minimizes the sloughing of the soil into the hole that is often caused by entrainment of the incoming flow of water. Polymer slurries are viscous, but they do not form cakes on the wall; rather, they simply continue to flow into the soil, so new slurry must be added continuously. The unit weight of a bentonite slurry is between 3 and 10% higher than the unit weight of water, whereas the unit weight of a polymer slurry is less than 3% higher than that of water. The chemical composition of slurries should be checked before use (Brown et al. 2010).

If slurry is insufficient to keep the hole open, a steel casing can be lowered in the open hole and advanced as drilling progresses, to prevent collapse. After the hole is drilled, the casing may be left in place permanently or retrieved. Once the hole is opened, a steel reinforcement cage is lowered in the center of the hole. Then a tremie pipe is lowered to the bottom of the hole and concrete is poured into the hole from the bottom up. Because concrete is heavier than bentonite slurry, the concrete displaces the slurry upward, to overflow in a desanding pit, for example. It is very important to keep the bottom of the tremie pipe below the concrete level to prevent contamination of the concrete by the slurry. If the bottom of the tremie pipe is raised above the concrete-mud interface (called burping the tremie) during concreting, there is a possibility that some slurry or soil may become trapped in the concrete. This would create a weak inclusion or defect in the bored pile. Onshore, the slurry is recirculated, but for offshore drilled and grouted piles, the slurry is wasted on the

ocean floor. Once the hole is full of concrete, it is allowed to cure; thereafter, the bored pile is complete.

In summary, there are three main procedures for placing a bored pile (Brown et al. 2010):

1. Dry method (Figure 18.2)
2. Casing method (Figure 18.3)
3. Wet method (Figure 18.4)

Note that often a bored pile is constructed by using a combination of two or three of the methods listed here. In addition to those methods, two other techniques are sometime used for bored piles: base grouting and underreams (also called bells). *Base grouting* consists of injecting grout under pressure at the base of the bored pile after the concrete is sufficiently hard (Figure 18.5). This increases the pressure at the base by reaction against the side friction of the bored pile. This increase in pressure stiffens and strengthens the soil under the pile point and actually prestresses the pile against the soil. This technique aims at decreasing the settlement and increasing the capacity of the pile under load. *Underreams* or *bells* are created by lowering a special drilling tool to

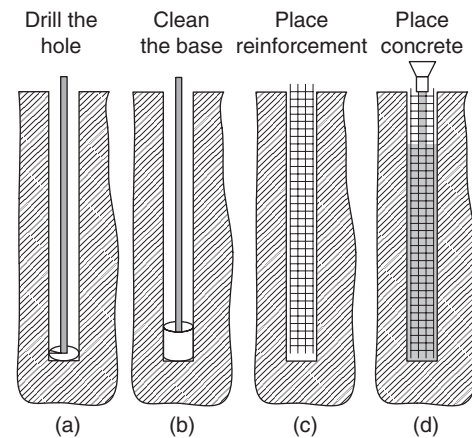


Figure 18.2 Installation of bored piles: Dry method (After Brown et al. 2010).

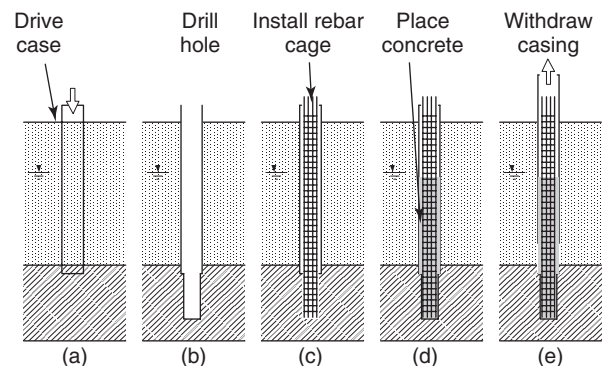


Figure 18.3 Installation of bored piles: Casing method (After Brown et al. 2010).

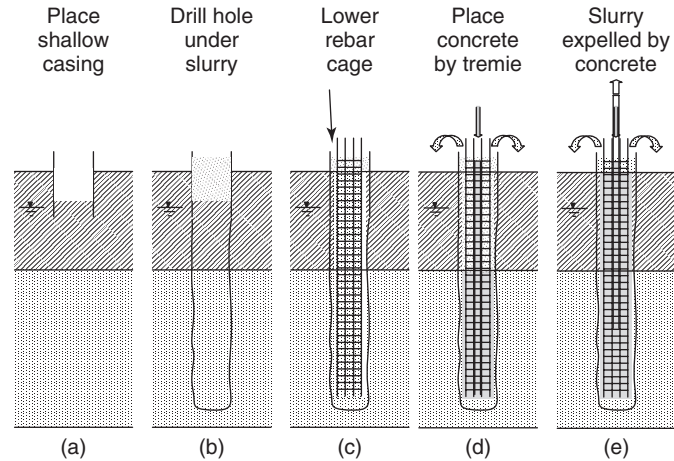


Figure 18.4 Installation of bored piles: Wet method (After Brown et al. 2010).

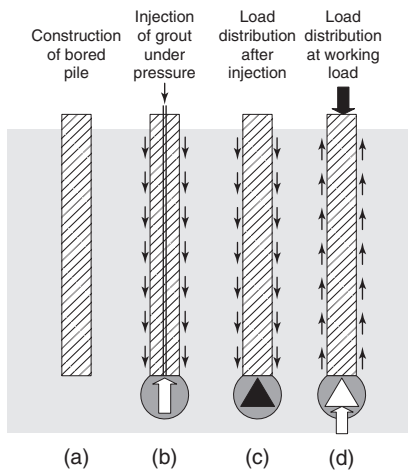


Figure 18.5 Installation of bored piles: Base grouting (After Brown et al. 2010).

the bottom of the hole before concreting takes place. This tool expands sideways and creates a cone-shaped opening by rotation (Figure 18.6). The angle of the cone with the horizontal is commonly in the range of 45 to 60 degrees. The purpose of an underream or bell is to increase the point resistance of a bored pile or the uplift capacity without having to increase the diameter over the entire length of the pile.

Some of the important issues in bored piles installation are as follows (ADSC-DFI 2004):

1. For bored piles drilled dry, one must ensure that the concrete that falls in the hole is not segregated by hitting against the reinforcing bars.
2. One must also ensure that there is enough room between the outside rebar and the soil for the concrete aggregates to fit properly.
3. For bored piles constructed under slurry and in sand, it is important to de-sand the slurry as drilling progresses (settling pond). If not, sand will settle at the bottom of

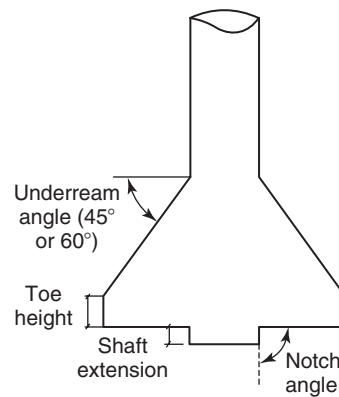


Figure 18.6 Installation of bored piles: Underream or bell (After Brown et al. 2010).

the hole and form a soft, compressible cushion that will hinder the settlement performance of the pile.

4. For bored piles constructed under slurry, it is also important not to keep the slurry in the hole too long. If it stays in the hole too long, the slick bentonite cake that forms on the wall of the hole will become very thick and will significantly decrease the friction capacity of the shaft.
5. In all cases, it is important to clean any loose soil from the bottom of the shafts just before concreting, to minimize settlement due to recompression of the excavated soil.

An experiment was conducted for two bored piles 1 m in diameter and 10 m long in sand (Briaud et al. 2000). In the first case, the contractor was asked to do the worst job possible (Pile 1) and in the second case the contractor was asked to do the best job possible (Pile 2). For Pile 1, the contractor did not de-sand the slurry, left the slurry in place in the finished hole for 72 hours, and did not clean the bottom of the pile. A 0.3 m thick cushion of soft sand was observed at the bottom of the pile and a 10 mm thick layer of bentonite

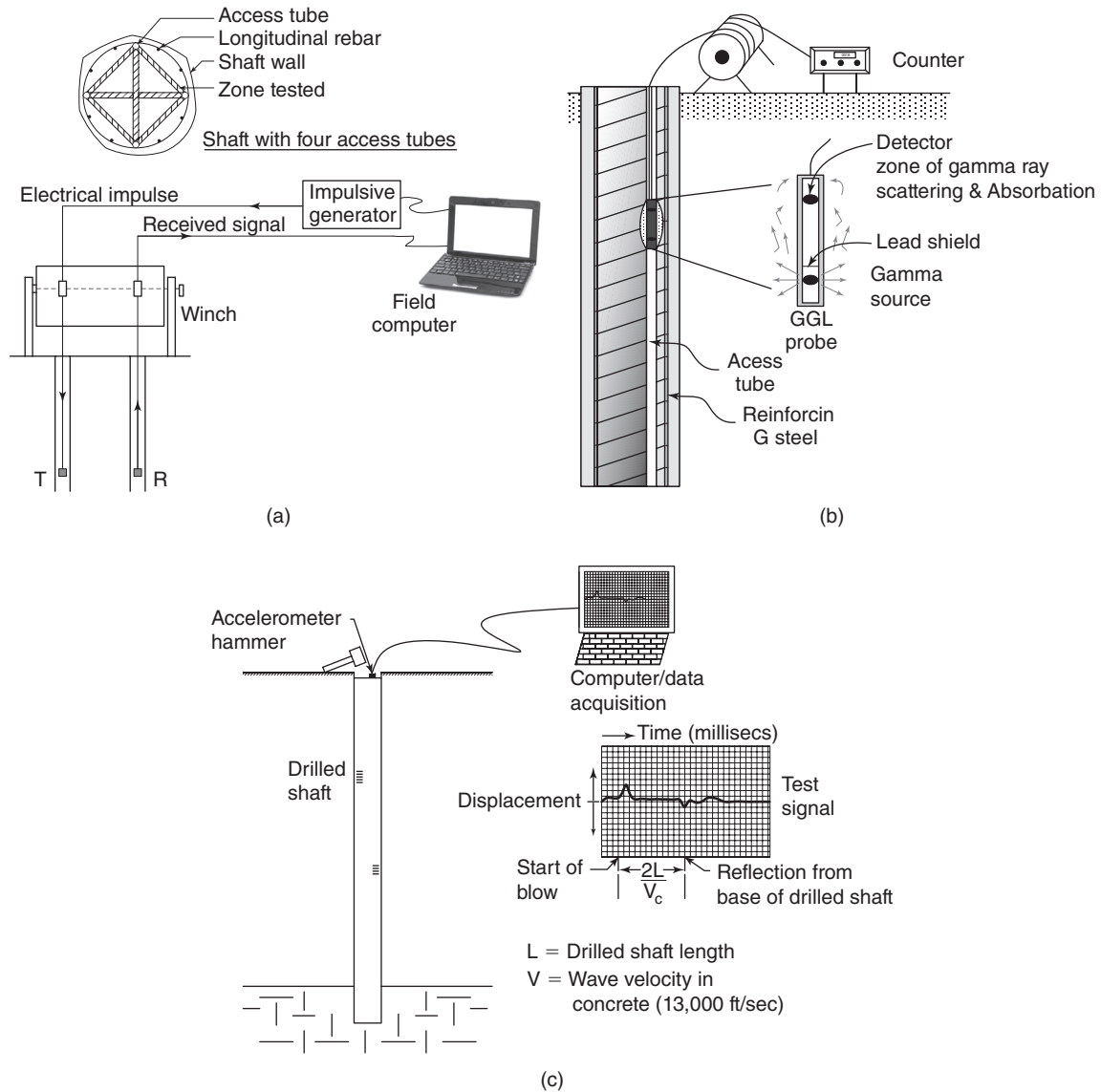


Figure 18.7 NDT techniques for bored piles: (a) Cross hole logging. (b) Gamma-gamma logging. (c) Sonic echo and impulse response (After Brown et al. 2010).

mud was measured on the walls of the bored pile hole by horizontal sampling. For Pile 2, the contractor was careful not to make any of those errors. Both piles were concreted, cured, and load tested to 150 mm of penetration. At 150 mm of penetration, Pile 1 carried only 1500 kN, whereas Pile 2 carried 4500 kN. The load distribution in the pile was measured with extensometers. Most of the difference in load came from the friction, which was reduced by a factor of 10; the point resistance was the same in both cases. This shows how important it is always to control the quality of foundation construction.

Drilled and grouted piles are also bored piles. These piles are installed by drilling a hole dry or under slurry; lowering a steel element such as an H beam, a steel pipe, or a rebar in the center; and filling the annulus between the reinforcement

and the soil with grout. Offshore casings for oil wells are placed that way. *Micropiles* are small-diameter versions of bored piles or drilled and grouted piles. *Augercast piles* were initially installed in such a way that the drilling, lowering of the reinforcement, and grouting were done in a single down-and-up process. This was very efficient, but was limited to smaller diameters, and the reinforcement was also limited to a centralized bar or small casing placed through the center of the hollow stem auger used to drill the hole. Now augercast piles are drilled with larger diameter augers, the auger is retrieved, and a reinforcement cage with centralizers is lowered in the hole full of cement paste before the cement sets.

Deep soil mixing is yet another process leading to stronger elements placed in the ground to carry the load from a structure. This process consists of drilling the soil with a cement

slurry and mixing the soil and cement in place while drilling. The cement and the soil harden into a soil-cement column made of a material with a strength intermediate between soil and concrete. The cement volume is around 20% of the soil volume and typical column diameters are around 1 m. The strength of this material varies significantly, but an unconfined compression strength equal to 2 MPa is not uncommon.

18.3.2 Nondestructive Testing of Bored Piles

Nondestructive testing (NDT) can be used on any deep foundation member. However, it is most often used in conjunction with the evaluation of onshore bored pile foundations. Several methods can be used (Figure 18.7):

1. Cross hole sonic logging
2. Gamma-gamma logging
3. Sonic echo
4. Impulse response

Cross Hole Sonic Logging

The cross hole sonic logging technique requires that at least two access holes and casings be left in the bored pile during construction. This is achieved by attaching the casings to the reinforcing cage. The casings are typically around 50 to 57 mm in diameter and should be very well connected to the bored pile to avoid loss of signal across the interface. A source transmitter is lowered in one of the access casings while a receiver is lowered to the same depth in another casing. The source emits a compression wave signal and the time t needed to receive the signal across the bored pile at the receiver is monitored. The compression wave speed is calculated as:

$$v = \frac{d}{t} \quad (18.6)$$

where v is the wave speed, d is the distance from the source to the receiver, and t is the travel time. The compression wave speed v in sound concrete is about 4000 m/s, in water is 1500 m/s, in air is 300 m/s, and in soils is anywhere from 400 to 2000 m/s. Therefore, any values much lower than 4000 m/s will be an indication of a problem with the bored pile. Table 18.1 gives an indication of how to rate concrete for various velocity readings. It is also possible to place the source and the receiver at different depths in the bored pile and

Table 18.1 Concrete Rating from Wave Speed

| Compression Wave Speed | Concrete Quality |
|------------------------|------------------|
| 3600 to 4000 m/s | Good |
| 3200 to 3600 m/s | Questionable |
| < 3200 m/s | Poor/defective |

(After Brown et al. 2010.)

across different horizontal paths. The data are then inverted to get a three-dimensional rendition of the bored pile. This is called cross hole tomography (Hollema and Olson 2002).

Gamma-Gamma Logging

The gamma-gamma logging technique requires that an access tube be left in the bored pile during construction. A gamma ray source and a gamma ray detector are placed in the same cylindrical probe and lowered in the access tube. Gamma rays are beams of photons; some of the photons bounce back to the detector and are counted upon arrival. The gamma ray arrivals are recorded in counts per second (cps). There is a reasonably linear correlation between the concrete density and the log base 10 of the cps:

$$\gamma_{conc} = a \log(cps) + b \quad (18.7)$$

where γ_{conc} is the unit weight of concrete, cps is the gamma ray count recorded at the detector per second, and a and b are calibration constants. The radius of influence of the gamma ray test is about half the distance between the source and the detector on the probe. In most cases, the radius of influence is less than 0.2 m. The result of a gamma-gamma logging test is a profile of unit weight along the bored pile. This profile gives many values of the unit weight, thereby allowing one to calculate a mean and standard deviation. Any unit weight value that is less than 3 standard deviations below the mean reading for the pile is considered anomalous (Brown et al. 2010).

Sonic Echo Method

The sonic echo technique does not require any access tube in the bored pile. Thus, it can be used even if plans were not made ahead of time to NDT the bored piles. However, it is not as reliable as the more rigorous cross hole or gamma-gamma testing. The sonic echo test consists of hitting the top of the bored pile with a carpenter-size hammer and recording the return signal at a geophone glued to the top of the pile. The departure and arrival of the compression-tension wave are recorded and the distance travelled is calculated according to a known wave speed. If the wave encounters a necking defect (reduction in concrete cross section), then it returns as a tension wave. If the wave encounters a bulb defect (increase in cross section), then it returns as a compression wave. Hence, the sign of the return wave indicates whether the defect is a necking or a bulb.

The reason for the return wave being a compression or a tension wave is explained as follows: If you hit a set of billiard balls lined up in a row (Figure 18.8) with a hammer, the last ball will leave the row. The reason is that the compression wave you generate with the hammer propagates through the balls and gets to the end. Finding no resistance, it tries to go back as a tension wave, but because there is no tension capacity between the balls, the last ball leaves. Now, if the billiard balls are in line but the last one is against a wall, and

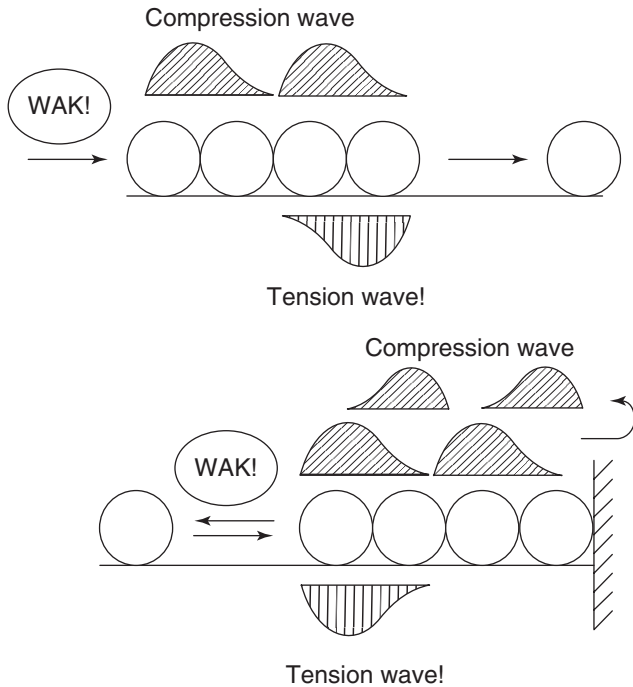


Figure 18.8 Impacts on billiard balls.

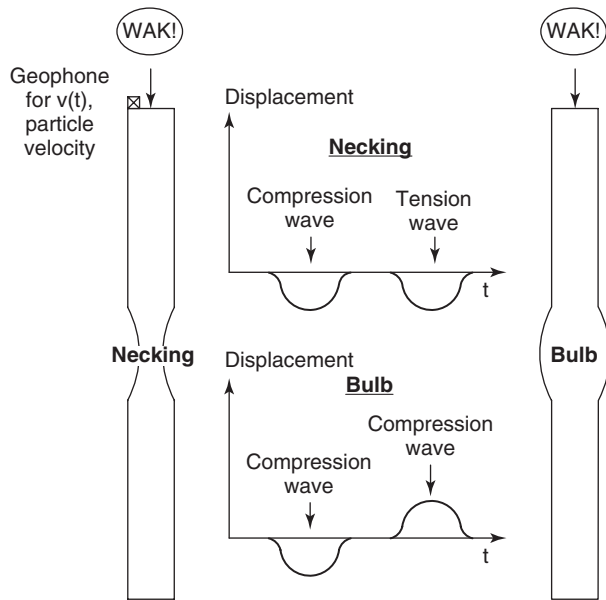


Figure 18.9 Sonic echo idealized signals.

if you hit the first one with a hammer, it is the first one that leaves the lineup. The reason is that the compression wave propagates through the balls, hits the wall, and returns as a compression wave back toward the first ball. There it finds no resistance and returns as a tension wave. Because there is no tension capacity between the balls, the first one leaves. The same thing happens in a bored pile. If the compression wave hits a necking defect (low resistance), it returns as a tension

wave; if it hits a bulb defect (high resistance), it returns as a compression wave (Figure 18.9).

Some of the limitations of the sonic echo method are:

1. The soil strength affects the intensity of the return wave. Pile length-to-diameter ratios larger than 10 in rock are unlikely to give satisfactory returns. In soft soils, however, length-to-diameter ratios of up to 50 can give satisfactory returns.
2. The interface of soil layers with contrasting strengths can create some return waves that must be distinguished from defects in the bored pile.
3. The smallest defect that can be detected improved from about 50% in 1993 (Baker et al. 1993; Briaud et al. 2002) to 10% in 2001 (Iskander et al. 2001).
4. An important distinction must be made between an anomaly and a defect. What may be detected as an anomaly may not represent a defect that would make a bored pile unusable.

Impulse Response Method

The impulse response technique is similar to the sonic echo method, but in this case the head of the hammer is instrumented with a dynamic load cell. During the impact that generates the wave propagation, the force-time signal of the hammer is recorded through this load cell. In addition, the velocity is recorded at the pile top. The force-time signal and the velocity time signal are then transformed into the frequency domain to create the force spectrum F and the velocity spectrum V . The ratio V/F is called the *mobility* and is plotted against the frequency (Figure 18.10).

Interpretation of the mobility curve proceeds as follows (Finno and Gassman 1998). The slope of the initial part of the mobility curve gives the small strain stiffness of the bored pile-soil system. The distance between peaks on the mobility curve gives the pile length or the distance between anomalies:

$$\Delta f = \frac{v_{conc}}{2L} \tag{18.8}$$

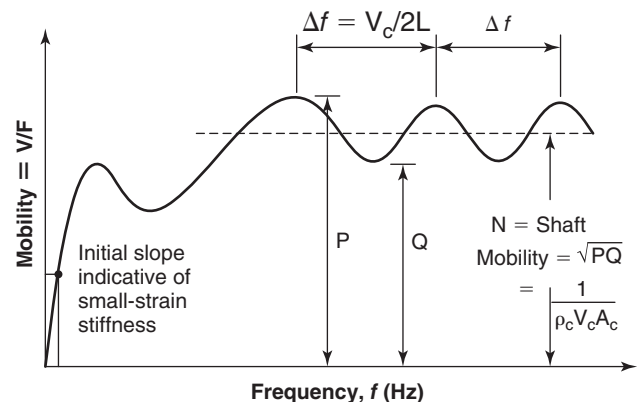


Figure 18.10 Mobility curve from an impulse response test.

where Δf is the distance between frequency peaks on Figure 18.10, v_{conc} is the compression wave velocity in concrete, and L is the length of the pile or the distance between anomalies. The mean value of the ratio V/F (Figure 18.10) is the inverse of the impedance:

$$\left(\frac{V}{F}\right)_{\text{mean}} = \frac{1}{I} = \frac{1}{\rho_c v_c A_c} \quad (18.9)$$

where $(V/F)_{\text{mean}}$ is the mean mobility from the mobility curve (Figure 18.10), I is the impedance of the system, ρ_c is the mass density of the concrete, v_c is the compression wave velocity in the concrete, and A_c is the cross-sectional area of the concrete pile.

Impedance Log Method

The impedance log technique is a derivative of the impulse response method. As mentioned regarding the impulse response method, the variation in impedance as a function of frequency can be generated. By comparing the mobility curve with the mobility curve for an infinitely long and constant-diameter bored pile, the variation in impedance as a function of depth can be generated (Hertlein 2009). This *impedance log* represents a two-dimensional rendition of the bored pile cross section as a function of depth (Figure 18.11). Note that in this rendition, because the impedance I is the product of $\rho_c v_c A_c$, all changes in mass density, wave velocity, and area are interpreted as changes in area. The impedance log has the advantage of giving a picture of the bored pile.

18.3.3 Installation of Driven Piles

A pile can be driven into the ground either by impact hammers or vibratory hammers. *Impact hammers* are big, heavy masses,

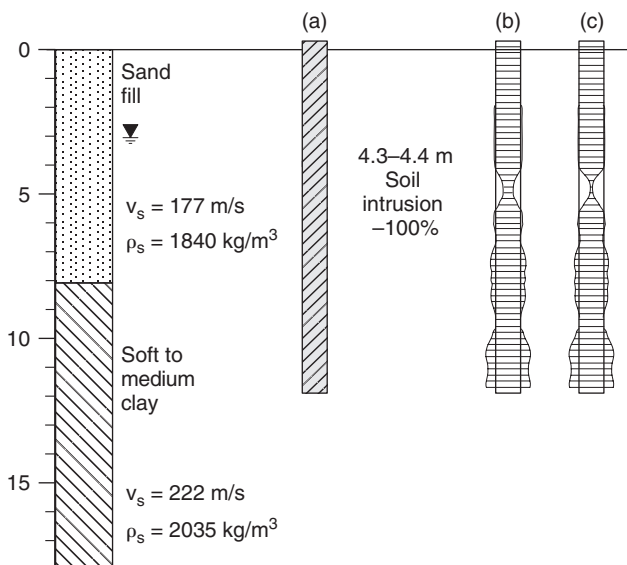


Figure 18.11 Example of impedance log of a bored pile (After Brown et al. 2010).

called *rams*, that are lifted and dropped repeatedly on the top of a pile to drive it into the ground. These hammers are of different types: steam hammers, diesel hammers, and hydraulic hammers. Steam hammers, the oldest types, use compressed steam to lift the ram; they may be single acting or double acting. In a single-acting hammer, the steam pressure lifts the ram which then falls under its own weight. In a double-acting hammer, the steam pressure also lifts the ram, but when the ram is ready to fall, the steam pressure acts on top of the ram to accelerate it downward, thereby increasing the force at impact. Diesel hammers, which use an explosion of ignited diesel fuel to lift the ram, can also be single acting or doubling acting. Hydraulic hammers use the hydraulic action of a piston. Hammers are rated in terms of maximum energy that can be delivered (drop height times weight of ram); these energies range from 20 kN.m or kJ to 800 kJ onshore and can reach up to 3000 kJ for offshore underwater hydraulic hammers. A cushion is placed between the hammer and the pile top to limit the stress generated in the pile material (soften the blow) by the hammer impact. Cushions made of wood are common and thicknesses can range from 25 to 100 mm. Sometimes a pile cap is also placed between the hammer and the pile. Pile driving formulas and the wave equation analysis (Lowery et al. 1967) are used to make calculations regarding drivability, hammer size, pile stresses, and pile capacity. Piles onshore are typically driven until a chosen blow count for a given hammer is reached. This blow count is usually around 75 blows per 0.3 meters of penetration. Offshore piles are usually driven to a penetration depth regardless of the blow count required.

Vibratory hammers grab the top of the pile and shake it vertically into the soil. The vibration is created by eccentrically rotating masses and the peak force is generated by the static weight of the hammer plus the centrifugal vibrating force. Although the frequency can vary from 10 to 100 Hz, the most common vibratory hammers operate at around 25 to 30 Hz. Resonance of the hammer-pile system is rarely reached, as it is typically higher than 30 Hz unless the pile is very long. Low-frequency, high-weight vibratory hammers (e.g., 1500 kN at 10 Hz) are used to drive large piles and caissons. Medium-frequency vibratory hammers (e.g., 250 kN at 25 Hz) are most common and are used for driving sheet pile and small piles. They work particularly well in sands where vibrations easily displace the soil particles. High-frequency vibratory hammers (e.g., 90 to 120 Hz) are rare and aim at reaching hammer-pile system resonance. Methods based on empirical formulas rooted in energy consideration as well as variances of the wave equation analysis are used to analyze these systems (Warrington 1992; Chua et al. 1987; Rausche 2002). The advantage of vibratory driving is that it is usually faster than impact driving, with a penetration rate that can be 10 times faster. The drawback is that it has limited penetration capability and does not develop residual stresses in the pile at the end of driving like impact-driven piles. As a result, a vibrodriven pile tends to exhibit more settlement

at working loads than an impact-driven pile, although both may have the same ultimate load (Briaud et al. 1990). Sometimes vibratory-driven piles are impact driven at the end of penetration to benefit from the advantages of both methods.

18.3.4 Pile Driving Formulas

Pile driving analysis started by assuming that the pile motion into the soil under each blow was a rigid body motion. Under this assumption, the energy conservation equation gives:

$$R_{ud} = \frac{Wh}{s} \quad (18.10)$$

where W is the weight of the hammer, h is the drop height, R_{ud} is the ultimate pile capacity at the time of driving, and s is the penetration of the pile. This simple equation turns out to be riddled with problems:

1. The fall of the ram is not unimpeded (e.g., friction) and there are other energy losses (e.g., compression of the cushion), so that the energy delivered to the pile is not Wh but a fraction of Wh' . This can be written as eWh where e is the efficiency of the driving system; e values are very difficult to quantify unless special measurements are made during driving, and can vary from 0.3 to 0.9.

2. The pile is not a rigid body; it compresses and rebounds during each hammer blow. This compression and rebound uses up energy that is not used to advance the pile penetration. This elastic energy is often represented by a term equal to $R_{ud}c/2$ (Figure 18.12) and is added to the resistance side of the energy equation (Eq. 18.10).

3. The movement of the pile during the driving process is best represented by a wave propagation in the pile. This process is not consistent with a single energy equation such as Eq. 18.10. This process is better represented by what is called the *wave equation analysis*.

4. If the static ultimate capacity R_{us} is the quantity sought from Eq. 18.10, then the dynamic component of R_{ud} due to rate and inertia effects must be subtracted from R_{ud} to get R_{us} .

Nevertheless, various forms of Eq. 18.10 have been proposed and used. The incentive was clearly the simplicity and great usefulness of this equation. Referring to Figure 18.12, the energy used in driving the pile is equated to the effective energy delivered by the hammer, and an improved version of Eq. 18.10 is:

$$R_{ud} = \frac{eWh}{s + \frac{c}{2}} \quad (18.11)$$

where R_{ud} is the ultimate capacity of the pile at the time of driving; e is the efficiency of the driving system; W is the weight of the ram; h is the height of drop (Wh is the rated energy of the hammer); s is the net downward movement of the pile after the blow, often called the *permanent set*; and c is the elastic rebound of the pile (c is usually taken as 5 mm, based

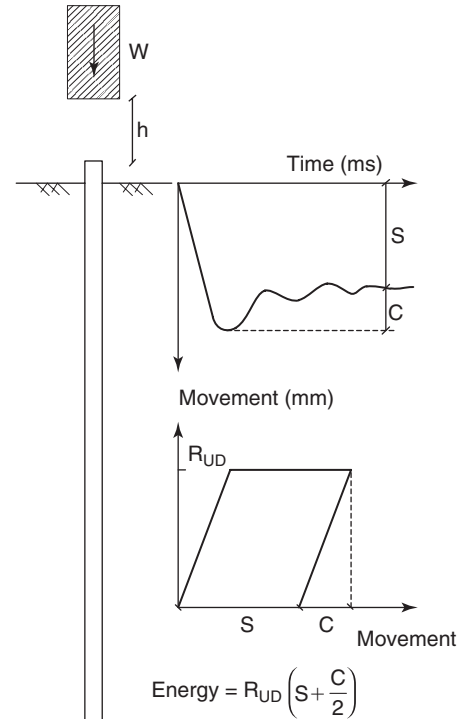


Figure 18.12 Pile driving event.

on experience). If the number of blows per 300 mm penetration is N , then the permanent set s is equal to $s = 300/N$. In order to include the effect of water stress dissipation and soil relaxation on the ultimate capacity, it is very desirable to use the blow count $N_{redrive}$ from re-driving the pile a good while after the end of driving. Then Eq. 18.11 becomes:

$$R_{ud} = \frac{eWh(\text{mm})}{\frac{300}{N_{redrive}} + 2.5} \quad (18.12)$$

This equation indicates how the pile resistance at the time of re-driving is linked to the blow count. The R-N curve (Figure 18.13) gives the following information:

1. It gives the pile resistance at the time of driving R_{ud} for an observed value of the blow count N .
2. Alternatively, if R_{ud} is known, if a reasonable blow count N for the end of driving is selected, and if the efficiency e of the system can be estimated, then the rated hammer energy Wh required to drive the pile can be obtained.
3. Equation 18.12 is a hyperbola with an asymptotic value of the pile resistance at the time of driving $R_{ud(\text{max})}$ of:

$$R_{ud(\text{max})} = \frac{eWh(\text{mm})}{2.5} \quad (18.13)$$

This is the maximum resistance that can be overcome by the hammer.

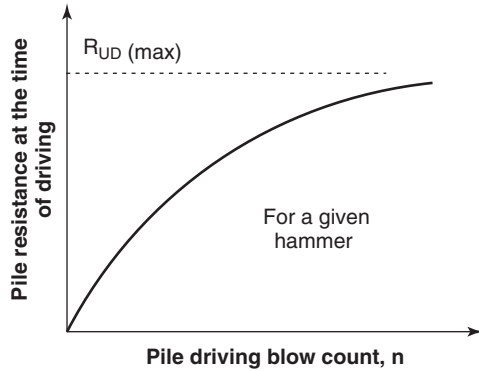


Figure 18.13 Pile driving R-N curve.

4. If a load test is performed to obtain the static ultimate capacity after driving R_{us} , the ratio K between R_{us} and R_{ud} can be calculated and used to evaluate R_{us} from the R_{ud} values on other piles.

One of the shortcomings of the pile driving equation is that it considers rigid body motion of the pile. In fact, a compression wave imparted by the hammer propagates down the pile and back up the pile in a time ranging from 5 to 20 milliseconds. This phenomenon must be accounted for to arrive at a more satisfactory analysis of the driving event.

18.3.5 Wave Propagation in a Pile

Before we talk about the wave equation for pile driving analysis, let's talk about wave propagation in a pile. We will apply the general principle to develop the solution for the displacement problem described in section 11.4.3.

1. We zoom in on an element of pile dz long (Figure 18.14).
2. We identify the knowns and unknowns, including the stresses in the pile element, the inertia force associated with the element mass, and the soil friction on the side of the element.
3. The fundamental equation in this case is the equation of motion:

$$\sum F = ma \quad \text{or} \quad (\sigma + d\sigma)A - \sigma A + fPdz = \rho Adz \frac{d^2u}{dt^2} \quad (18.14)$$

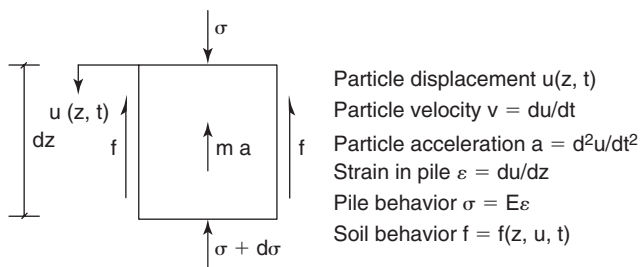


Figure 18.14 Element of pile.

where σ is the normal stress in the pile, A is the cross-sectional area of the pile, f is the shear stress at the interface, P is the pile perimeter, dz is the element length, ρ is the mass density of the pile, u is the pile particle displacement, and t is the time.

4. The constitutive equation for the pile is:

$$\sigma = E\epsilon = E \frac{du}{dz} \quad (18.15)$$

where E is the pile modulus of elasticity, ϵ is the strain in the pile, and z is the depth. This equation ignores the influence of confinement on the pile. This confinement plays a minor role because the stress in the pile is typically much larger than the confining stress from the surrounding soil.

5. The constitutive equation for the soil links the shear stress f at the pile soil interface to the displacement u of the pile. The shear stress f is then a function of u , and of the depth z if the soil is not uniform, and also the time t :

$$f = f(u, z, t) \quad (18.16)$$

6. Equations 18.14 through 18.16 are regrouped to give the wave equation:

$$\frac{d^2u}{dz^2} - \frac{\rho}{E} \frac{d^2u}{dt^2} + \frac{P}{AE} f = 0 \quad (18.17)$$

7. The boundary and initial conditions are the hammer impact velocity at $z = 0$ and $t = 0$ and the point resistance from the soil at $z = L$ and $t = 0$. The wave equation program solves this equation by stepping into time, as will be shown later.

The wave speed $c = dz/dt$ is different from the pile particle velocity $v = du/dt$. The wave speed c is typically thousands of times larger than the pile particle velocity. The wave travels down and up the pile during the few milliseconds of impact, whereas the particle only moves around its point of equilibrium. When a particle in the pile moves, it pushes its neighbor, which moves in turn. The very slight delay between the movements of these two neighbors is what creates the propagation of the wave. Of course, the stiffer the pile is, the faster the neighbor feels the push; thus, c is higher for stiffer materials. In contrast, the denser the pile is, the harder it is for the particle to move its neighbor, so c is lower for higher-density materials. The equation for the wave speed (compression) is derived as follows. We will use the case of a compression wave propagating in a pile without surrounding soil.

$$\frac{d^2u}{dz^2} = \frac{\rho}{E} \frac{d^2u}{dt^2} \quad (18.18)$$

In this instance it is convenient to change variables:

$$x = z + \sqrt{\frac{E}{\rho}} t \quad \text{and} \quad y = z - \sqrt{\frac{E}{\rho}} t \quad (18.19)$$

Then Eq. 18.18 becomes:

$$\frac{d^2u}{dx^2} = 0 \tag{18.20}$$

for which the solution is of the form:

$$u = f(x) + g(y) = f\left(z + \sqrt{\frac{E}{\rho}}t\right) + g\left(z - \sqrt{\frac{E}{\rho}}t\right) \tag{18.21}$$

Let's now consider the position of the wave at time t and $t + \Delta t$ (Figure 18.15). At time t , the wave is at a depth z , at time $t + \Delta t$ the wave is at a depth $z + \Delta z$, and the wave speed is $c = \Delta z/\Delta t$. The two functions f and g represent two waves, one coming down and one coming up in the pile. Let's consider one of the two waves represented by function f . The displacement $u(t)$ at time t and depth z is $u = f\left(z + \sqrt{\frac{E}{\rho}}t\right)$ and the displacement $u(t + \Delta t)$ at time $t + \Delta t$ and depth $z + \Delta z$ is $u = f\left(z + \Delta z + \sqrt{\frac{E}{\rho}}(t + \Delta t)\right)$. Because we have unimpeded propagation of the wave, the two values of u must be equal for all values of t and z . This requires that:

$$\Delta z = \sqrt{\frac{E}{\rho}} \Delta t \quad \text{and} \quad c = \sqrt{\frac{E}{\rho}} \tag{18.22}$$

where c is the wave speed.

The impedance I is defined as the ratio between the force and the velocity. The relationship is established as follows.

$$F = \sigma A = E\varepsilon A = E \frac{du}{dz} A = E \frac{du}{dt} \frac{dt}{dz} A = \frac{EA}{c} v = Iv \tag{18.23}$$

where F is the force generated by the impact, σ is the normal stress, A is the cross-sectional area, E is the modulus of elasticity, ε is the normal strain, u is the particle displacement, z is the depth, t is the time, c is the wave speed, v is the particle velocity, and I is the impedance equal to EA/c .

Equation 18.21 indicates that the particle velocity is made of the influence of a wave going down plus a wave going up in the pile. Similarly, the force F is made of a force going

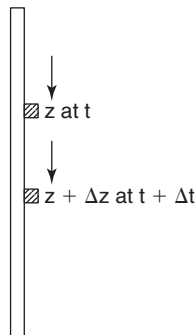


Figure 18.15 Wave location at time t and $t + \Delta t$.

down plus a force going up:

$$F = AE \frac{du}{dz} = AE \left(\frac{df_{\downarrow}}{dz} + \frac{dg_{\uparrow}}{dz} \right) = F_{\downarrow} + F_{\uparrow} \tag{18.24}$$

The equation for the particle velocities is also similar:

$$v = \frac{du}{dt} = \frac{df_{\downarrow}}{dt} + \frac{dg_{\uparrow}}{dt} = v_{\downarrow} + v_{\uparrow} \tag{18.25}$$

Note that:

$$\frac{df_{\downarrow}}{dz} = c \frac{df_{\downarrow}}{dt} \quad \text{and} \quad \frac{dg_{\uparrow}}{dz} = -c \frac{dg_{\uparrow}}{dt} \tag{18.26}$$

Therefore, using the impedance I , defined as:

$$I = \frac{AE}{c} \tag{18.27}$$

we get the following relationships:

$$F_{\uparrow} = 0.5(F + Iv) = Iv_{\uparrow} \tag{18.28}$$

$$F_{\downarrow} = 0.5(F - Iv) = -Iv_{\downarrow} \tag{18.29}$$

18.3.6 Wave Equation Analysis

In 1960, Smith proposed a calculation scheme to include the wave propagation in the analysis. This was the beginning of the modern pile driving analysis. The equations proposed by Smith are based on a discretization of the hammer, the cushion, the pile, and the soil. This discretization breaks the pile into elements that have a mass M and a spring constant K (Figure 18.16). The hammer, the cap-block, the helmet,

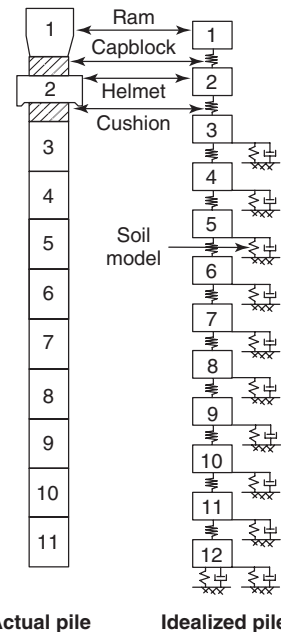


Figure 18.16 Discretization of the pile for wave equation analysis. (After Lowery et al. 1967).

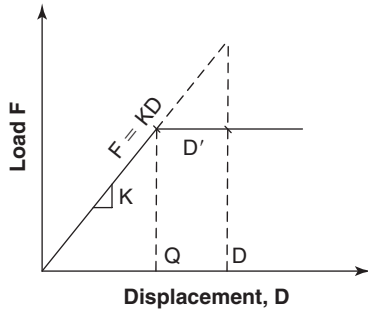


Figure 18.17 Soil model. (After Lowery et al. 1967).

and the cushion can also be represented by an element with a mass and a spring constant to represent their compressibility under load. The soil is represented as a series of springs tied to the pile elements with a dashpot for dynamic effects and a sliding block for maximum resistance. The soil model for the static resistance is an elastic, perfectly plastic model, as shown in Figure 18.17. The movement required to reach the plastic plateau is called the quake Q . The dynamic resistance of the soil is obtained from the static resistance by:

$$R_{DYN} = R_{STA}(1 + Jv) \quad (18.30)$$

where R_{DYN} and R_{STA} are the dynamic and static resistance of the soil respectively, v is the particle velocity of the pile element, and J is a damping coefficient. Table 18.2 gives the values for Q and J originally recommended by Coyle et al. (1973). Tables 18.3 and 18.4 give the values currently recommended in the GRLWEAP manual (2012). GRLWEAP

Table 18.2 Original Values of Quake Q and Damping Coefficient J

| Soil Type | Side Damping | Point Damping | Side Quake | Point Quake |
|-----------|--------------|---------------|------------|-------------|
| Clay | 0.65 s/m | 0.03 s/m | 2.5 mm | 2.5 mm |
| Silt | 0.33 s/m | 0.50 s/m | 2.5 mm | 2.5 mm |
| Sand | 0.16 s/m | 0.50 s/m | 2.5 mm | 2.5 mm |

(Lowery et al. 1967)

Table 18.3 Recommended Quake Q

| Soil Type | Pile Type or Size | Side Quake | Point Quake |
|---------------------------|--|------------|--------------------|
| All soil types | All pile types | 2.5 mm | |
| All soil types, soft rock | Nondisplacement piles (unplugged) | | 2.5 mm |
| Very dense and hard soils | Displacement piles with diameter or width D (solid or plugged) | | $D(\text{mm})/120$ |
| Loose or soft soils | Displacement piles with diameter or width D (solid or plugged) | | $D(\text{mm})/60$ |
| Hard rock | All types | | 1 mm |

(GRLWEAP 2012.)

Table 18.4 Recommended Damping Coefficient J

| Soil Type | Side Damping | Point Damping |
|----------------------|--------------|---------------|
| Coarse-grained soils | 0.16 s/m | |
| Fine-grained soils | 0.65 s/m | |
| All soils | | 0.50 s/m |

(GRLWEAP 2012.)

makes additional comments regarding the quake values:

1. Nondisplacement piles are sheet piles, H piles, or open-ended pipe piles that are not plugging during driving.
2. Displacement piles are solid piles (concrete piles) or piles that plug during driving.
3. Typically, pipe piles with diameters larger than 900 mm will not plug, whereas H piles and pipe piles with diameters smaller than 500 mm will plug during driving.
4. For vibratory-driven piles in fine-grained soils, the quake value should be doubled.
5. For vibratory-driven piles in all soils, the damping values should be doubled.

The equations used to solve the wave equation are as follows:

$$D(m, t) = D(m, t - 1) + V(m, t - 1)\Delta t \quad (18.31)$$

where $D(m, t)$ is the displacement of mass number m at the time step number t , $V(m, t - 1)$ is the velocity of mass number m at time step number $t - 1$, and Δt is the time

increment. This time increment must be very small, as the entire event may take only 20 milliseconds. Samson et al. (1963) recommend that Δt be less than:

$$\Delta t \leq \frac{\Delta L}{\sqrt{\frac{E}{\rho}}} \quad (18.32)$$

where ΔL is the pile element length, E is the pile modulus of elasticity, and ρ is the mass density of the pile material. This ensures that the wave does not propagate past one element during one time step. Once the displacements of all the pile elements are calculated, the compression of the springs between the pile elements can be calculated:

$$C(m, t) = D(m, t) - D(m + 1, t) \quad (18.33)$$

where $C(m, t)$ is the compression of spring number m at time step number t , and $D(m, t)$ is the displacement of the mass number m at time step number t .

Once the spring compressions are known, the force in the spring can be calculated:

$$F(m, t) = C(m, t)K(m) \quad (18.34)$$

where $F(m, t)$ is the force in spring number m at time step number t and $K(m)$ is the spring constant for spring number m .

The soil resistance is calculated as follows:

$$R(m, t) = (D(m, t) - D'(m, t))K'(m)(1 + JV(m, t - 1)) \quad (18.35)$$

where $R(m, t)$ is the dynamic soil resistance on the side of mass m or under the last mass at time step number t ; $D(m, t)$ is the displacement of mass number m at time step number t ; $D'(m, t)$ is the displacement beyond the quake if $D(m, t)$ is larger than the quake (if not, $D'(m, t)$ is zero); $K'(m)$ is the soil spring for mass number m ; J is the soil damping factor; and $V(m, t - 1)$ is the velocity of mass number m at time step number $t - 1$. Then the velocity of the element is calculated as follows:

$$V(m, t) = V(m, t - 1) + (F(m - 1, t) - F(m, t) - R(m, t)) \frac{g \Delta t}{W(m)} \quad (18.36)$$

where $V(m, t)$ is the velocity of mass number m at time step number t , $F(m - 1, t)$ is the force in spring $m - 1$ above mass number m at time step number t , $F(m, t)$ is the force in spring m below mass number m at time step number t , $R(m, t)$ is the dynamic soil resistance on the side of mass number m at time step number t , g is the acceleration due to gravity, Δt is the time step, and $W(m)$ is the weight of mass number m . In this string of equations, Eq. 18.34 is the constitutive equation

for the pile, Eq. 18.35 is the constitutive equation for the soil, and Eq. 18.36 is the fundamental equation ($F = Ma$).

Several computer programs have been written to automate the calculations, which consist of stepping into time and making a set of calculations within each time step. These programs include MICROWAVE (Lowery 1993), GRLWEAP (2012), and TNOWAVE (2012). The first two use the equations described in this subsection; the last one uses the method of characteristics. The best way to understand the calculations is to go through a simple example.

Example of Wave Equation Calculations

A square concrete pile (Figure 18.18) has a cross section 0.3 m by 0.3 m and a length of 8 m. The concrete modulus E_{conc} is 2×10^7 kN/m² and the concrete unit weight is 25 kN/m³. The hammer weighs 20 kN and strikes the pile at 3 m/s. Between the hammer and the pile is an oak cushion that has the same cross-sectional area as the pile, a thickness of 0.20 m, a modulus E_{cush} equal to 2×10^6 kN/m², and a unit weight of 7 kN/m³. The pile is driven into a sand with a point resistance of 500 kN, a quake of 2.5 mm, and a damping coefficient of $J = 0.2$ s/m.

The following idealizations are made to simplify the calculations. Such extreme simplifications are not necessary when using one of the computer programs mentioned earlier. The hammer is idealized as a rigid mass with a weight W_1 equal to 20 kN. The cushion is idealized as a spring with no mass; the spring constant K_1 comes from the equation giving the compression C of a column:

$$C = \frac{FL}{AE} \quad \text{or} \quad K = \frac{F}{C} = \frac{AE}{L} \quad (18.37)$$

where F is the force in the column, L is the length of the column, A is the column cross section, and E is the modulus of the column material. Therefore:

$$K_1 = \frac{0.3 \times 0.3 \times 2 \times 10^6}{0.2} = 900 \text{ kN/mm} \quad (18.38)$$

The pile itself is decomposed into two elements. (In a computer program, at least 10 elements are recommended.) Both elements are 4 m long and have weights W_2 and W_3 equal to:

$$W_2 = W_3 = 0.3 \times 0.3 \times 4 \times 25 = 9 \text{ kN} \quad (18.39)$$

The elasticity or springiness of each pile element is characterized by a spring K_2 , given by:

$$K_2 = K_3 = \frac{0.3 \times 0.3 \times 2 \times 10^7}{4} = 450 \text{ kN/mm} \quad (18.40)$$

The soil model is the point resistance model for the pile represented by an elastic, perfectly plastic model. The spring (Figure 18.12) is given by:

$$K' = \frac{500}{2.5} = 200 \text{ kN/mm} \quad (18.41)$$

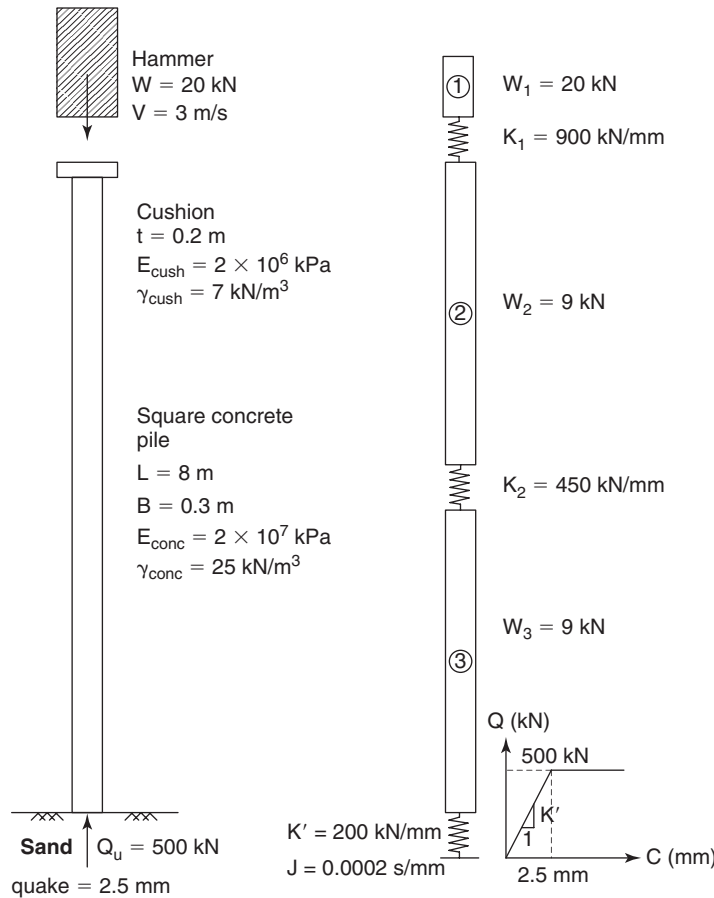


Figure 18.18 Example of wave equation analysis for a simple pile.

Figure 18.18 shows the real pile and the idealized pile. Note that I have placed the spring for pile element 2 under the pile segment, ignored the spring K_3 , and kept only the spring K' under the pile point. If we wished to keep K_3 , we would have to put it in series with K' . The time step is chosen by using Eq. 18.32:

$$\Delta t \leq \frac{4}{\sqrt{\frac{2 \times 10^7}{2500}}} = 0.045s \quad (18.42)$$

This value of Δt is very large because the length of the pile element is very large, to simplify the calculations. We would normally have a pile element that is much smaller than 4 m. Nevertheless, we will use a time step of 0.0005 seconds. The results of all calculations for the first four time steps are shown in Table 18.5.

Residual stresses are generated in an impact-driven pile in the following way. During the last hammer blow, the pile goes down, say, 7 mm, and mobilizes the upward resistance of the soil in both friction and point resistance. Then the pile rebounds, and in doing so it reverses the direction of the friction stresses. Indeed, it takes very little movement for the friction to be mobilized (say, 2 mm). However, because

it takes a lot more movement to totally decompress the pile point—say, 10 mm—the soil still pushes upward on the pile at the pile point. Equilibrium establishes itself at the end of the blow between the downward friction load and the upward point load (Figure 18.19). This creates a residual compression load in the pile. Thus, impact-driven piles end up being prestressed in the soil and their settlement is minimized because of this phenomenon. Briaud and Tucker (1984) showed how the wave equation can be used to simulate residual stresses. Under the first blow simulation, the pile is driven from a stress-free initial state, but the wave equation calculations end up with the residual stresses prediction. Using the residual loads from the output at the end of the first blow simulation as input to the second blow simulation allows one to simulate the influence of residual stresses. This influence makes pile driving easier, particularly for hard driving (e.g., Figure 18.20). Post grouting of bored piles is a way to establish beneficial residual stresses in bored piles and reduce potential settlement.

18.3.7 Information from Pile Driving Measurements (PDA, Case, CAPWAP)

Several methods are available to obtain the static capacity of the pile from dynamic measurements made at the top

Table 18.5 Wave Equation Calculations

| | 1 | 2 | 3 | 4 | 5 | 6 | 7 |
|---|---------|------|----------|----------|----------|----------|----------|
| A | Time | s | 0.000 | 0.0005 | 0.001 | 0.0015 | 0.002 |
| B | D(1,t) | mm | 0.000 | 1.500 | 2.834 | 3.897 | 4.672 |
| C | D(2,t) | mm | 0.000 | 0.000 | 0.368 | 1.296 | 2.708 |
| D | D(3,t) | mm | 0.000 | 0.000 | 0.000 | 0.045 | 0.241 |
| E | C(1,t) | mm | 0.000 | 1.500 | 2.467 | 2.601 | 1.964 |
| F | C(2,t) | mm | 0.000 | 0.000 | 0.368 | 1.250 | 2.467 |
| G | F(1,t) | kN | 0.000 | 1350.000 | 2219.923 | 2341.013 | 1767.614 |
| H | F(2,t) | kN | 0.000 | 0.000 | 165.544 | 562.706 | 1110.058 |
| I | R(3,t)s | kN | 0.000 | 0.000 | 0.000 | 9.022 | 48.211 |
| J | R(3,t)d | kN | 0.000 | 0.000 | 0.000 | 9.185 | 51.990 |
| K | V(1,t) | mm/s | 3000.000 | 2668.913 | 2124.476 | 1550.343 | 1116.836 |
| L | V(2,t) | mm/s | 0.000 | 735.750 | 1855.387 | 2824.564 | 3182.932 |
| M | V(3,t) | mm/s | 0.000 | 0.000 | 90.221 | 391.890 | 968.537 |

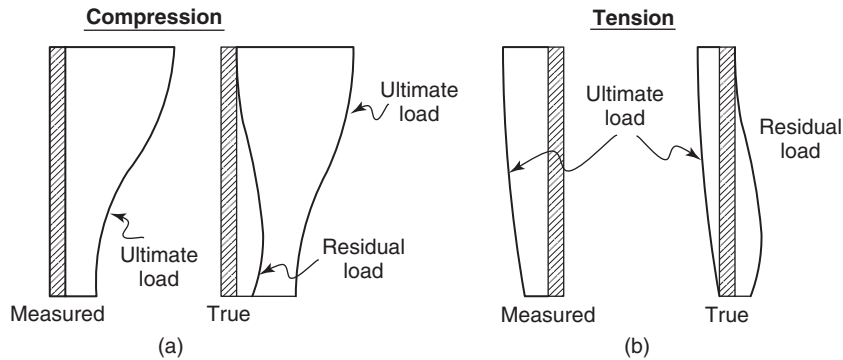


Figure 18.19 Residual load in an impact-driven pile.

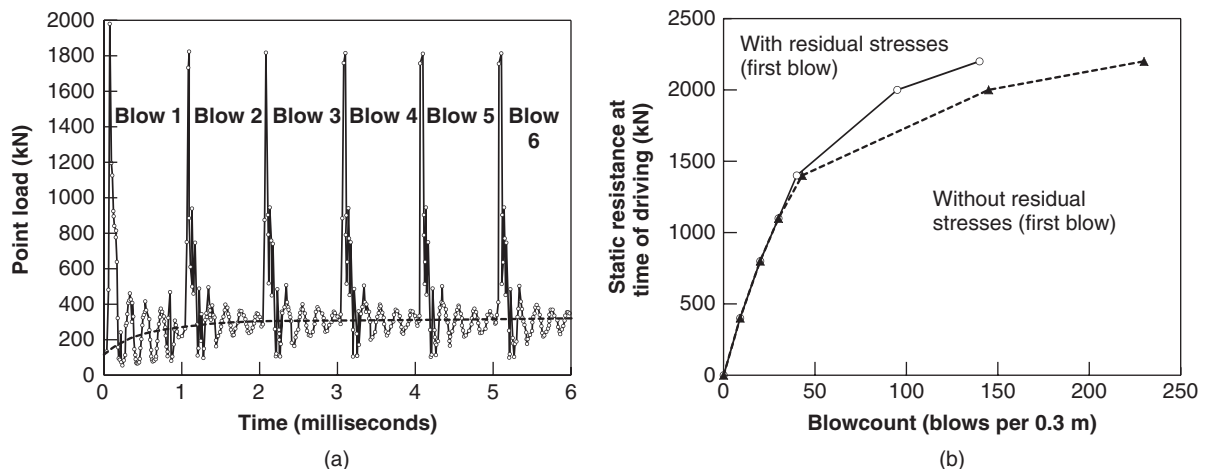


Figure 18.20 Pile driving R-N curve for a pile with and without residual stresses. (Briaud and Tucker 1984).

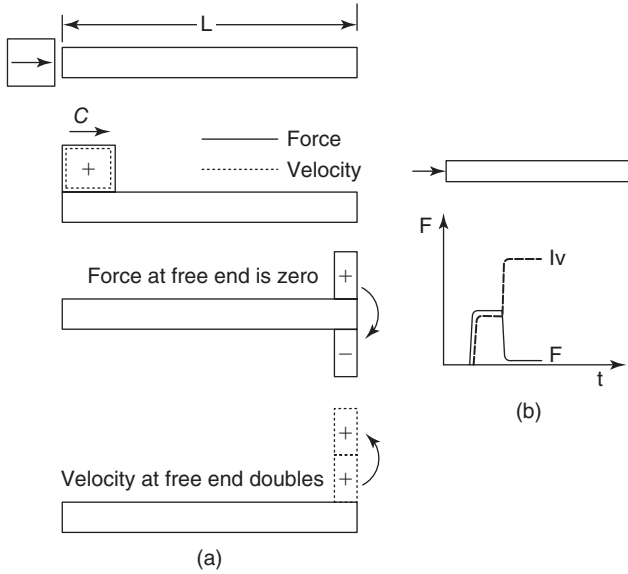


Figure 18.21 Free-end pile signal: (a) Pile. (b) Signal. (After Hannigan et al. 1998)

of the pile. The notion of making such measurements goes back a long way, but the credit for commercializing the idea goes to George Goble. Dynamic measurements made at the top of the pile usually include two strain gages and two accelerometers. ASTM has a standard for this test: D4945–89, entitled “Standard Method for High Strain Testing of Piles.” The purpose of the strain gages is to obtain the force in the pile during the impact of the hammer and the purpose of the accelerometers is to obtain the acceleration as a function of time and then the velocity by integration of the acceleration signal. The pile driving analyzer or PDA (Likins and Hussein 1988) is a device used to record, digitize, and process the strain and acceleration signals measured at the pile head.

Understanding the signals is important. The following example helps in this process. Imagine a pile suspended horizontally from the ceiling and hit at one end (Figure 18.21). There is no soil surrounding it and the end of the pile is free. Then the compression force in the pile will be proportional to the particle velocity ($F = Iv$, from Eq. 18.23). Now the wave is racing along the pile at the wave speed c . When it gets to the end of the pile, the compression force F finds no resistance and reflects as a tension force, but the magnitude of the particle velocity doubles while the wave speed is unchanged (see Eqs. 18.24 to 18.26). The F and Iv signals are as shown in Figure 18.21. This would be close to a case of easy driving with very little point resistance. Now let’s say that the pile is still suspended from the ceiling and it is hit at one end, but the other end is against a strong wall (Figure 18.22). When the compression wave gets to the wall, it cannot displace it. As a result, the compression force doubles and the velocity vanishes; the F and Iv signals are shown in Figure 18.22. Again, see Eqs. 18.24 to 18.26 for the mathematical reason. This would be close to hard driving into a strong bearing

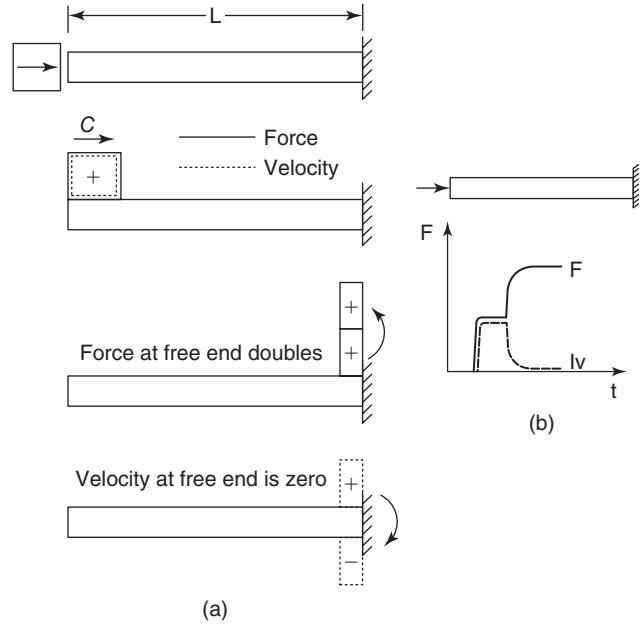


Figure 18.22 Fixed-end pile signal: (a) Pile. (b) Signal. (After Hannigan et al. 1998)

layer. Actual force and impedance times velocity signals for different driving conditions are shown in Figure 18.23 (Hannigan et al. 1998).

The Case Method

The Case Method (Likins and Hussein 1988) is a simple method for obtaining the dynamic and static pile capacity from the force and velocity signals. It is rooted in Eq. 18.43, which states that:

$$R_D = F - Ma \tag{18.43}$$

where R_D is the pile resistance, F is the force at the top of the pile, M is the mass of the pile, and a is the acceleration of the pile. This equation is based on rigid motion. To recognize the influence of the wave, Eq. 18.43 is modified empirically by taking average values of F and a during the time corresponding to the travel of the wave down and back up to the top of the pile:

$$R_D = 0.5(F_{(t_1)} + F_{(t_1+2L/c)}) - M \frac{(v_{(t_1+2L/c)} - v_{(t_1)})}{(t_1 + 2L/c - t_1)} \tag{18.44}$$

where R_D is the dynamic resistance of the pile, $F_{(t_1)}$ is the force at the top of the pile read at a time equal to t_1 , t_1 is the time corresponding to the first peak of the force signal, $F_{(t_1+2L/c)}$ is the force at the top of the pile read at a time equal to $(t_1 + 2L/c)$, L is the length of the pile, c is the wave speed in the pile material, M is the mass of the pile, $v_{(t_1)}$ is the velocity at the top of the pile read at the time t_1 , and $v_{(t_1+2L/c)}$ is the velocity at the top of the pile read at a time $(t_1 + 2L/c)$ (Figure 18.24). The term $2L/c$ corresponds

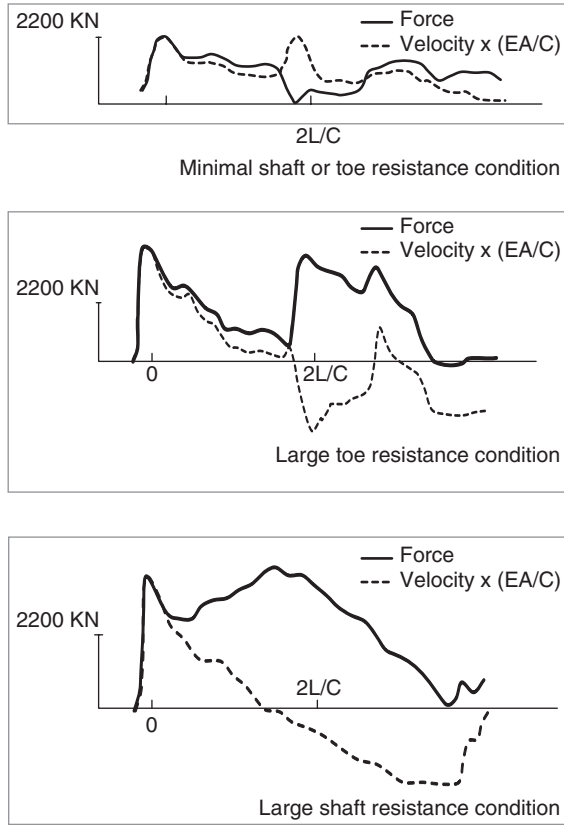


Figure 18.23 Actual force and impedance times velocity signals for different conditions. (After Hannigan 1990)

to the time necessary for the wave to travel to the bottom of the pile and back to the top, so $(t_1 + 2L/c)$ corresponds to the first return of the wave. Figure 18.24 shows a record of force-time signal at the top of a pile.

Eq. 18.44 can be rewritten as:

$$R_D = 0.5(F_{(t_1)} + F_{(t_1+2L/c)} + I(v_{(t_1)} - v_{(t_1+2L/c)})) \quad (18.45)$$

where I , the impedance of the pile, is given by:

$$I = \frac{AE}{c} = \frac{Mc}{L} \quad (18.46)$$

In this equation A is the cross-sectional area of the pile, E is the modulus of the pile material, c is the wave speed, M is the

mass of the pile, and L is the length of the pile. Figure 18.24 shows as a dashed line the signal obtained by multiplying the velocity measured at the top of the pile (actually integrated from accelerometer measurements) by the pile impedance I . The resistance R_D is the dynamic resistance of the pile. To get the static resistance of the pile R_S , a case damping factor J_c is used:

$$R_D = R_S + J_c I v \quad (18.47)$$

The velocity v is chosen to be the pile point velocity v_{point} , which can be obtained from wave propagation theory as:

$$v_{point(t_1)} = \frac{F_{(t_1)} + I v_{(t_1)} - R_D}{I} \quad (18.48)$$

where $v_{point(t_1)}$ and $v_{(t_1)}$ are the pile point and pile top velocities respectively, evaluated at the time t_1 corresponding to the first peak of the force signal; $F_{(t_1)}$ is the force at the pile top at time t_1 ; I is the pile impedance; and R_D is the dynamic resistance at the time of driving. Regrouping Eqs. 18.45, 18.47, and 18.48 gives the static capacity of the pile as:

$$R_S = 0.5((1 - J_c)(F_{(t_1)} + I v_{(t_1)}) + (1 + J_c)(F_{(t_1+2L/c)} - I v_{(t_1+2L/c)})) \quad (18.49)$$

The recommended Case damping coefficients are shown in Table 18.6.

Table 18.6 Case Damping Coefficient J_c .

| Soil Type | Case Damping Coefficient J_c |
|-------------|--------------------------------|
| Clean sands | 0.10 to 0.15 |
| Silty sands | 0.15 to 0.25 |
| Silts | 0.25 to 0.40 |
| Silty clays | 0.40 to 0.70 |
| Clays | 0.70 to 1.00 |

(Likins and Hussein 1988.)

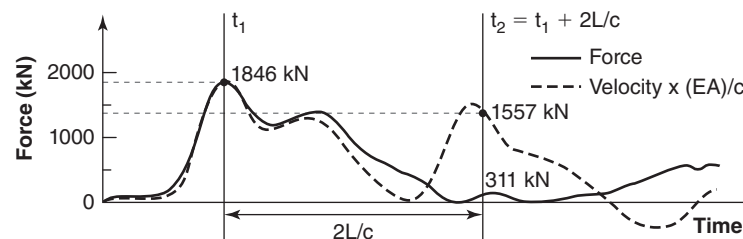


Figure 18.24 Force and impedance times velocity signals at the top of a pile. (After Likins and Hussein 1988.)

The CAPWAP Method

The CAPWAP method (Goble et al. 1993) makes use of the wave equation analysis described in section 18.3.5 and solves the inverse problem. It progresses by iterations to curve-fit the pile response determined in a wave equation model to the measured response of the actual pile during one hammer blow. The measured acceleration is used as input to the pile model and reasonable estimates are made for the soil resistance, quake, and damping parameters. The force-time signal at the pile head is calculated using a wave equation program and compared to the measured force-time signal. The input parameters, including the soil-resistance distribution, quake, and damping, are modified until the match between the measured and calculated signals is deemed satisfactory. Figure 18.25 shows an example of a comparison between measured and calculated force signals for a pile. Once an acceptable match is achieved, the solution yields an estimate of the ultimate static capacity, the distribution of soil resistance along the pile, and the quake and damping parameters. CAPWAP (PDI, CAse Pile Wave Analysis Program, 2012) and DLTWAVE (Dynamic Load Testing WAVE, TNO, 2012) are two programs that can be used.

Note that the soil resistance predicted from data collected during pile driving is tied to the blow count. Indeed, if the blow count is high, the pile penetration per blow is low and the associated pile capacity is low (Figure 18.26). However, if a much bigger hammer is brought in and the pile penetration per blow increases significantly, the soil resistance predicted from such measurement on the same pile can be much higher. For a given pile, the bigger the hammer, the larger the predicted soil resistance is. Figure 18.26 indicates the reason for this observation.

18.3.8 Suction Caissons

Suction caissons have become very popular in the last decade for the foundation of offshore platforms and offshore wind turbines. They consist of upside-down coffee cans (large ones!) pushed into the seafloor by sucking water out of the inside (Figure 18.27).

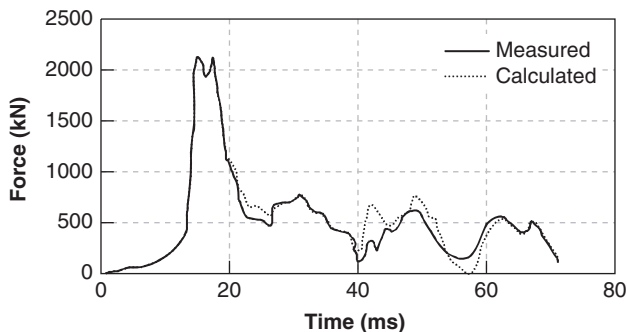


Figure 18.25 Signal matching using CAPWAP. (After Goble et al. 1993.)

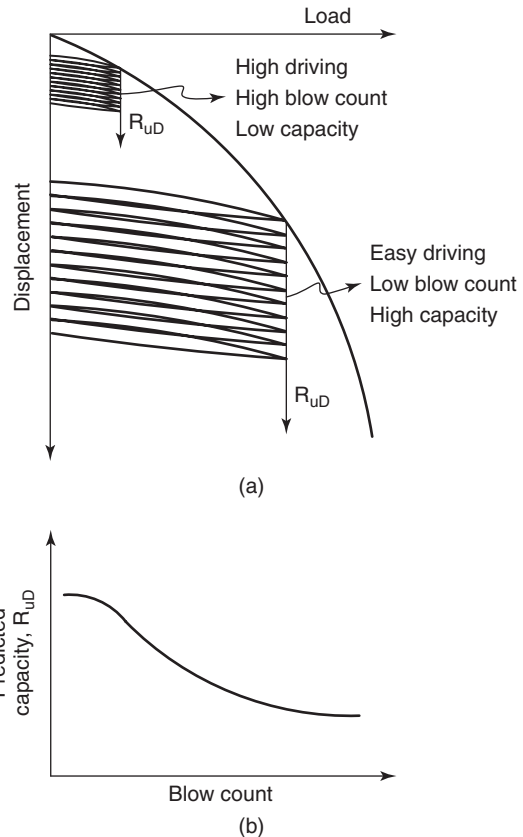


Figure 18.26 Predicted capacity depends on blow count and hammer size.

They are used primarily in clays, but occasionally have to penetrate through sand layers. In clays they have aspect ratios around 5 to 1, with diameters in the range of 3 to 6 m and lengths in the range of 15 to 30 m. Capacities in clays vary from 5 to 20 MN. Sand layers can offer high resistance to penetration; as a result, in sand, the aspect ratio is usually reduced, with values of around 2 to 1. The differential pressure between the inside and the outside of the caisson must be large enough to create a downward force that can overcome the soil resistance to penetration. In clays, this penetration resistance Q_{tot} is calculated as follows (API-RP 2SK, 2012):

$$Q_{tot} = Q_{side} + Q_{tip} = \alpha s_u A_{wall} + (N_c s_u + \gamma' z) A_{tip} \tag{18.50}$$

where Q_{side} is the soil friction resistance on the outside and the inside of the wall of the suction caisson, Q_{tip} is the area at the tip of the caisson corresponding to the thickness of the wall, α is the adhesion factor during installation (taken, for example, as the ratio of the residual shear strength over the peak shear strength), s_u is the average peak undrained shear strength obtained from direct simple shear tests, A_{wall} is the area of the inside wall plus the outside wall in contact with the soil, N_c is the bearing capacity factor (taken as 7.5), γ' is the effective unit weight of the soil, z is the final penetration depth, and A_{tip} is the area of the tip of the caisson corresponding to the cross-sectional area of the wall.

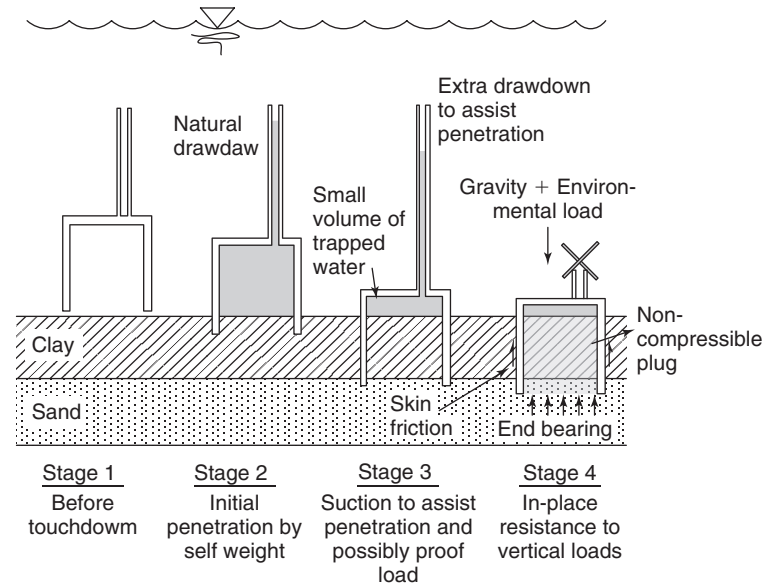


Figure 18.27 Installation of a suction caisson.

The underpressure Δu_{req} needed to enable installation of the suction caisson can then be calculated as:

$$\Delta u_{req} = \frac{Q_{tot} - W'}{A_{in}} \quad (18.51)$$

where Δu_{req} is the difference in pressure between the top and bottom of the roof of the suction caisson, Q_{tot} is the total resistance at full penetration, W' is the submerged weight of the suction caisson, and A_{in} is the area under the roof of the caisson where the underpressure is acting.

The amount of suction that can be generated has a limit which is set by any associated failure mechanism. For example, an excessive underpressure could create an inverse bearing capacity failure ($N_c s_u$) and excessive plug movement inside the wall of the caisson (αs_u). The failure underpressure can then be evaluated as follows:

$$\Delta u_{crit} = N_c s_u + \frac{\alpha s_u A_{wall}}{A_{in}} \quad (18.52)$$

where Δu_{crit} is the underpressure that would create inward failure of the soil, N_c is the bearing capacity factor (taken as 6.2 to 9 depending on the relative embedment; see Figure 17.7), s_u is the undrained shear strength measured in a direct simple shear test, α is the adhesion factor during installation (taken, for example, as the ratio of the residual shear strength over the peak shear strength), s_u is the average peak undrained shear strength obtained from direct simple shear tests, A_{wall} is the area of the inside wall in contact with the soil, and A_{in} is the area under the roof of the caisson where the underpressure is acting. Similar rules have been developed for suction caissons in sand (Andersen et al. 2008). The actual underpressure used is limited to Δu_{crit} divided by a factor of safety equal to 1.5, for operation at a safe level.

18.3.9 Load Testing (Static, Statnamic, Osterberg)

Static Load Tests

Static load tests are still the best way to obtain the load settlement curve for a pile (ASTM D1143). Most typically, these tests consist of installing two or more reaction piles on each side of the test pile, placing a beam across the two reaction piles, and pushing or pulling on the test pile with a jack (Figure 18.28). The load is measured by a load cell between the beam and the jack, while the settlement of the pile is measured by dial gages or LVDTs connected to a settlement beam with supports far away from the test pile. The result of the load test is a load settlement curve (Figure 18.29) up to the capacity of the test pile, the capacity of the reaction system, or the target load for proof tests. For more advanced load tests, the test pile is instrumented with strain gages or extensometers to measure the load in the pile at different depths. This is very useful when separate measurements are needed for the load carried in friction and the load carried in point resistance. For driven piles, the instrumentation should be read right after driving to obtain the distribution of the residual loads.

The ultimate load is obtained from the load settlement curve. For piles in fine-grained soils, the ultimate load is usually clearly identifiable as a plunging load. For coarse-grained soils, the ultimate load is much harder to identify because the curve tends to gradually curve without a plunging load. In this case, an ultimate load criterion is used. There are many such criteria; the most appropriate ultimate load definition seems to be the load corresponding to a settlement s (Figure 18.29) equal to:

$$s = \frac{B}{10} + \frac{PL}{AE} \quad (18.53)$$

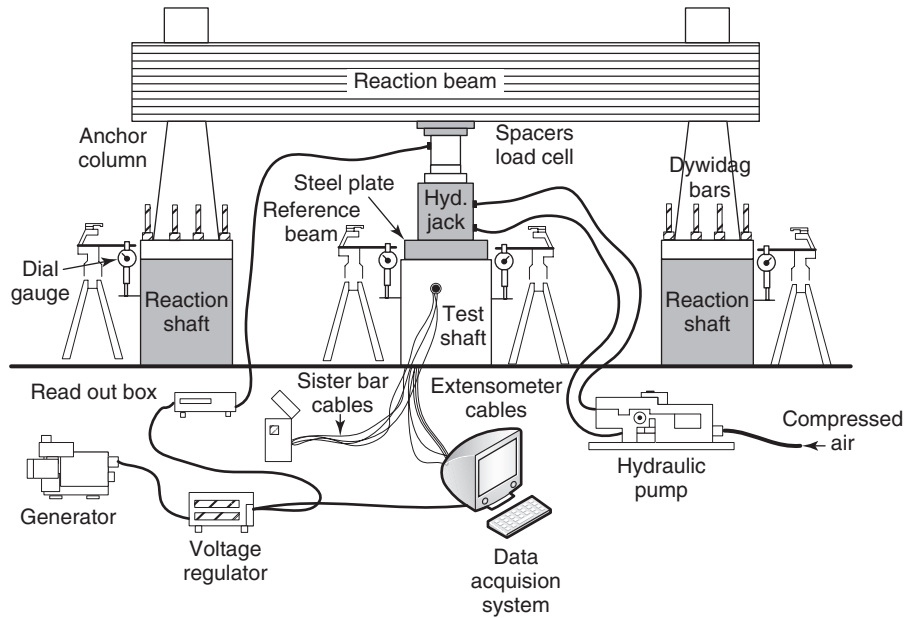


Figure 18.28 Load test setup.

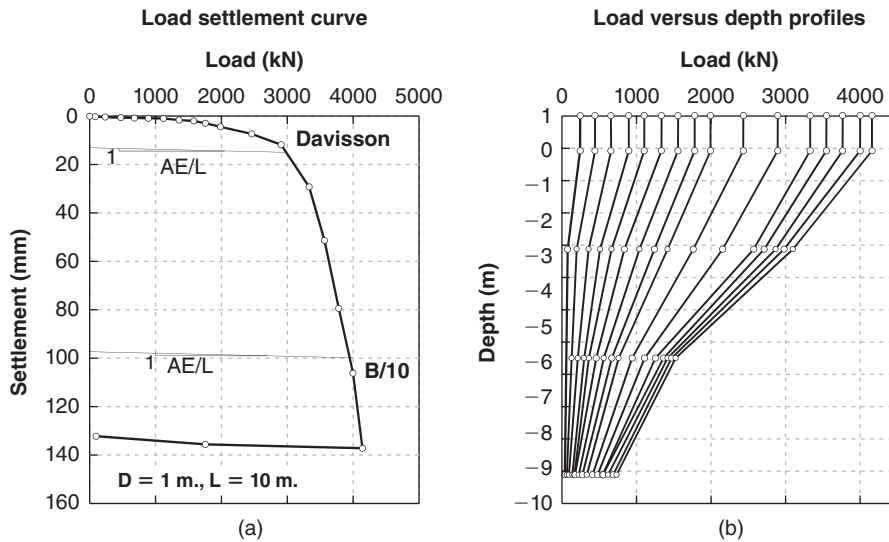


Figure 18.29 Results of an instrumented load test on a bored pile: (a) Load settlement curve. (b) Load versus depth profiles. (Briaud et al. 2000)

where B is the pile diameter, P is the load at the pile top, L is the pile length, A is the pile cross-sectional area, and E is the modulus of the pile material. The Davisson criterion (Figure 18.29) gives a load corresponding to a much smaller settlement:

$$s = 4 \text{ mm} + \frac{B}{120} + \frac{PL}{AE} \quad (18.54)$$

For a 1 m diameter, 10 m long concrete pile loaded to 5000 kN, the two criteria give a settlement s of 103 mm ($B/10$) and 15 mm (Davisson). It is clear that the Davisson criterion corresponds to a much smaller settlement than the $B/10$ criterion.

Osterberg Load Cell Test

The Osterberg load cell test (Figure 18.30) is another form of static load test. The Osterberg cell or O-cell was developed by Jorge Osterberg (1984). The idea is to place a hydraulic flat jack at the bottom of the pile, so that after pile installation the jack can be inflated, thereby pushing the pile upward against the point resistance. During the test, the soil friction acts downward on the pile and the point resistance acts upward. The test ends when the ultimate friction load or the point resistance load is reached, whichever comes first. If the friction load is the smaller of the two, the ultimate friction load is determined, but only a lower bound of the

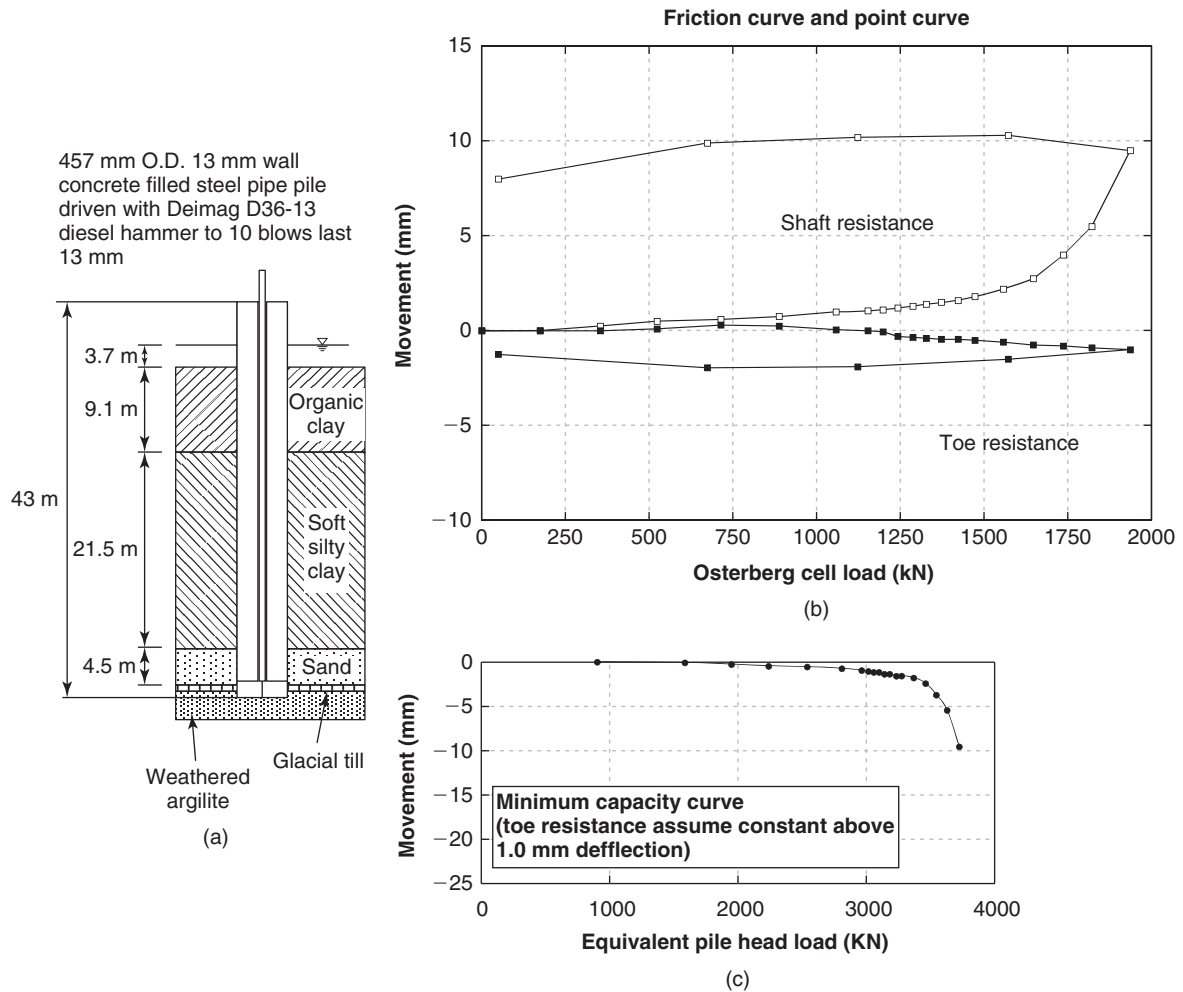


Figure 18.30 Osterberg load test. (a) Osterberg test. (b) Load test results, friction curve, and point curve. (c) Reconstructed top load top movement. (After Hannigan et al. 1998.)

ultimate point resistance is obtained. If the point resistance is the smaller of the two, the ultimate point load is determined, but only a lower bound of the ultimate friction resistance is obtained. In this case, the drawback can be mitigated by placing the O-cell along the pile at a location that balances the load above and the load below the O-cell position. Generally, ASTM Standard D1143 is followed, and loads as high as 300 MN have been generated on large piles. The cost of an O-cell test seems to be about one-third to two-thirds of the cost of a conventional load test, with more savings being realized as the maximum load necessary increases. Figure 18.30 shows an example of results from an O-cell test. There is one load settlement curve for the friction and one load settlement curve for the point resistance. These two curves are added to reconstruct the top load top settlement curve for the pile; however, this reconstructed curve assumes that either the friction or the point resistance remains constant at the end of testing (conservative).

The Statnamic Load Test

The Statnamic load test (Figure 18.31) was developed by Berminghammer (Bermingham and Janes 1989). It consists of placing a dynamic pressure chamber fueled by solid propellant on top of the pile and a large mass on top of the jack. When the fuel is ignited, the large mass is accelerated upward to about 20 g, and by reaction the same force acts downward on the pile. The loading event takes about 100 milliseconds. The load is measured through a dynamic load cell, the acceleration with an accelerometer, and the displacement through a laser beam on a target. Integrating the accelerometer data once for velocity and twice for displacement complements the data.

ASTM Standard D7383 is followed, and loads as high as 50 MN have been generated. Figure 18.32 shows an example of the data collected. The load F_{sm} measured during the Statnamic test is composed of the static resistance of the soil F_s , the rate effect component of the soil F_d , and the inertia

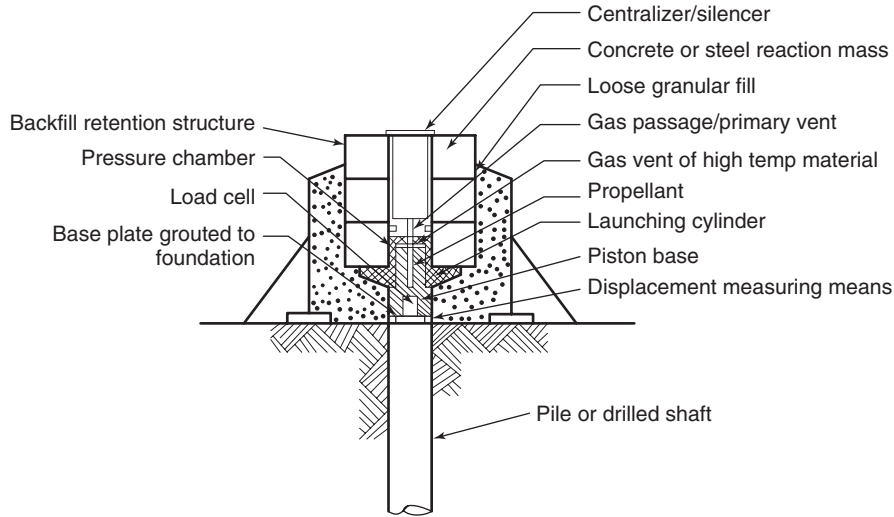
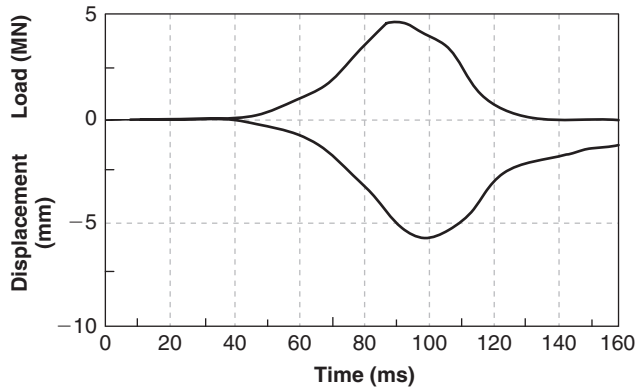
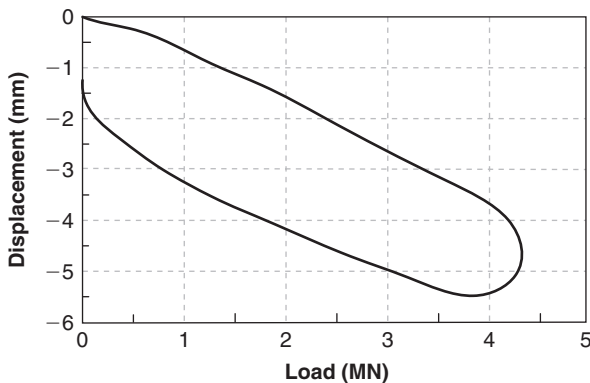


Figure 18.31 Original Statnamic set up. (Bermingham and Janes 1989)



(a) Load and displacement versus time



(b) Load vs. displacement curve

Figure 18.32 Statnamic load test data. (After Hannigan et al. 1998)

force F_i due to accelerating the pile and surrounding soil:

$$F_{sm}(t) = F_s(t) + F_d(t) + F_i(t) \quad (18.55)$$

The purpose of the test is to obtain the static resistance F_s . The rate effect force F_d is considered to be linearly proportional to the velocity:

$$F_d(t) = Cv(t) \quad (18.56)$$

where C is a damping factor similar to the J values for the wave equation analysis. Furthermore, the force F_i can be expressed as:

$$F_i(t) = Ma(t) \quad (18.57)$$

where M is the mass of the pile and $a(t)$ is the measured acceleration at the top of the pile. Here it is assumed that the entrained soil mass is negligible and that rigid body motion prevails. At the point of maximum displacement on the unloading part of the load settlement curve (point A in Figure 18.33), the velocity is zero and therefore the force F_d is zero. Then, if it is assumed that at A the displacement is large enough to mobilize the ultimate pile capacity, the load at point A is the sum of the static ultimate capacity of the pile F_{su} and the inertia force F_i :

$$F_{sm}(t_A) = F_{su}(t_A) + Ma(t_A) \quad (18.58)$$

where $F_{sm}(t_A)$ is the load measured in the Statnamic test at time t_A , t_A is the time corresponding to the largest displacement during the Statnamic test (point A in Figure 18.33), M is the mass of the pile, and $a(t_A)$ is the acceleration measured at the pile top at time t_A .

The damping coefficient C can be obtained by using the maximum load measured at point B on the load settlement curve as follows:

$$C = \frac{F_{sm}(t_B) - F_{su}(t_A) - Ma(t_B)}{v(t_B)} \quad (18.59)$$

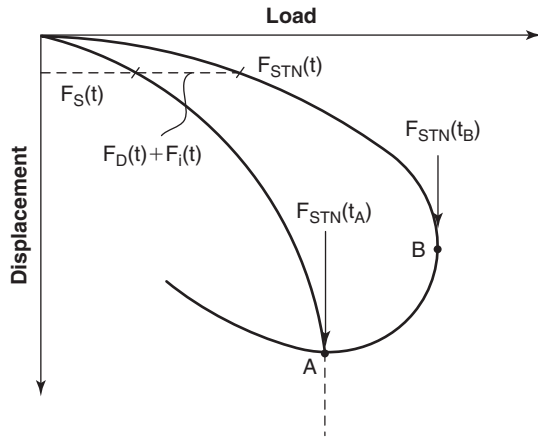


Figure 18.33 Obtaining the static curve from a Statnamic load test. (After Hannigan et al. 1998)

where $F_{sm}(t_B)$ is the load measured in the Statnamic test at time t_B , t_B is the time corresponding to the largest load during the Statnamic test (point B in Figure 18.33), M is taken as the mass of the pile, $a(t_B)$ is the acceleration measured at the pile top at time t_B , $F_{su}(t_A)$ is the static load obtained from Eq. 18.58, and $v(t_B)$ is the velocity measured at the top of the pile a time t_B . If it is further assumed that C is a constant during the load test, then point by point and for any given time t , the static load F_s versus displacement curve can be obtained from:

$$F_s(t) = F_{sm}(t) - Cv(t) - Ma(t) \quad (18.60)$$

Figure 18.33 shows the result of such a procedure.

18.4 VERTICAL LOAD: SINGLE PILE

If a pile is installed in the ground, is left to rest until it gains its full capacity, and is then load tested, the results of the load test could look like the load settlement curve of Figure 18.29. At the beginning of the load test, the load increases proportional to the settlement. This is the linear part of the behavior, and it is usually within this range of loads that the settlement of a single pile is calculated. When the load increases past that point, permanent deformations occur, nonlinear behavior becomes apparent, and, at high loads, a small increase in load leads to a large increase in settlement of the pile.

In clay, that part of the curve usually exhibits a plunging failure mode where the pile simply cannot sustain any increase in load. In sand, however, that part of the curve usually exhibits a continuous increase in load as a function of settlement. The reason for this difference is that during a typical load test, the behavior under the point of a pile in clay is undrained (for saturated soils), whereas the behavior in sand is drained. Under undrained conditions, the shear strength is nearly constant regardless of the total stress increase (plunging failure of the pile), whereas under drained conditions the shear strength increases with the total stress increase and so

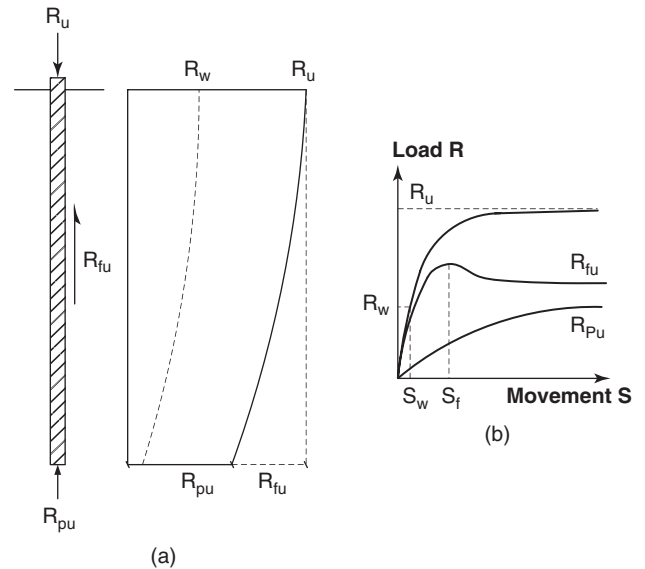


Figure 18.34 Load distribution in a single pile.

does the pile resistance. The distribution of the load in the pile is shown in Figure 18.34.

The issues to be discussed next—always in the simple case of a single pile—include how to estimate the ultimate load of the pile, estimate the settlement of the pile, negotiate downdrag problems, and handle shrink-swell situations.

18.4.1 Ultimate Vertical Capacity for a Single Pile

The ultimate load R_u of a single pile (Figure 18.35) is given by:

$$R_u = R_{uf} + R_{up} = \sum_{i=1}^n f_{ui} A_{si} + p_u A_p \quad (18.61)$$

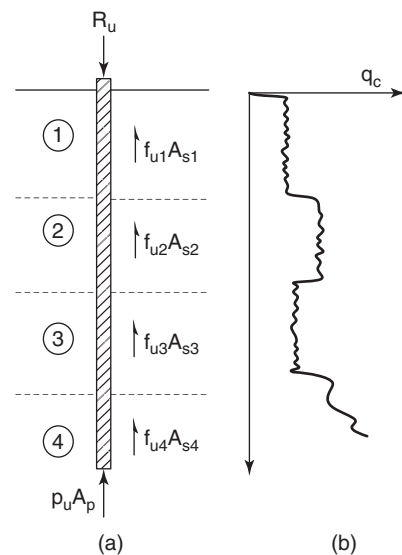


Figure 18.35 Vertical capacity of a single pile.

Table 18.7 Methods for Ultimate Capacity of Single Piles

| | Bored Piles | Driven Piles |
|----------------------|--|--|
| Fine-Grained Soils | LPC-PMT method LPC-CPT method FHWA, 2010 | LPC-PMT method LPC-CPT method API RP2A Effective stress method |
| Coarse-Grained Soils | LPC-PMT method LPC-CPT method FHWA, 2010 | LPC-PMT method LPC-CPT method API RP2A Briaud-Tucker SPT method |

where R_{uf} is the ultimate resistance in friction, R_{up} is the ultimate resistance in point bearing, A_{si} is the side area of the i^{th} pile element, f_{ui} is the ultimate friction between the soil and the pile acting on the i^{th} pile element, A_p is the area of the pile point, and p_u is the ultimate bearing pressure of the soil at the pile point.

Many methods exist for estimating the values of f_u and p_u . Most of them are empirical with some theoretical content. The methods listed in Table 18.7 have been selected for presentation in this book.

LPC-PMT Method

The LPC-PMT method (Frank, 1999, 2013, Norme Francaise AFNOR P94-262) was developed by the Laboratories des

Ponts et Chaussees after 30 years of instrumented load testing of piles by Bustamante and his colleagues. It is not restricted to a pile type or a soil type. It makes recommendations of f_u and p_u for bored piles and driven piles and for fine-grained soils and coarse-grained soils. It is based on the limit pressure from the pressuremeter test (PMT). Although the PMT is not a very common test in many countries, it has the significant advantage over all other tests of being possible in almost all soils and rock. The steps to follow for the LPC-PMT method are:

1. Classify the soil according to Table 18.8.
2. Identify the pile type on Table 18.9 and Table 18.10.

Table 18.8 Soil Classification for LPC-CPT and LPC-PMT Methods

| SOIL TYPE | STRENGTH | PMT p_L^* (MPa) | CPT q_c (MPa) | SPT N (bpf) | Shear Strength s_u (kPa) |
|--------------------------|-------------------|----------------------|--------------------|----------------|-------------------------------|
| Clay, Silt | Very soft to soft | < 0.4 | < 1 | | < 75 |
| | Firm | 0.4 to 1.2 | 1 to 2.5 | | 75 to 150 |
| | Stiff | 1.2 to 2 | 2.5 to 4 | | 150 to 300 |
| | Very stiff | > 2 | > 4 | | > 300 |
| Sand, Gravel | Very loose | < 0.2 | < 1.5 | < 3 | |
| | Loose | 0.2 to 0.5 | 1.5 to 4 | 3 to 8 | |
| | Medium dense | 0.5 to 1 | 4 to 10 | 8 to 25 | |
| | Dense | 1 to 2 | 10 to 20 | 25 to 42 | |
| | Very dense | > 2 | > 20 | 42 to 58 | |
| Chalk | Soft | < 0.7 | < 5 | | |
| | Weathered | 0.7 to 3 | 5 to 15 | | |
| Marl and Marly Limestone | Intact | > 3 | > 15 | | |
| | Soft | < 1 | < 5 | | |
| | Hard | 1 to 4 | 5 to 15 | | |
| Rock | Very hard | > 4 | > 5 | | |
| | Weathered | 2.5 to 4 | | | |
| | Fissured | > 4 | | | |

(After Frank 2013 and Norme Francaise AFNOR P94-262)

Table 18.9 Choosing the Friction Parameters for the LPC-PMT Method.

| Friction curve | Clay, Silt | | Sand, Gravel | | Chalk | | Marl and Marly Limestone | | Weathered rock | |
|----------------------------------|------------|-----------------|--------------|-----------------|----------|-----------------|--------------------------|-----------------|----------------|-----------------|
| | Q1 | | Q2 | | Q3 | | Q4 | | Q5 | |
| | α | f_{lim} (kPa) | α | f_{lim} (kPa) | α | f_{lim} (kPa) | α | f_{lim} (kPa) | α | f_{lim} (kPa) |
| Bored, dry | 1.1 | 90 | 1.0 | 90 | 1.8 | 200 | 1.5 | 170 | 1.6 | 200 |
| Bored, mud | 1.25 | 90 | 1.4 | 90 | 1.8 | 200 | 1.5 | 170 | 1.6 | 200 |
| Bored w. casing (left in place) | 0.7 | 50 | 0.6 | 50 | 0.5 | 50 | 0.9 | 90 | - | - |
| Bored w. casing (retrieved) | 1.25 | 90 | 1.4 | 90 | 1.7 | 170 | 1.4 | 170 | - | - |
| Driven concrete | 1.1 | 130 | 1.4 | 130 | 1.0 | 90 | 0.9 | 90 | - | - |
| Driven metal (closed end) | 0.8 | 90 | 1.2 | 90 | 0.4 | 50 | 0.9 | 90 | - | - |
| Driven metal (open end) | 1.2 | 90 | 0.7 | 50 | 0.5 | 50 | 1.0 | 90 | 1.0 | 90 |
| Driven H pile | 1.1 | 90 | 1.0 | 130 | 0.4 | 50 | 1.0 | 90 | 0.9 | 90 |
| Driven sheet pile | 0.9 | 90 | 0.8 | 90 | 0.4 | 50 | 1.2 | 50 | 1.2 | 90 |
| Micropiles (single injection) | 2.7 | 200 | 2.9 | 380 | 2.4 | 320 | 2.4 | 320 | 2.4 | 320 |
| Micropiles (repeated injections) | 3.4 | 200 | 3.8 | 440 | 3.1 | 440 | 3.1 | 440 | 3.1 | 500 |

(After Frank 2013 and Norme Francaise AFNOR P94-262)

Table 18.10 Bearing Capacity Factor k_p for LPC-PMT Method

| | Clay, Silt | | Sand, Gravel | | Chalk | | Marl and Marly Limestone | | Weathered rock | |
|----------------------------------|------------|--|--------------|--|-------|--|--------------------------|--|----------------|--|
| | | | | | | | | | | |
| Bored, dry | 1.15 | | 1.1 | | 1.45 | | 1.45 | | 1.45 | |
| Bored, mud | 1.15 | | 1.1 | | 1.45 | | 1.45 | | 1.45 | |
| Bored w. casing (left in place) | 1.15 | | 1.1 | | 1.45 | | 1.45 | | 1.45 | |
| Bored w. casing (retrieved) | 1.15 | | 1.1 | | 1.45 | | 1.45 | | 1.45 | |
| Driven concrete | 1.35 | | 3.1 | | 2.3 | | 2.3 | | 2.3 | |
| Driven metal (closed end) | 1.35 | | 3.1 | | 2.3 | | 2.3 | | 2.3 | |
| Driven metal (open end)* | 1.0 | | 1.9 | | 1.4 | | 1.4 | | 1.2 | |
| Driven H pile* | 1.3 | | 3.1 | | 1.7 | | 2.2 | | 1.5 | |
| Driven sheet pile* | 1.0 | | 1.0 | | 1.0 | | 1.0 | | 1.2 | |
| Micropiles (single injection) | 1.15 | | 1.1 | | 1.45 | | 1.45 | | 1.45 | |
| Micropiles (repeated injections) | 1.15 | | 1.1 | | 1.45 | | 1.45 | | 1.45 | |

*For vibrodriven piles, use one half of these k_p values.

(After Frank 2013 and Norme Francaise AFNOR P94-262)

- From Table 18.9, read the designation of the f_{soil} curve to be used (Q1 to Q5) as well as the α value and the maximum allowable value for f_{soil} called f_{lim} .
- Enter the proper curve on Figure 18.36a and read the value of f_{soil} corresponding to the value of the net limit pressure p_L^* defined as $p_L - \sigma_{oh}$ where p_L is the PMT limit pressure and σ_{oh} is the total horizontal stress at rest at the depth of the pressuremeter test that gave the value of p_L . The value of f_u to be used in Eq. 18.61 is

$$\text{given by: } f_u = \alpha f_{soil} \leq f_{lim} \quad (18.62)$$

- Repeat steps 1 through 4 to obtain the values of f_{ui} for all values of p_{Li}^* in the soil profile next to the pile.
- The value of p_u is given by:

$$p_u = k_p p_L^* \quad (18.63)$$

where p_L^* is the average net limit pressure within 1.5B below the pile point, and B is the pile point diameter or width.

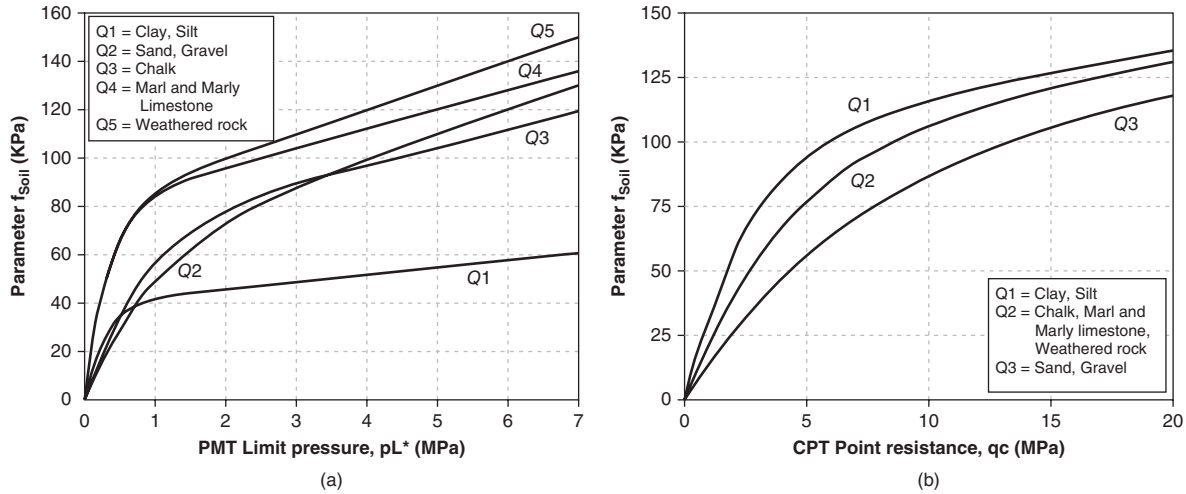


Figure 18.36 (a) Soil friction vs. PMT limit pressure curves and (b) vs. CPT point resistance curves. (After Frank 2013 and Norme Francaise AFNOR P94-262)

7. Obtain k_p for Eq. 18.63 from Table 18.10 and calculate p_u .
8. Calculate the ultimate vertical capacity R_u of the single pile according to Eq. 18.61.

LPC-CPT Method

The LPC-CPT method (Frank 1999, 2013; Norme Francaise AFNOR P94-262) was developed by the Laboratories des Ponts et Chaussées after 30 years of instrumented load testing of piles by Bustamante and his colleagues. It was developed in parallel with the LPC-PMT method as CPT soundings were performed at each load test site. It is not restricted to a pile type or a soil type. It makes recommendations of f_u and p_u for bored piles and driven piles and for fine-grained soils and coarse-grained soils. It is based on the point resistance of the cone penetrometer test (CPT). Although the CPT is a very popular test, which is becoming even more popular as time goes by, it is limited to soils that can be penetrated with a 200 kN truck to sufficient depth for pile design. The steps to follow for the LPC-CPT method are:

1. Classify the soil according to Table 18.8.
2. Identify the pile type on Table 18.11 and Table 18.12
3. From Table 18.11, read the designation of the f_{soil} curve to be used (Q1 to Q5) as well as the α value and the maximum allowable value for f_{soil} called f_{lim} .
4. Enter the proper curve on Figure 18.36b and read the value of f_{soil} corresponding to the value of the CPT point resistance q_c at the depth where f_u is required. The value of f_u to be used in Eq. 18.61 is given by:

$$f_u = \alpha f_{soil} \leq f_{lim} \quad (18.64)$$

where f_{lim} is the maximum permissible value of f_u .

5. Repeat steps 1 through 4 to obtain the values of f_{ui} for all values of q_c in the CPT sounding next to the pile.
6. The value of p_u is given by:

$$p_u = k_c q_c \quad (18.65)$$

where q_c is the average CPT point resistance within 1.5B below the pile point, and B is the pile point diameter or width and k_c a bearing capacity factor.

7. Obtain k_c for Eq. 18.65 from Table 18.12 and calculate p_u .
8. Calculate the ultimate vertical capacity R_u of the single pile according to Eq. 18.61.

FHWA Method for Bored Piles in Fine-Grained Soils

The FHWA method evolved from the initial recommendations of O'Neill and Reese (1999) and was modified by Brown et al. (2010). It gives the following recommendations for f_u and p_u :

From ground surface to depth of 1.5 m:

$$f_u = 0 \quad (18.66)$$

For the rest of the pile and $s_u < 150$ kPa:

$$f_u = 0.55s_u \quad (18.67)$$

For the rest of the pile and $150 < s_u < 250$ kPa:

$$f_u = \left(0.55 - 0.1 \left(\frac{s_u}{p_a} - 1.5 \right) \right) s_u \quad (18.68)$$

where s_u is the undrained shear strength of the soil at the depth where f_u is calculated.

$$p_u = N_c s_u \quad (18.69)$$

where N_c is 9 unless the bored pile has length-to-diameter ratio less than 3, in which case N_c is given by Figure 17.7 (see section 17.6.1), s_u is the undrained shear strength of the soil averaged over 2B below the point of the bored pile, and B is the pile point diameter.

FHWA Method for Bored Piles in Coarse-Grained Soil

This FHWA method also evolved from the initial recommendations of O'Neill and Reese (1999) and was modified by

Table 18.11 Choosing the Friction Parameters for LPC-CPT Method

| Friction curve | Clay, Silt | | Sand, Gravel | | Chalk | | Marl and Marly Limestone | | Weathered Rock | |
|----------------------------------|------------|-----------------|--------------|-----------------|----------|-----------------|--------------------------|-----------------|----------------|-----------------|
| | Q1 | | Q3 | | Q2 | | Q2 | | Q2 | |
| | α | f_{lim} (kPa) | α | f_{lim} (kPa) | α | f_{lim} (kPa) | α | f_{lim} (kPa) | α | f_{lim} (kPa) |
| Bored, dry | 0.55 | 90 | 0.7 | 90 | 0.8 | 200 | 1.4 | 170 | 1.5 | 200 |
| Bored, mud | 0.65 | 90 | 1.0 | 90 | 0.8 | 200 | 1.4 | 170 | 1.5 | 200 |
| Bored w. casing (left in place) | 0.35 | 50 | 0.4 | 50 | 0.25 | 50 | 0.85 | 90 | - | - |
| Bored w. casing (retrieved) | 0.65 | 90 | 1.0 | 90 | 0.75 | 170 | 0.13 | 170 | - | - |
| Driven concrete | 0.55 | 130 | 1.0 | 130 | 0.45 | 90 | 0.85 | 90 | - | - |
| Driven metal (closed end) | 0.4 | 90 | 0.85 | 90 | 0.2 | 50 | 0.85 | 90 | - | - |
| Driven metal (open end) | 0.6 | 90 | 0.5 | 50 | 0.25 | 50 | 0.95 | 90 | 0.95 | 90 |
| Driven H pile | 0.55 | 90 | 0.7 | 130 | 0.2 | 50 | 0.95 | 90 | 0.85 | 90 |
| Driven sheet pile | 0.45 | 90 | 0.55 | 90 | 0.2 | 50 | 1.25 | 50 | 1.15 | 90 |
| Micropiles (single injection) | 1.35 | 200 | 2.0 | 380 | 1.1 | 320 | 2.25 | 320 | 2.25 | 320 |
| Micropiles (repeated injections) | 1.7 | 200 | 2.65 | 440 | 1.4 | 440 | 2.9 | 440 | 2.9 | 500 |

(After Frank 2013, Norme Francaise AFNOR P94-262)

Table 18.12 Bearing Capacity Factor k_c for LPC-CPT Method

| | Clay, Silt | | Sand, Gravel | | Chalk | | Marl and Marly Limestone | | Weathered Rock | |
|----------------------------------|------------|--|--------------|--|-------|--|--------------------------|--|----------------|--|
| | | | | | | | | | | |
| Bored, dry | 0.4 | | 0.2 | | 0.3 | | 0.3 | | 0.3 | |
| Bored, mud | 0.4 | | 0.2 | | 0.3 | | 0.3 | | 0.3 | |
| Bored w. casing (left in place) | 0.4 | | 0.2 | | 0.3 | | 0.3 | | 0.3 | |
| Bored w. casing (retrieved) | 0.4 | | 0.2 | | 0.3 | | 0.3 | | 0.3 | |
| Driven concrete | 0.45 | | 0.4 | | 0.4 | | 0.4 | | 0.4 | |
| Driven metal (closed end) | 0.45 | | 0.4 | | 0.4 | | 0.4 | | 0.4 | |
| Driven metal (open end)* | 0.35 | | 0.25 | | 0.15 | | 0.15 | | 0.15 | |
| Driven H pile* | 0.4 | | 0.4 | | 0.35 | | 0.2 | | 0.20 | |
| Driven sheet pile* | 0.35 | | 0.15 | | 0.15 | | 0.15 | | 0.15 | |
| Micropiles (single injection) | 0.45 | | 0.2 | | 0.3 | | 0.3 | | 0.25 | |
| Micropiles (repeated injections) | 0.45 | | 0.2 | | 0.3 | | 0.3 | | 0.25 | |

*For vibrodriven piles, use one half of these k_c values.

(After Frank 2013, Norme Francaise AFNOR P94-262)

Brown et al. (2010). It gives the following recommendations for f_u and p_u :

$$f_u = K \tan \delta \sigma'_{ov} = \beta \sigma'_{ov} = (1 - \sin \varphi') \left(\frac{\sigma'_p}{\sigma'_{ov}} \right)^{\sin \varphi'} \tan \varphi' \sigma'_{ov} \quad (18.70)$$

where K is taken as the at-rest horizontal earth pressure coefficient, δ is taken as the effective stress friction angle φ' , σ'_{ov} is the vertical effective stress at rest in the soil at the depth where f_u is calculated, β is $K \tan \delta$, and σ'_p is

the effective stress preconsolidation pressure of the soil. The value of σ'_p can be estimated by:

$$\sigma'_p \text{ (kPa)} = 47(N_{60})^m \quad (\text{Mayne 2007a; 2007b}) \quad (18.71)$$

$$\sigma'_p \text{ (kPa)} = 15N_{60} \quad (\text{Kulhawy and Chen 2007}) \quad (18.72)$$

where N_{60} is the SPT blow per 0.3 m corrected for 60% of maximum energy, and m is 0.6 for clean quartz sands and 0.8 for silty sands and sandy silts. O'Neill and Reese (1999)

gave a value of β related to the depth z in meters at which f_u is calculated:

$$\beta = 1.5 - 0.244[z(\text{m})]^{0.5} \quad \text{with} \quad 0.25 \leq \beta \leq 1.2 \quad (18.73)$$

The FHWA 2010 method retained the previous recommendation for p_u as:

$$p_u (\text{kPa}) = 60N_{60} \quad (18.74)$$

where N_{60} is the SPT blow per 0.3 m corrected for 60% of maximum energy averaged over 2B below the point of the bored pile, with B being the pile point diameter.

API-RP2A Method for Driven Piles in Fine-Grained Soils

The API-RP2A method also evolved over the years and is now based on the work of Randolph and Murphy (1985). It gives the following recommendations for f_u and p_u :

$$f_u = \alpha s_u = 0.5 \left(\frac{s_u}{\sigma'_{ov}} \right)^{-0.5} s_u \quad \text{for} \quad \frac{s_u}{\sigma'_{ov}} \leq 1 \quad (18.75)$$

$$f_u = \alpha s_u = 0.5 \left(\frac{s_u}{\sigma'_{ov}} \right)^{-0.25} s_u \quad \text{for} \quad \frac{s_u}{\sigma'_{ov}} > 1 \quad (18.76)$$

where s_u is the undrained shear strength, and σ'_{ov} is the vertical effective stress at rest in the soil at the depth where f_u is calculated. Then p_u is obtained by:

$$p_u = 9s_u \quad (18.77)$$

Effective Stress Method for Driven Piles in Fine-Grained Soil

The effective stress method theoretically gives the long-term capacity of a pile in fine-grained soil because it uses the effective stress approach and the drained strength parameters of the soil. It is fundamentally correct, but the parameters that enter into the calculations are more difficult to obtain accurately than those for the total stress method (such as API-RP2A) for the same case. It appears that much precision is lost through adding steps and complexity in the calculations. At this time, it seems that simplicity wins over theoretical correctness. As research progresses, it is likely that theoretical correctness will prevail. Nevertheless, this method gives the following recommendations for f_u and p_u :

$$f_u = K \tan \delta \sigma'_{ov} = \beta \sigma'_{ov} \quad (18.78)$$

The problem is to obtain reliable and accurate values of β . The following values have been proposed (Jeanjean 2012):

$$\beta = (1 - \sin \varphi') OCR^{0.5} \tan \varphi' \quad (18.79)$$

where φ' is the effective stress friction angle of the soil, and OCR is the overconsolidation ratio (defined as the ratio of the preconsolidation pressure σ'_p over the vertical effective stress σ'_{ov}). Briaud and Tucker (1997) proposed the values shown in Table 18.13.

For the ultimate point pressure p_u , there is very little data available to make a recommendation, so one could use the ultimate bearing capacity of a shallow foundation. The

Table 18.13 Proposed Values of β for Clays

| Soil Type | β value |
|-------------------------------|---------------|
| Soft clays and soft silts | 0.2 to 0.25 |
| Medium clays and medium silts | 0.25 to 0.30 |
| Stiff clays and stiff silts | 0.3 to 0.35 |

(Briaud and Tucker 1997.)

following equation seems to fit the FHWA recommendations quite well (Hannigan et al. 1998).

For φ' between 25 and 40 degrees:

$$p_u = N_q \sigma'_{ov} = 400(\tan \varphi')^6 \sigma'_{ov} \quad (18.80)$$

API-RP2A Method for Driven Piles in Coarse-Grained Soils

The API-RP2A method gives the following recommendations for f_u and p_u :

$$f_u = K \tan \delta \sigma'_{ov} \quad (18.81)$$

where K is the horizontal earth pressure coefficient (taken as 0.8), δ is the friction angle of the pile soil interface, and σ'_{ov} is the vertical effective stress at rest in the soil at the depth where f_u is calculated. Then p_u is obtained by:

$$p_u = N_q \sigma'_{ov} \quad (18.82)$$

where N_q is the bearing capacity factor. Recommendations for δ and N_q are presented in Table 18.14.

Briaud-Tucker SPT Method for Driven Piles in Coarse-Grained Soils

This method (Briaud and Tucker 1984) was developed for sands and gravels, and for driven piles only. It makes use of the SPT blow count N and is based on a database of pile load tests that included measured residual loads in the piles at the end of driving and before load testing. The values of f_u and p_u are given by:

$$f_u (\text{kPa}) = 5 (N)^{0.7} \quad (18.83)$$

$$p_u (\text{kPa}) = 1000 (N)^{0.5} \quad (18.84)$$

where N is the SPT blow count (blows per 0.3 m). The database used to develop these equations was populated with uncorrected N values, but it seems logical to use N_{60} if the energy is measured or can be estimated during the SPT. Indeed, most of the data came from U.S. pile load tests where drill rigs generate about 60% of maximum energy on the average.

18.4.2 Miscellaneous Questions about the Ultimate Capacity of a Single Pile

Minimum Thickness of the Bearing Layer

A question about the minimum thickness of the bearing layer arises when the layer in which the point of the pile ends has a finite thickness and is underlain by a weaker layer. The

Table 18.14 Recommended Values of δ and N_q

| Soil Type | Density | Angle δ | Limiting Friction (kPa) | Bearing Factor N_q | Limiting Point Pressure (kPa) |
|-----------|------------|----------------|-------------------------|----------------------|-------------------------------|
| Sand | Very loose | 15 | 48 | 8 | 1900 |
| Sand-silt | Loose | | | | |
| Silt | Medium | | | | |
| Sand | Loose | 20 | 67 | 12 | 2900 |
| Sand-silt | Medium | | | | |
| Silt | Dense | | | | |
| Sand | Medium | 25 | 81 | 20 | 4800 |
| Sand-silt | Dense | | | | |
| Sand | Dense | 30 | 96 | 40 | 9600 |
| Sand-silt | Very dense | | | | |
| Gravel | Dense | 35 | 115 | 50 | 12000 |
| Sand | Very dense | | | | |

(API-RP 2A 2000.)

question is: How thick should the bearing layer be to generate the full p_u capacity of that layer? One of the important factors is the difference in strength between the bearing layer and the underlying layer. One of the best ways to answer this question is to perform a failure load analysis (see section 17.6.3). Short of that, and if the difference in strength between the bearing layer and the underlying layer is not extreme (say, less than 4 to 1), then a thickness to pile width ratio of more than 4 may be appropriate.

$$\frac{H}{B} > 4 \quad (18.85)$$

where H is the distance between the pile point location and the bottom of the bearing layer and B is the pile diameter or width. One very important observation is that at 4 times the pile width, the thickness of the bearing layer may sustain the capacity of a single pile—but the question is very different for a pile group.

Which Area to Consider for A_s and A_p in Equation 18.61

For solid piles such as bored piles and concrete or timber driven piles, and also for closed-end pipe piles, the issue is clear: The side area should be the pile perimeter times the pile segment length. The question arises in the case of open-end pipe piles and H piles. These piles may plug or not plug during driving and later on during loading. Whether the pile plugs or not depends on the soil type, the pile diameter, and the loading. Some piles may not plug during driving, but most common-size piles plug during subsequent slow loading. It is common practice to calculate the ultimate load R_u (plug) corresponding to a plugged condition on the one hand, and then R_u (unplug) corresponding to an unplugged condition on the other, and to take the minimum of the two as the failure load R_u . For an open-end pipe pile, the plugged condition would be the addition of the outside friction plus the point

capacity using the total area, whereas the unplugged condition would be the friction on the outside and the inside of the pile plus the point capacity on the thickness of the pipe wall.

$$\text{Plugged case} \quad R_{u(\text{plug})} = \sum f_{ui} \pi D \Delta L_i + p_u \frac{\pi D^2}{4} \quad (18.86)$$

$$\text{Unplugged case} \quad R_{u(\text{unplug})} = \sum 2f_{ui} \pi D \Delta L_i + p_u \pi D t \quad (18.87)$$

$$\text{Ultimate capacity} \quad R_u = \text{Min}(R_{u(\text{plug})}, R_{u(\text{unplug})}) \quad (18.88)$$

where D is the pile diameter, ΔL is the pile segment length, and t is the wall thickness. The recommendations in Table 18.15 are made by Frank 2013, Norme Francaise AFNOR P94-262.

Compression vs. Tension

An important thing to know is whether the friction in compression is the same as the friction in tension. One issue is

Table 18.15 Pile Areas to Be Used in Ultimate Capacity Calculations according to Frank (2013), Norme Francaise AFNOR P94-262

| | Point | Side |
|--|---------------------------|-------------------|
| Open-end pipe $D = \text{diameter}$ | $A_p = \frac{\pi D^2}{4}$ | $A_s = \pi DL$ |
| H pile $B = \text{width of flange}$ $W = \text{height of web}$ | $A_p = BW$ | $A_s = 2(B + W)L$ |

the Poisson's effect, which makes the pile expand laterally when in compression and contract laterally when in tension. This creates a lower lateral stress in tension than in compression, thereby leading to less friction capacity in tension than in compression. Counter to this is the fact that soil masses tend to relax and creep around piles and maintain horizontal stresses in the long term. This was measured by placing total stress pressure cells on driven piles and monitoring the horizontal pressure as a function of time (Briaud and Tucker 1989). Another problem is that the failure surface of the pile in compression may be different from the failure surface of the pile in tension. This was observed on 23 m long H piles in sand that had an ultimate load in friction-tension equal to one-half of the ultimate load in friction-compression (Briaud et al. 1984). The American Petroleum Institute recommends the same friction coefficient in compression and in tension for long pipe piles in clay and in sand. All in all, it appears that significantly different friction capacities in tension and in compression are the exception rather than the rule; however, they can exist and probably more so for short piles.

Should I Add γd or Not Add γd to the Expression Giving p_u ?

The question about adding γd is related to the following two expressions:

$$p_u = ks \quad (18.89)$$

$$p_u = ks + \gamma d \quad (18.90)$$

where p_u is the ultimate point pressure, k is a bearing capacity factor, s is a soil strength measurement (CPT q_c , PMT p_L , SPT N , undrained shear strength s_u), γ is the soil unit weight, and d is the depth of the foundation below the nearby ground surface. The answer is that at the level of the foundation, the actual p_u value is given by Eq. 18.90. Thus, if Eq. 18.90 is used, then the weight of the foundation must be included on the load side of the ultimate limit state equation. If it is assumed that the pressure exerted by the weight of the foundation plus backfilling is equal to the pressure of the overburden on each side of the foundation, then the two cancel out and the term γd can be ignored. Generally, it is best to add γd and include the weight of the foundation on the load side, especially in more complex cases where the cancellation may not apply.

What about Buoyancy when the Foundation Is Under Water?

The problem of buoyancy is again associated with the term γd or the vertical total stress at the depth of the foundation σ_{ov} . If the total weight of the foundation is W and the water pressure under the foundation is u_w , applied over the bottom surface A_p of the foundation, the buoyant weight is $W' = W - u_w A_p$. The point resistance $p_u A_p$ contains the term $\gamma d A_p$ (or better,

$\sigma_{ov} A_p$) and therefore includes the buoyancy force of the foundation. Indeed, $\sigma_{ov} A_p$ is the sum of $\sigma'_{ov} A_p$ and $u_w A_p$, which is the buoyancy force. So there are two alternatives:

1. Use the buoyant weight W' of the pile and then use $\sigma'_{ov} A_p$.
2. Use the total weight W of the pile and then use $\sigma_{ov} A_p$.

It is usually best to use the total weight and the total vertical stress at the foundation level.

Rate of Loading Effect

Soils are somewhat viscous, so if the rate of loading or straining is not changed much, the difference in the pile ultimate capacity can be neglected. If, however, there is a drastic change in loading rate or strain rate, then the difference must be included in the calculations. For example, most of the calculation methods presented in section 18.4.1 are based on load test databases where the pile was pushed to large displacements in several hours. However, under a building or a bridge, the pile will experience the load for the design life of the structure, which may be 75 years, for example. In contrast, the rise time of a hurricane wave against an offshore structure may be only 3 seconds. In these two cases, the ultimate capacity would be significantly affected. The model used for the undrained shear strength of saturated clays (see section 15.8) is extended to pile capacities (Briaud and Garland 1985):

$$\frac{R_{u1}}{R_{u2}} = \left(\frac{t_1}{t_2} \right)^{-n} \quad (18.91)$$

where R_{u1} is the ultimate pile resistance when loaded to failure in a time t_1 and R_{u2} is the ultimate pile resistance when loaded to failure in a time t_2 . Values of the viscous exponent n vary from 0.01 to 0.03 for sand and from 0.02 to 0.08 for clays (see Figure 15.18). So, if a pile has a capacity of 1000 kN according to usual methods associated with load tests averaging 3 hours, and if that pile is loaded in 3 s by a hurricane wave, then the load will be such that:

$$\frac{R_{u1}}{1000} = \left(\frac{3}{3 \times 3600} \right)^{-0.05} = 1.5 \quad (18.92)$$

The capacity R_{u1} of the pile during the hurricane is 50% larger than the capacity calculated by conventional methods. However, if Eq. 18.91 is applied to long-term loading under a 75-year-old building, the capacity becomes:

$$\frac{R_{u1}}{1000} = \left(\frac{75 \times 365 \times 24}{3} \right)^{-0.05} = 0.54 \quad (18.93)$$

The capacity R_{u1} of the pile after 75 years would be 50% smaller than the capacity calculated by conventional methods. The data upon which Eq. 18.91 is based are mostly populated with tests done in less than 3 hours; therefore, using this model for the long-term capacity of piles is not based on data.

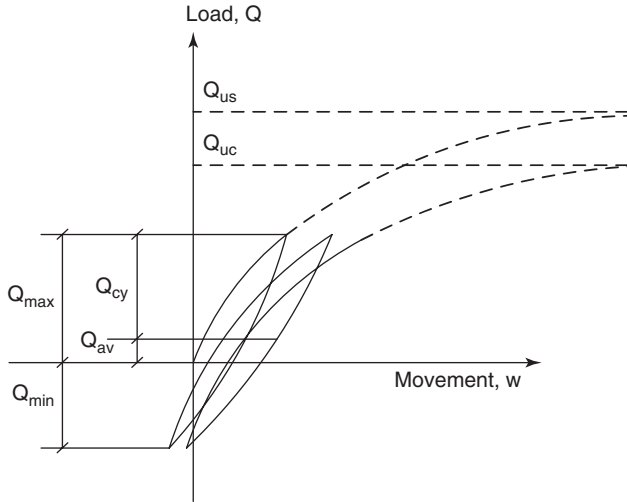


Figure 18.37 Cyclic loading of piles.

Cyclic Loading Effect

Soils are sensitive to cyclic loading and tend to weaken with the accumulation of cycles. Figure 18.37 shows the load settlement curve for a pile subjected to cyclic loading. Two main parameters are defined: the cyclic amplitude ratio R_{cy} and the average load ratio R_{av} :

$$R_{cy} = \frac{Q_{max} - Q_{min}}{2Q_{us}} \quad \text{and} \quad R_{av} = \frac{Q_{max} + Q_{min}}{2Q_{us}} \quad (18.94)$$

where Q_{us} is the vertical ultimate capacity of the pile under static monotonic loading, and Q_{max} and Q_{min} are the maximum and minimum load applied respectively during cyclic loading. The ultimate cyclic capacity Q_{uc} is the maximum load that can be reached when performing a monotonic test to

failure at the end of the cycles. Note also that Q_{cy} and Q_{av} are the cyclic load amplitude and the average load respectively. If a test reaches failure after N cycles, then Q_{uc} is equal to Q_{max} for N cycles. If the load does not change direction during loading (always compression, for example), it is called *one-way cyclic loading*. If it does change direction (compression to tension, for example), it is called *two-way cyclic loading*. The most severe loading seems to be symmetrical two-way cyclic loading where R_{av} is equal to zero.

Studies have been performed and recommendations made to quantify the influence of R_{cy} and R_{av} on the ratio Q_{uc}/Q_{us} . One of them is the work of Karlsrud et al. (1986) at NGI. The results, shown in Figure 18.38, indicate that for these tests and for full reversal of load ($Q_{av} = 0$), the cyclic capacity Q_{uc} is 35 to 50% of the static capacity Q_{us} depending on the number of cycles to failure.

Briaud and Felio (1986) studied the impact of cyclic vertical loading on the response of piles by quantifying the increase in vertical movement as a function of the number of cycles. After collecting a database of 16 studies on cyclic full-scale pile load tests and 10 studies on model pile load tests, they used the following power law model:

$$\frac{s(N)}{s(1)} = N^a \quad (18.95)$$

where $s(N)$ and $s(1)$ are the movement of the pile top for the N th and first cycle respectively, N is the cycle number, and a is the cyclic exponent. Figure 18.38 shows the range of a values obtained as a function of the cyclic load ratio Q_{max}/Q_{us} .

Prediction Method vs. Design Method

A distinction should be made between a prediction method and a design method (Figure 18.39). The goal of a prediction

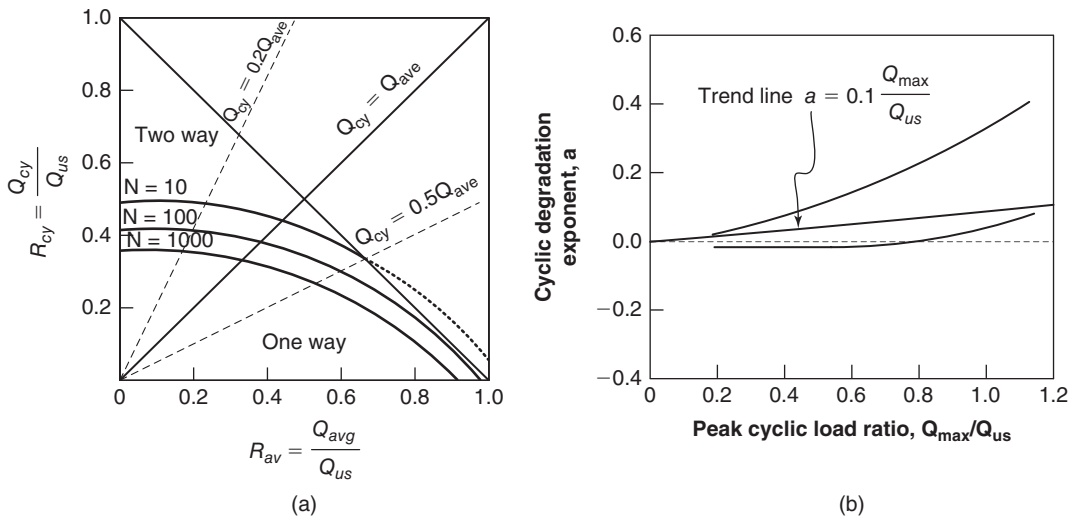


Figure 18.38 Results of two studies on cyclic loading of piles in clays: (a) Karlsrud et al. (1986). (b) Briaud and Felio (1986).

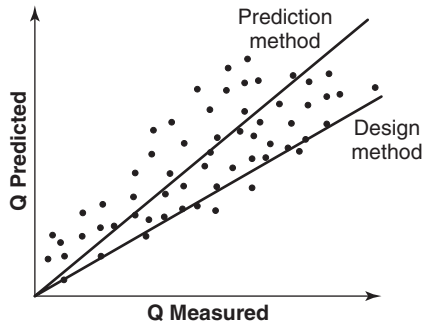


Figure 18.39 Difference between a prediction method and a design method.

method is for the calculated value to be as close as possible to the measured value on the average. The goal of a design method is to minimize the number of times the calculated value is unsafe. This is a big difference, and for ultimate pile capacity a design method will tend to give lower values than a prediction method. This also brings into play the issue of precision versus accuracy. An *accurate method* is a method that gives the right answer on the average. A *precise method* is a method that exhibits very little scatter around the mean. A precise and accurate method is a method that gives the right answer on the average with very little scatter around the mean; that is, very little uncertainty. An inaccurate but precise method is more desirable than an imprecise but accurate method. Indeed, it is easier to apply a calibration factor to the mean value of an inaccurate but precise method than to reduce the scatter of an imprecise but accurate method.

Resistance Factor

To use the LRFD approach, one must have the load factors γ and resistance factors ϕ in Eq. 18.3. These factors are given in the codes or guidelines specific to each method. For the load factors γ , see Table 17.1. For the resistance

factors, some methods make a distinction between the side friction resistance factor ϕ_f and the point resistance factor ϕ_p . Some methods use one global resistance factor ϕ . Table 18.16 shows suggested ranges of global resistance factors as collected from various sources.

Length Effect on Ultimate Capacity

The length of the pile may have an effect on the pile capacity. This is particularly clear when the soil is overconsolidated and the pile is long. Here is why. Overconsolidated soils exhibit a peak shear strength followed by a lower to much lower residual shear strength. Long piles, when loaded, exhibit much more movement at the pile top than at the pile point because of the elastic compression of the pile (same in tension). At ultimate load, the displacement at the pile top will be large enough to be on the residual part of the strength curve while, at the pile point, the displacement will just reach the peak strength. As a result, the ultimate load will be lower than the one obtained by using the peak shear strength all along the pile for obtaining f_u . The best way to quantify the influence of pile length on ultimate load is to use a settlement analysis at large displacement. This topic is covered in section 18.4.3.

18.4.3 Settlement of a Single Pile

The settlement of the top of a pile s_{top} is equal to the settlement of the point of the pile s_{point} plus the compression of the pile:

$$s_{top} = s_{point} + \frac{PL}{A_{cs}E_p} \tag{18.96}$$

where P is the average load in the loaded portion of the pile, L is the length of pile under load, A_{cs} is the pile cross section, and E_p is the modulus of elasticity of the pile material. The load in the pile is Q_{top} at the top and Q_{point} at the point

Table 18.16 Estimated Resistance Factor ϕ for Ultimate Limit State in Pile Design

| | Bored Piles | | Driven Piles | |
|----------------------|----------------|--------------------------|--------------------------|--------------------------|
| | Method | Resistance factor ϕ | Method | Resistance factor ϕ |
| Fine-grained soils | LPC-PMT method | 0.5 to 0.6 | LPC-PMT method | 0.5 to 0.6 |
| | LPC-CPT method | 0.5 to 0.6 | LPC-CPT method | 0.5 to 0.6 |
| | FHWA, 2010 | 0.35 to 0.45 | API RP2A | 0.6 to 0.7 |
| | | | Effective stress method | 0.3 to 0.4 |
| Coarse-grained soils | LPC-PMT method | 0.5 to 0.6 | LPC-PMT method | 0.5 to 0.6 |
| | LPC-CPT method | 0.5 to 0.6 | LPC-CPT method | 0.5 to 0.6 |
| | FHWA, 2010 | 0.45 to 0.55 | API RP2A | 0.6 to 0.7 |
| | | | Briaud-Tucker SPT method | 0.35 to 0.45 |

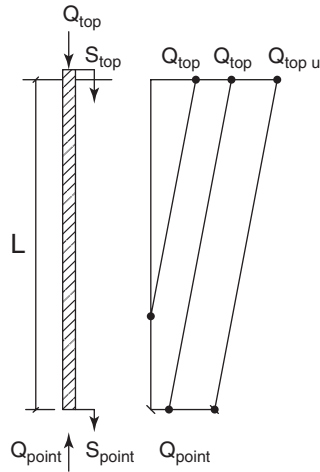


Figure 18.40 Load distribution in the pile.

(Figure 18.40). If the friction is constant between the top and the point of the pile, Eq. 18.96 becomes:

$$s_{top} = s_{point} + \frac{(Q_{top} + Q_{point})L}{2A_{cs}E_p} \quad (18.97)$$

As a preliminary estimate, $(Q_{top} + Q_{point})/2$ is often taken as $0.6Q_{top}$. Of course this is an estimated average. For friction piles where most of the pile capacity comes from the side friction, $0.6Q_{top}$ would likely be larger than the true average load, and in fact L is likely not the total length of the pile, as the load becomes zero along the pile length. For an end-bearing pile, though, $0.6Q_{top}$ may be too small, as much of the load is carried in point resistance. The settlement s_{point} is related to the load at the point through a load transfer curve that can be idealized as an elastic, perfectly plastic curve (Figure 18.41). The slope of the elastic part is a spring constant k_p such that:

$$Q_{point} = k_p s_{point} \quad (18.98)$$

Then Eq. 18.97 becomes:

$$s_{top} = \frac{Q_{point}}{k_p} + \frac{(Q_{top} + Q_{point})L}{2A_{cs}E_p} \quad (18.99)$$

The spring constant k_p has been related to the modulus of the soil under the point through theory. The relationship for a closed-end circular pile (Randolph and Wroth 1978) is:

$$Q_{point} = k_p s_{point} = \left(\frac{DE_s}{1-\nu^2} \right) s_{point} \quad (18.100)$$

where D is the diameter of the pile point, and E_s and ν are the modulus and the Poisson's ratio of the soil below the pile point. In terms of pressure p under the pile point, the equation becomes:

$$p = \frac{4E_s}{\pi D(1-\nu^2)} s_{point} \quad (18.101)$$

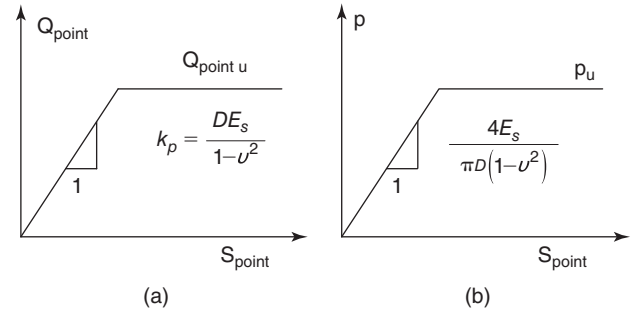


Figure 18.41 Point load transfer curve model.

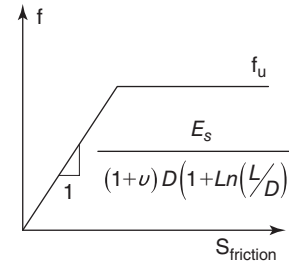


Figure 18.42 Friction load transfer curve model.

The friction load transfer curve can also be represented by an elastic, perfectly plastic curve (Figure 18.42). The slope of the elastic part of the friction transfer curve (Frank, Zhao 1982) is given by:

$$f = \frac{E_s}{(1+\nu)(1+Ln(L/D))D} s_{friction} \quad (18.102)$$

where f is the friction stress at the interface between the pile and the soil, E_s and ν are the soil modulus and the Poisson's ratio at depth z where the friction is generated, L is the embedded pile length, D is the pile diameter, and $s_{friction}$ is the downward movement of the pile at depth z .

We still do not know what the load distribution is in the pile for a given load at the top. Solving this problem requires a load transfer curve analysis, which is best explained through an example (Figure 18.43).

A 0.3 m diameter closed-end pipe pile with a 5 mm thick wall is driven 10 m below the ground surface. The steel has a modulus of 2×10^8 kPa. The soil is made of 9 m of a soft clay underlain by a thick layer of dense sand. The modulus of the soft clay is 5×10^3 kPa, and the modulus of the sand layer is 10^5 kPa. The drained Poisson's ratio is 0.35 for both soils. The ultimate friction f_u in the soft clay at the pile-soil interface is 20 kPa, and in the dense sand f_u is 80 kPa. The ultimate point pressure under the pile point in the dense sand is 10,000 kPa.

1. Divide the pile into a number of elements. We would typically use a minimum of 10 elements for the computer solution. For this hand calculation, we will use only 3 elements, as shown in Figure 18.43.

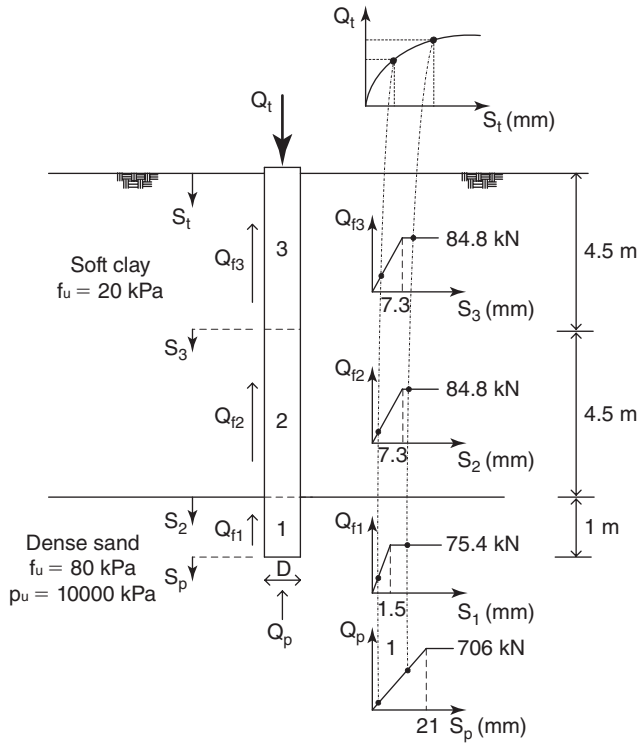


Figure 18.43 Pile problem and load transfer curves.

- Prepare the load transfer curves for each element: three friction curves for elements 1, 2, and 3 and one point curve under element 1. To prepare these curves, the elastic slopes of Eqs. 18.101 and 18.102 are used together with the ultimate values of f_u and p_u . These curves are shown in Figure 18.43.
- Assume a point movement of 1 mm and calculate the point load corresponding to that movement using Eq. 18.100:

$$Q_{point} = \left(\frac{0.3 \times 100000}{1 - 0.35^2} \right) \times 0.001 = 34.2 \text{ kN} \quad (18.103)$$

This corresponds to point 1 on the point load transfer curve in Figure 18.43.

- Evaluate the friction f_1 mobilized in element 1 by reading the friction transfer curve for a movement of 1 mm (Eq. 18.102):

$$f_1 = \frac{100000}{(1 + 0.35)(1 + Ln(10/0.3))0.3} \times 0.001 = 54.8 \text{ kPa} < 80 \text{ kPa} \quad (18.104)$$

More correctly speaking, we should first calculate the movement at the midpoint in element 1 and then use that movement to obtain the friction value from the transfer curve. This would require an iteration. For simplicity in these hand calculations, we will use the

movement at the bottom of the element to obtain the friction value in that element.

- Calculate the load carried in friction in element 1:

$$Q_{friction1} = f_1 \pi D \Delta L_1 = 54.8 \times 3.14 \times 0.3 \times 4.5 = 51.6 \text{ kN} \quad (18.105)$$

- Calculate the movement at the bottom of element 2:

$$s_2 = s_{point} + \frac{\left(Q_p + \frac{Q_{f1}}{2} \right) \Delta L_1}{A_{cs} E_p} = 1 + \frac{(34.2 + \frac{51.6}{2}) 1000}{3.14 \times 0.3 \times 0.005 \times 2 \times 10^8} = 1.063 \text{ mm} \quad (18.106)$$

- Evaluate the friction f_2 mobilized in element 2 by reading the friction transfer curve for the movement s_2 (Eq. 18.102):

$$f_2 = \frac{5000}{(1 + 0.35)(1 + Ln(10/0.3))0.3} \times 0.001063 = 2.91 \text{ kPa} < 20 \text{ kPa} \quad (18.107)$$

- Calculate the load carried in friction in element 2:

$$Q_{friction2} = f_2 \pi D \Delta L_2 = 2.91 \times 3.14 \times 0.3 \times 4.5 = 12.3 \text{ kN} \quad (18.108)$$

- Calculate the movement at the bottom of element 3:

$$s_3 = s_2 + \frac{\left(Q_p + Q_{f1} + \frac{Q_{f2}}{2} \right) \Delta L_2}{A_{cs} E_p} = 1.063 + \frac{(34.2 + 51.6 + \frac{12.3}{2}) 4500}{3.14 \times 0.3 \times 0.005 \times 2 \times 10^8} = 1.502 \text{ mm} \quad (18.109)$$

- Evaluate the friction f_3 mobilized in element 3 by reading the friction transfer curve for the movement s_3 (Eq. 18.102):

$$f_3 = \frac{5000}{(1 + 0.35)(1 + Ln(10/0.3))0.3} \times 0.001439 = 3.94 \text{ kPa} < 20 \text{ kPa} \quad (18.110)$$

- Calculate the load carried in friction in element 3:

$$Q_{friction3} = f_3 \pi D \Delta L_3 = 3.94 \times 3.14 \times 0.3 \times 4.5 = 16.7 \text{ kN} \quad (18.111)$$

12. Calculate the movement at the top of element 3:

$$\begin{aligned} s_{top} &= s_3 + \frac{(Q_p + Q_{f1} + Q_{f2} + \frac{Q_{f3}}{2}) \Delta L_3}{A_{cs} E_p} \\ &= 1.502 + \frac{(34.2 + 51.6 + 12.3 + \frac{16.7}{2}) 4500}{3.14 \times 0.3 \times 0.005 \times 2 \times 10^8} \\ &= 2.01 \text{ mm} \end{aligned} \quad (18.112)$$

13. Calculate the load at the top of the pile:

$$\begin{aligned} Q_{top} &= Q_p + Q_{f1} + Q_{f2} + Q_{f3} \\ &= 34.2 + 51.6 + 12.3 + 16.7 = 114.8 \text{ kN} \end{aligned} \quad (18.113)$$

14. Now we have a point on the top load versus top movement curve for the vertically loaded pile. A second point can be generated by going back to step 3 and assuming a point movement of, say, 2 mm and repeating steps 3 to 13 to get the corresponding values of Q_{top} and s_{top} . Point by point, the load settlement curve for the pile is generated in this fashion.

Note that typically it takes very little displacement to mobilize the ultimate friction, whereas it takes more displacement to mobilize the ultimate point resistance. The displacement associated with full friction mobilization is often estimated to be 2.5 mm, while the displacement associated with full point resistance mobilization can be 10 mm or more.

18.5 VERTICAL LOAD: PILE GROUP

Piles are often installed in groups (Figure 18.45) to carry higher loads under columns of buildings, bridges, dams, and other structures. Again the questions of ultimate resistance and settlement arise.

18.5.1 Ultimate Vertical Capacity of a Pile Group

What we want to know is if a group of n piles, each having an isolated ultimate capacity R_{us} , will have an ultimate capacity of n times R_{us} . The first estimate of R_{ug} for the group can be written as:

$$R_{ug} = enR_{us} \quad (18.114)$$

where R_{ug} is the ultimate capacity of the pile group, e is the efficiency of the pile group, n is the number of piles in the group, and R_{us} is the ultimate capacity of one pile. The efficiency e of the group may be smaller than 1, but sometimes is larger than 1. Two cases are identified: sand and clay.

Sand

For sand, a further distinction is made between bored piles and driven piles. For bored piles, the current AASHTO recommendation (2010) is to use efficiencies as follows:

$$\text{Bored pile groups in sand } e = 0.67 \text{ for } s/B = 2.5 \quad (18.115)$$

$$\text{Bored pile groups in sand } e = 1.0 \text{ for } s/B > 4 \quad (18.116)$$

where e is the group efficiency, s is the center-to-center pile spacing, and B is the pile diameter. For values of s/B between 2.5 and 4, extrapolation is used. For driven pile groups in sand, it is reasonable to think that the efficiency depends on the relative density of the sand. In loose sands, driving piles in a group would densify the sand more than driving a single pile would. Thus, the efficiency of a driven pile group in loose sand should be higher than 1. In very dense sand, however, the pile driving could not make the sand any denser, so the efficiency of the driven pile group would not be enhanced.

A large-scale experiment was performed to check if the efficiency of driven pile groups in loose sand was larger than 1 (Briaud et al. 1989). A five-pile group was driven in place, as was a separate reference single pile (Figure 18.44). The piles were closed-end steel pipe piles with a diameter of 0.273 m, an embedded length of 9.15 m, and a wall thickness of 9.3 mm. The soil was a clean, fine sand hydraulic fill with the following properties: dry unit weight 15.7 kN/m³, water content 23%, friction angle 35.4°, SPT blow count 15 blows per 0.3 m, CPT point resistance averaging 6200 kPa, and a PMT limit pressure averaging 500 kPa. The piles were instrumented with strain gages to obtain the residual load due to driving and (separately) the load carried in friction and in point resistance during load testing. The single pile and the pile group were load tested (pushed) to a penetration of 40 mm and exhibited plunging failure. At that penetration the single pile carried an ultimate load of 505 kN and the pile group an ultimate load of 2499 kN for an efficiency of 0.99. However, it is interesting to note that although the top load was the same for the single pile and each pile in the group, the distribution of point load and friction load was quite different. The ultimate point load was 360 kN for the single pile and 240 kN per pile in the group, leading to a point efficiency of 0.67. The ultimate load carried in friction was 150 kN for the single pile and 270 kN per pile in the group, leading to a friction efficiency of 1.8. The significant difference in point load between the single pile and the piles in the group was attributed to the difference in residual stresses. When a single pile is driven, it locks in a residual point load. Driving additional piles in the group next to the first pile releases the residual point load and decreases its beneficial effect. The significant difference in friction load between the single pile and the piles in the group was attributed to the difference in horizontal stresses. When a single pile is driven, it generates a certain horizontal stress. Driving additional piles in the group next to the first pile increases the horizontal stresses and therefore the pile friction. Based on these results, it may be best to write the efficiency equation for a pile group as:

$$R_{ug} = n(e_f R_{ufs} + e_p R_{ups}) \quad (18.117)$$

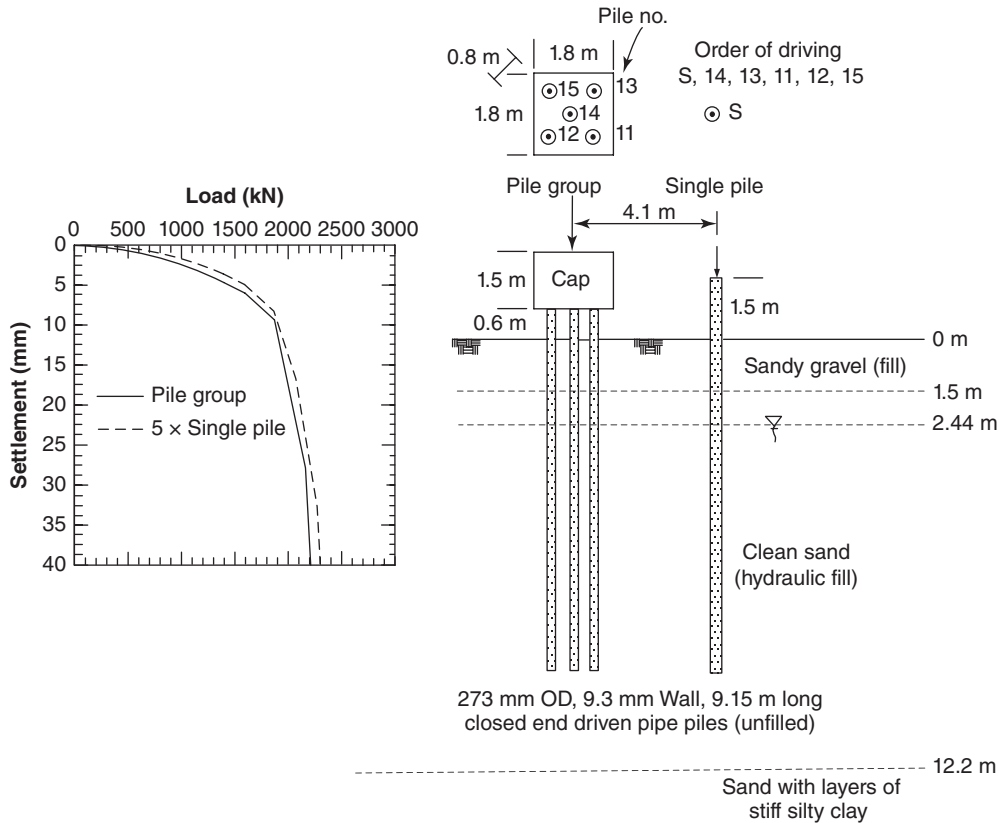


Figure 18.44 Pile group load test and results.

where R_{ug} is the ultimate capacity of the pile group, n is the number of piles in the group, e_f and e_p are the efficiencies of the pile group in friction and in point resistance respectively, and R_{ufs} and R_{ups} are the ultimate capacity of one pile in friction and in point resistance respectively. The pile group load test just described suggests e_f and e_p values of 0.67 and 1.8 respectively. In the case history just described, the increase in friction balanced the decrease in point resistance perfectly. Shorter piles that rely more on point resistance would have global efficiencies e lower than 1, and longer piles that rely more on friction resistance would have global efficiencies e higher than 1. In the absence of further evidence, it is suggested that the efficiency of driven piles in loose sand be taken as 1.

Clay

For clay, the group efficiency can be taken as 1, but it is very important also to check a second failure mechanism called *block failure*. This mechanism corresponds to the case where the pile group fails as a block, as shown in Figures 18.45 and 18.46. The ultimate capacity of the block is given by:

$$\begin{aligned}
 R_{ublock} &= R_{ublock}(friction) + R_{ublock}(point) \\
 &= 2(B_g + L_g)Df_u + B_gL_gP_u \quad (18.118)
 \end{aligned}$$

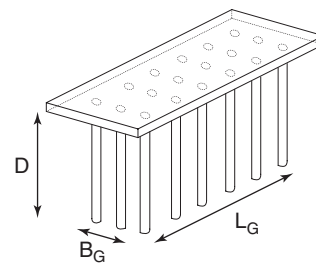


Figure 18.45 Pile group: (a) Closely spaced slender piles. (b) Strong layer not thick enough.

where the ultimate friction f_u is taken as the undrained shear strength s_u because the shearing will take place mostly in the clay, and p_u is $N_c s_u$ with N_c being obtained from the Skempton chart (see Figure 17.7). Note that for the single pile, N_c is likely equal to 9, because the relative embedment of the single pile, D/B , is often larger than 4; for the group, the relative embedment is much smaller, as it is equal to D/B_g . The ultimate capacity of the pile group is then the smaller of:

$$R_{ug} = \text{Min}(nR_{us}, R_{ublock}) \quad (18.119)$$

There are two cases in which R_{ublock} will be the smaller of the two (Figure 18.46). The first case is when the center-to-center pile spacing is small (say, 3 or less) and the piles are

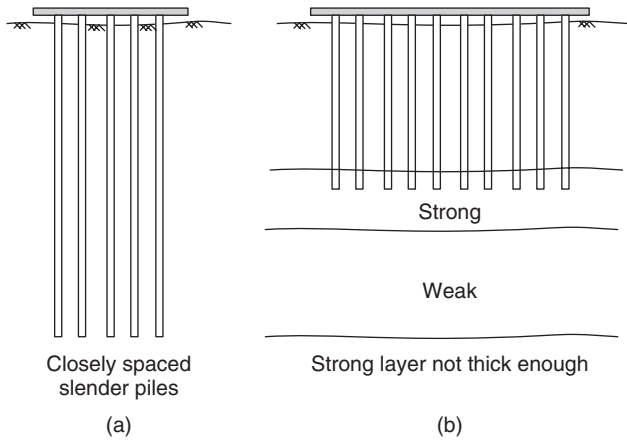


Figure 18.46 Cases where block failure is likely to control.

long and slender (say, $D/B > 30$). The second case is when the pile point is in a strong layer that gives a high single-pile ultimate capacity but is not thick enough to prevent the pile group from punching through into a weaker layer below. In this case the R_{us} (point) would involve the strength of the strong layer, whereas the R_{ublock} (point) would involve the strength of the weak layer below.

18.5.2 Settlement of Pile Groups

The settlement of a pile group can be much larger than the settlement of a single pile. The major difference is the increase in the depth of influence under the pile group compared to the single pile (Figure 18.47) and the accumulation of load effect from all the piles. Many empirical equations have been proposed to relate the settlement of the group s_g to the settlement of the single pile s_s . The following one is recommended by O'Neill (1983):

$$\frac{s_g}{s_s} = \sqrt{\frac{B_g}{B_s}} \tag{18.120}$$

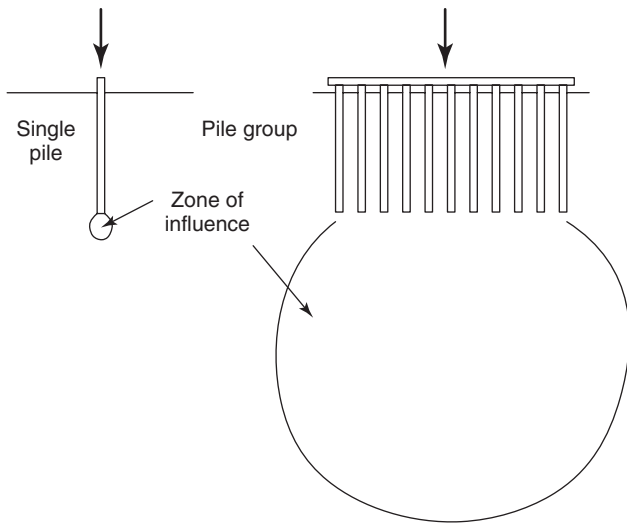


Figure 18.47 Difference in zone of influence between single pile and pile group.

where s_s is the settlement of the single pile under the working load Q , s_g is the settlement of the group under nQ , n is the number of piles in the group, B_g is the width of the group, and B_s is the width of the single pile. This equation indicates that the settlement of the group does not increase linearly with B_g but rather with the square root of B_g . This is corroborated by limited data (O'Neill 1983).

For large groups of piles in a uniform soil deposit, Terzaghi proposed to calculate the settlement of the group by considering that the group was equivalent to a spread footing having the dimensions B_g by L_g and located at a depth equal to $2/3$ of the pile embedded depth (Figure 18.48). If the piles penetrated through a weak layer into a strong layer (end-bearing piles), the equivalent footing is placed on top of the strong layer. If the penetration into the strong layer is significant, then the $2/3$ rule would apply to the strong layer (Figure 18.48). Note that such an approach gives a linear increase of s_g with B_g which is more severe than Eq. 18.120. The Terzaghi approach has been found to be conservative in some cases.

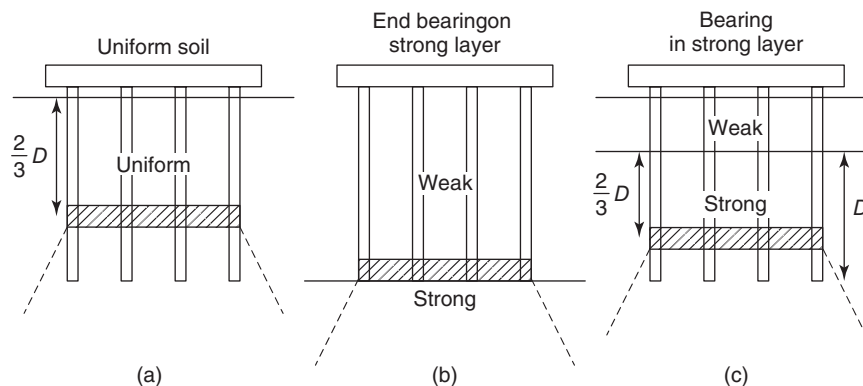


Figure 18.48 Terzaghi equivalent footing approach.

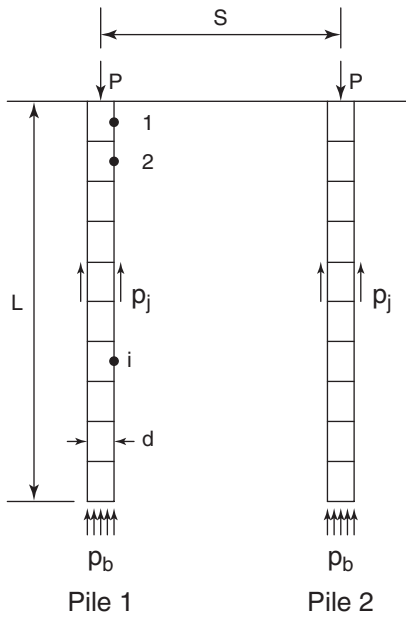


Figure 18.49 Influence of one pile on the other. (After Poulos and Davis, 1980)

A third approach to calculating the settlement of a pile group is to use a computer program that solves the problem of superposition of displacements induced by all piles (Poulos and Davis 1980). This is called the *interaction factor method*. Each pile stresses the soil surrounding it; therefore, each pile contributes to the global settlement at any other point. Each pile is first discretized as n pile elements versus depth (Figure 18.49). For a group of two identical and equally loaded piles, the movement of any node on pile 1 is given by:

$$[\rho_s] = \frac{d}{E_s} [I_1 + I_2][f] \quad (18.121)$$

where $[\rho_s]$ is the vector of the displacements at all nodes i (1 to n) of pile 1 (same as pile 2), d is the pile diameter, E_s is the soil modulus, $[f]$ is the vector of shear stresses at all nodes

j (1 to n) of pile 1 (same as pile 2), $[I_1 + I_2]$ is the $n + 1$ by $n + 1$ matrix ($n + 1$ because there are n friction elements and 1 point) of displacement influence factors containing elements I_{1ij} and I_{2ij} , and I_{1ij} and I_{2ij} are the displacement influence factors at element i on pile 1 caused by shear stress (friction) on element j of piles 1 and 2 respectively. These factors are obtained by integration of the Mindlin equation (1936). Note that the solution for pile 2 is the same, because the two piles are identical and equally loaded.

Of particular interest is the displacement at the top of one of the piles. By setting this displacement equal to 1, the distribution of shear stresses along the piles can be generated by solving Eq. 18.121. The interaction factor α is defined as:

$$\alpha = \frac{\text{additional settlement due to adjacent pile}}{\text{settlement of pile under its own load}} \quad (18.122)$$

Figure 18.50 shows the range of expected values for the interaction factor depending on the spacing between piles, the slenderness of the pile, and the relative stiffness between the pile and the soil.

In the general case of n identical piles, the settlement of pile k can be expressed as:

$$\rho_k = \rho_1 \sum_{\substack{j=1 \\ j \neq k}}^n (P_j \alpha_{kj}) + \rho_1 P_k \quad (18.123)$$

where ρ_k is the settlement of pile k , ρ_1 is the settlement of a single pile under a unit load, P_j is the load at the top of pile j , and α_{kj} is the interaction factor for spacing between piles k and j . Equation 18.123 can be written for all piles in the group, giving n equations. In addition, the load on the group can be written as:

$$P_G = \sum_{j=1}^n P_j \quad (18.124)$$

The $n + 1$ equations thus assembled can be solved for the boundary conditions imposed by the pile cap. Two simple conditions exist:

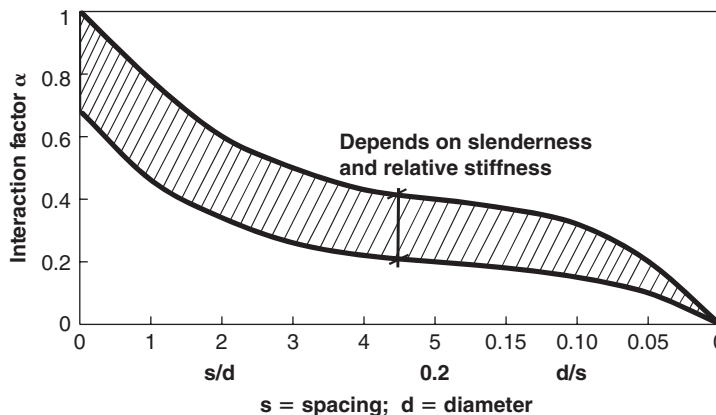


Figure 18.50 Interaction factor as a function of pile spacing. (After Poulos and Davis 1980)

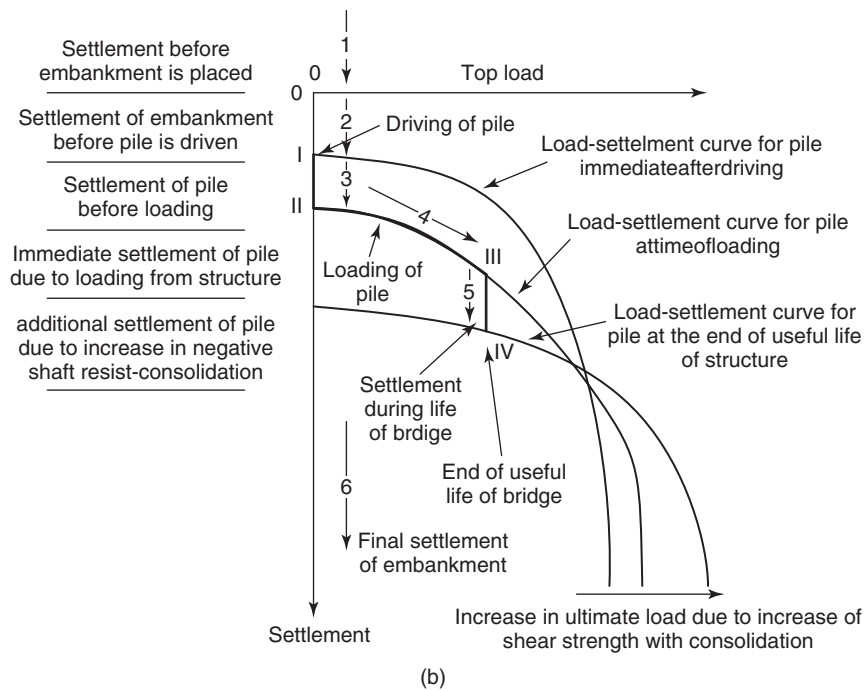
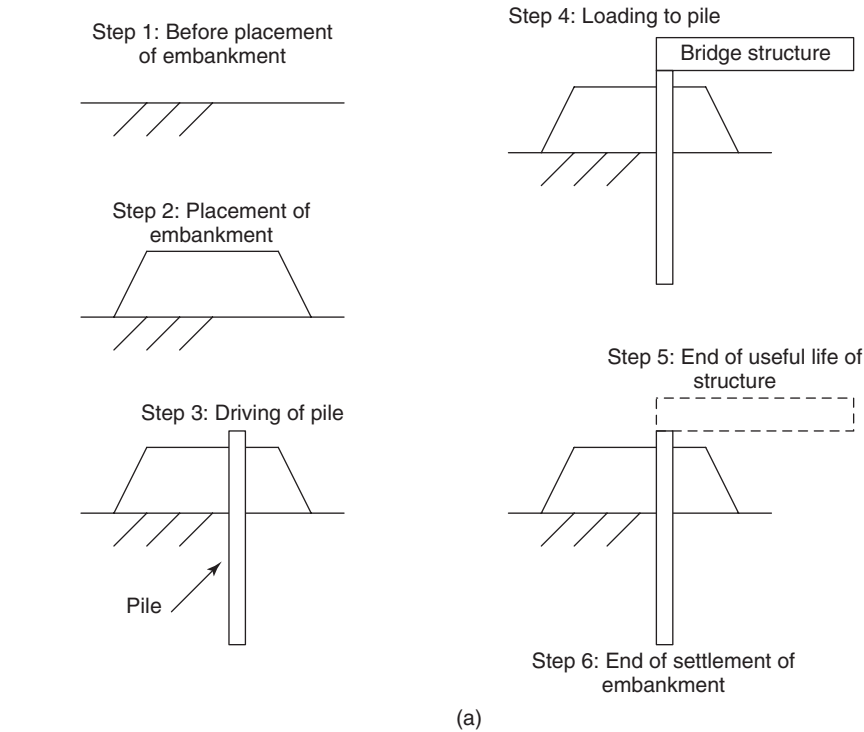


Figure 18.51 Construction sequence and settlement path for a case of downdrag: (a) Construction sequence. (b) Settlement path.

1. Equal load on all piles (perfectly flexible pile cap)
2. Equal settlement of all piles (perfectly rigid pile cap)

The program DEFPIG (Poulos 2012) automates these calculations. Other programs based on somewhat different

approaches include PIGLET (Randolph 1980) and FLPIER (Hoit et al. 1997). Of course it is now possible to use the general finite element method to model a group of piles and the surrounding soil in three dimensions and with nonlinear soil behavior.

18.6 DOWNDRAG

18.6.1 Definition and Behavior

In the normal case, the loaded pile moves down more than the soil surrounding it. *Downdrag* refers to the special case where the soil around the upper part of the pile moves downward more than the pile. This occurs, for example, when a pile is driven through a compressible layer into a stronger layer, and then an embankment is placed on the compressible layer, creating significant settlement of the ground surface. A construction sequence leading to downdrag and the associated settlement path are shown in Figure 18.51. Table 18.17 gives some clues indicating when downdrag might occur. A guideline manual for downdrag on uncoated and bitumen coated piles should be consulted for further information on downdrag (Briaud and Tucker 1997; <http://ceprofs.tamu.edu/briaud/>).

Table 18.17 Some Situations in which Downdrag Can Occur

| | |
|---|--|
| 1 | The total settlement of the ground surface will be larger than 100 mm |
| 2 | The settlement of the ground surface after the piles are installed will be larger than 10 mm |
| 3 | The height of the embankment to be placed on the ground surface exceeds 2 m |
| 4 | The thickness of the soft compressible layer is larger than 10 m |
| 5 | The water table will be drawn down by more than 4 m |
| 6 | The piles are longer than 25 m |

18.6.2 Downdrag on a Single Pile

A shallow, soft layer loaded by an embankment, for example, settles more than the pile, which may rest in a strong deeper layer. In this instance the soil drags the pile down during the soil settlement. Because the pile does not move downward as much as the soil, at the ground surface it looks like the pile is coming out of the ground. So, when you see piles coming slowly out of the ground, it could be downdrag. This downdrag load extends to the point where the settlement of the soil becomes equal to the settlement of the pile (Figure 18.52); that point is called the *neutral point* (NP). In the case of no downdrag, the load in the pile decreases from the top down to the pile point (Figure 18.52). In the case of downdrag, the load increases to the NP and then decreases to the pile point. In extreme cases the NP is at the pile point. The evolution of the loads during and after construction is shown in Figure 18.53 for the case of downdrag and no downdrag.

As with other foundation design problems, the two limit states must be satisfied: serviceability limit state (allowable settlement) and ultimate limit state (ultimate capacity). What is special about downdrag cases is that the serviceability limit state (allowable settlement criterion) controls the design much more often than does the case of no downdrag. Indeed, downdrag induces larger settlement of the pile and settlement calculations must be performed with this in mind. Also, one must check that the load at the NP, which is most often the highest load in the pile, will not crush the pile material. Two main equations are the basis for finding the location of the neutral point. Vertical equilibrium gives the following expression:

$$Q_t + F_n = F_p + Q_p \tag{18.125}$$

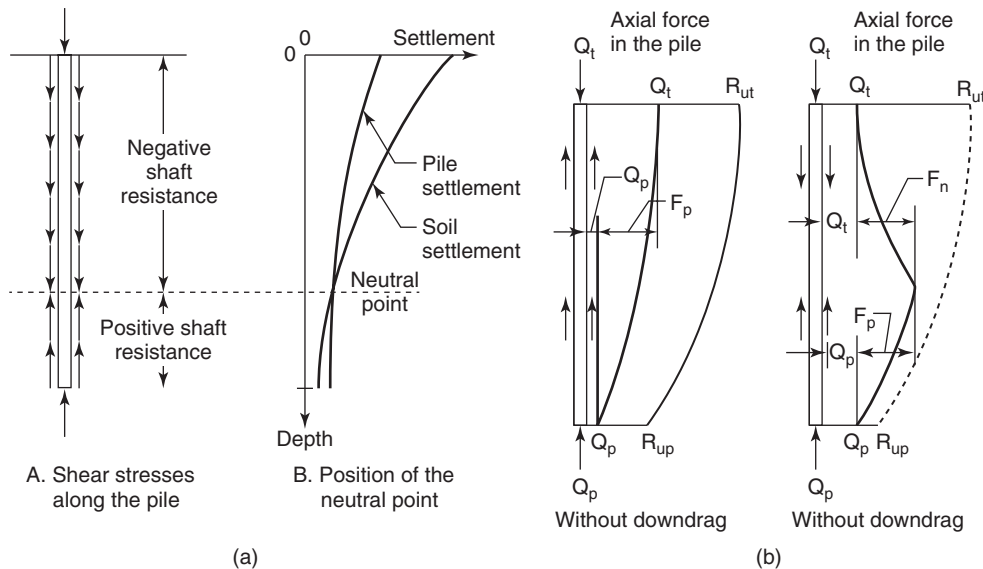


Figure 18.52 Settlement profile and load distribution: (a) Settlement profile. (b) Load distribution.

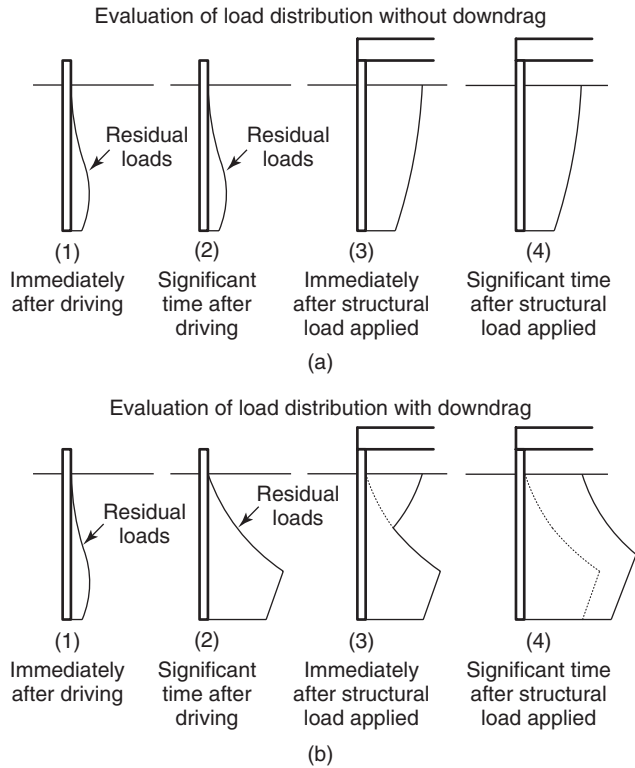


Figure 18.53 Evolution of the loads during and after construction.

where Q_t is the top load on the pile, F_n is the downdrag or negative friction load, F_p is the positive friction load, and Q_p is the point load (Figure 18.52). Compatibility of movement at the NP gives:

$$w_{NP(soil)} = w_{NP(pile)} \quad (18.126)$$

where $w_{NP(pile)}$ is the pile movement at the NP and $w_{NP(soil)}$ is the soil movement at the NP. These two equations are used together with an iteration procedure to find the depth of the NP. Although the necessary calculations have been automated in computer programs (e.g., PILNEG, available at <http://ceprofs.tamu.edu/briaud/>), these calculations are best illustrated through hand calculations.

18.6.3 Sample Downdrag Calculations

Consider the square concrete pile of Figure 18.54. It is 30 m long and 0.3 m × 0.3 m in cross section. The concrete has a modulus of elasticity of 2×10^7 kN/m². The soil develops an ultimate friction that is constant with depth (simplification) and equal to 25 kN/m². To simplify the problem further, it is assumed that the friction load transfer curve is rigid-perfectly plastic, so that any pile displacement generates the ultimate friction. The point resistance load transfer curve (Figure 18.54) is elastic-perfectly plastic, with an ultimate point resistance of 1000 kN and a 5 mm movement required to reach that ultimate value. The soil settlement profile shown in Figure 18.54 indicates that, at the pile point, the soil movement is zero (hard layer) and the ground surface settles 200 mm. The allowable settlement for the structure is 15 mm.

1. Find the ultimate capacity of the pile.

$$Q_u = 25 \times 1.2 \times 30 + 1000 = 1900 \text{ kN} \quad (18.127)$$

If the pile was not subjected to downdrag, we would apply the load and resistance factor design and end up

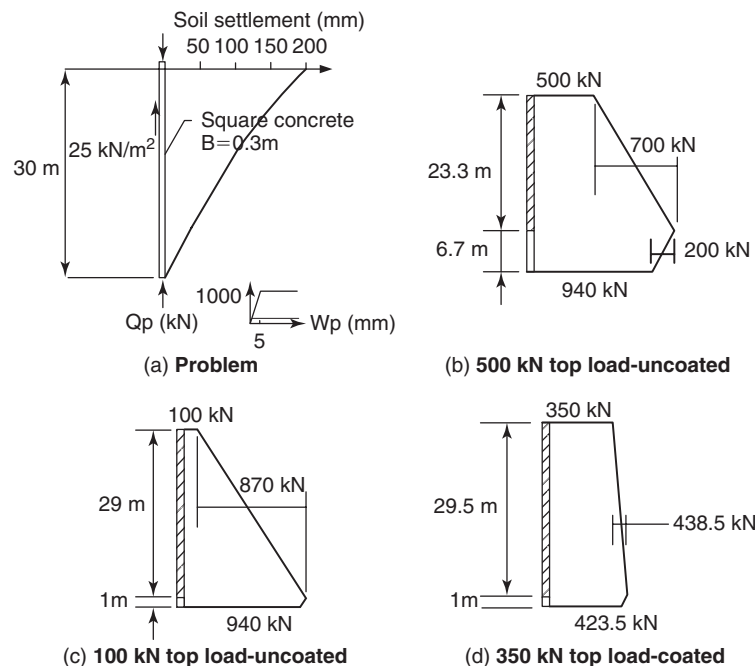


Figure 18.54 Example downdrag problem and results.

with a top load of around 800 kN for such a pile. Because we have downdrag, we need to reduce this load.

2. Try a top load of $Q_t = 500$ kN.

- a. Assume that the NP is at a depth of 20 m.

From the soil settlement profile, we read a soil movement at the assumed depth of the NP (20 m) of:

$$w_{NP(soil)} = 50 \text{ mm} \quad (18.128)$$

Vertical equilibrium of the pile gives us the load in the pile at the NP, Q_{NP} , and the point load Q_p (Eq. 18.125):

$$Q_{NP} = 500 + 25 \times 1.2 \times 20 = 1100 \text{ kN} \quad (18.129)$$

$$\begin{aligned} Q_p &= 500 + 25 \times 1.2 \times 20 - 25 \times 1.2 \times 10 \\ &= 800 \text{ kN} \end{aligned} \quad (18.130)$$

We can now use the point load transfer curve together with the calculated point load to obtain the corresponding point movement w_p :

$$w_p = 4 \text{ mm} \quad (18.131)$$

Then we can calculate the pile movement at the location of the neutral point by adding the elastic compression of the pile between the pile point and the NP. First, the average load in the pile between the pile point and the NP is:

$$Q_{ave} = \frac{800 + 1100}{2} = 950 \text{ kN} \quad (18.132)$$

The pile movement at the NP is:

$$\begin{aligned} w_{NP(pile)} &= 4 + \frac{950 \times 10}{0.3 \times 0.3 \times 2 \times 10^7} \times 1000 \\ &= 9.3 \text{ mm} \end{aligned} \quad (18.133)$$

Comparing Eq. 18.128 with Eq. 2a shows that the movement of the soil at the NP is quite different from the movement of the pile at the NP. Therefore, this cannot be the NP; our first guess was incorrect. Let's try another guess.

- b. Assume that the NP is at a depth of 29 m.

From the soil settlement profile, we read a soil movement at the NP of:

$$w_{NP(soil)} = 5 \text{ mm} \quad (18.134)$$

Vertical equilibrium of the pile gives us the point load, Q_p (Eq. 18.125):

$$\begin{aligned} Q_p &= 500 + 25 \times 1.2 \times 29 - 25 \times 1.2 \times 1 = 1340 \text{ kN} \\ & \quad (18.135) \end{aligned}$$

This is not possible because the ultimate point load is only 1000 kN. What would happen in this case is that the pile point would settle into the soil until the settlement of the pile point became sufficient for equilibrium to be reached. This would happen when (Eq. 18.125):

$$500 + F_n = F_p + 1000 \quad (18.136)$$

Knowing that:

$$F_n + F_p = 25 \times 1.2 \times 30 = 900 \text{ kN} \quad (18.137)$$

Then (Figure 18.54):

$$F_n = 700 \text{ kN} \quad \text{and} \quad F_p = 200 \text{ kN} \quad (18.138)$$

This means that the neutral point would be at a depth of:

$$z_{NP} = \frac{700}{25 \times 1.2} = 23.3 \text{ m} \quad (18.139)$$

From the soil settlement profile, we get a settlement at the NP of:

$$w_{NP(soil)} = 35 \text{ mm} \quad (18.140)$$

The mean load in the pile between the top and the NP is:

$$Q_{ave} = \frac{500 + 1200}{2} = 850 \text{ kN} \quad (18.141)$$

and the settlement at the top of the pile is:

$$w_{top} = 35 + \frac{850 \times 23.3}{0.3 \times 0.3 \times 2 \times 10^7} \times 1000 = 46 \text{ mm} \quad (18.142)$$

This is more than the allowable settlement, not to mention that the pile point would be at failure. We need to reduce the top load on the pile.

3. Try a top load of $Q_t = 100$ kN.

- a. Assume that the NP is at a depth of 25 m.

From the soil settlement profile, we read a soil movement at the NP of:

$$w_{NP(soil)} = 25 \text{ mm} \quad (18.143)$$

This is already larger than the allowable settlement, so we need to move the NP deeper.

- b. Assume that the NP is at a depth of 29 m.

From the soil settlement profile, we read a soil movement at the NP of:

$$w_{NP(soil)} = 5 \text{ mm} \quad (18.144)$$

Vertical equilibrium of the pile gives us the load in the pile at the NP, Q_{NP} , and the point load Q_p (Eq. 18.125):

$$Q_{NP} = 100 + 25 \times 1.2 \times 29 = 970 \text{ kN} \quad (18.145)$$

$$Q_p = 100 + 25 \times 1.2 \times 29 - 25 \times 1.2 \times 1 = 940 \text{ kN} \quad (18.146)$$

We can now use the point load transfer curve together with the calculated point load to obtain the corresponding point movement w_p :

$$w_p = 4.7 \text{ mm} \quad (18.147)$$

Then we can calculate the pile movement at the location of the neutral point by adding the elastic compression of the pile between the pile point and the NP. First, the average load in the pile between the pile point and the NP is:

$$Q_{ave} = \frac{940 + 970}{2} = 955 \text{ kN} \quad (18.148)$$

The pile movement at the NP is:

$$w_{NP(pile)} = 4 + \frac{955 \times 1}{0.3 \times 0.3 \times 2 \times 10^7} \times 1000 = 5.2 \text{ mm} \quad (18.149)$$

The movement of the soil at the NP is very close to the movement of the pile at the NP. Let's calculate the movement at the top of the pile. The mean load in the pile between the NP and the top of the pile is:

$$Q_{ave} = \frac{100 + 970}{2} = 535 \text{ kN} \quad (18.150)$$

and the movement of the top of the pile is:

$$w_{top} = 5 + \frac{535 \times 29}{0.3 \times 0.3 \times 2 \times 10^7} \times 1000 = 13.6 \text{ mm} \quad (18.151)$$

Therefore, the settlement at the top of the pile is allowable. However, the pile point is close to failure, and this pile, which would typically carry about 800 kN of load with no downdrag, is reduced to carrying 100 kN under precarious conditions. What if we coated that pile with a friction reducer such as bitumen? Let's say that this friction reducer reduces the friction from 25 kN/m² to 2.5 kN/m² (common for properly selected bitumen).

4. Try a top load of 350 kN on the coated pile.
 - a. Assume that the NP is at a depth of 29.5 m.

From the soil settlement profile, we read a soil movement at the NP of:

$$w_{NP(soil)} = 2.4 \text{ mm} \quad (18.152)$$

Vertical equilibrium of the pile gives us the load in the pile at the NP, Q_{NP} , and the point load Q_p (Eq. 18.125):

$$Q_{NP} = 350 + 2.5 \times 1.2 \times 29.5 = 438.5 \text{ kN} \quad (18.153)$$

$$Q_p = 350 + 2.5 \times 1.2 \times 29.5 - 25 \times 1.2 \times 0.5 = 423.5 \text{ kN} \quad (18.154)$$

We can now use the point load transfer curve together with the calculated point load to obtain the corresponding point movement w_p :

$$w_p = 2.2 \text{ mm} \quad (18.155)$$

Then we can calculate the pile movement at the location of the neutral point by adding the elastic compression of the pile between the pile point and the NP. First, the average load in the pile between the pile point and the NP is:

$$Q_{ave} = \frac{423.5 + 438.5}{2} = 431 \text{ kN} \quad (18.156)$$

The pile movement at the NP is:

$$w_{NP(pile)} = 2.2 + \frac{431 \times 0.5}{0.3 \times 0.3 \times 2 \times 10^7} \times 1000 = 2.3 \text{ mm} \quad (18.157)$$

The movement of the soil at the NP is very close to the movement of the pile at the NP. Let's calculate the movement at the top of the pile. The mean load in the pile between the NP and the top of the pile is:

$$Q_{ave} = \frac{350 + 438.5}{2} = 394.2 \text{ kN} \quad (18.158)$$

and the movement at the top of the pile is:

$$w_{top} = 5 + \frac{394.2 \times 29.5}{0.3 \times 0.3 \times 2 \times 10^7} \times 1000 = 11.5 \text{ mm} \quad (18.159)$$

Therefore, the settlement is acceptable. Note that the ultimate capacity of the pile is reduced because of the coating:

$$\begin{aligned} Q_u &= 2.5 \times 1.2 \times 29.5 + 25 \times 1.2 \times 0.5 + 1000 \\ &= 1103.5 \text{ kN} \end{aligned} \quad (18.160)$$

18.6.4 LRFD Provisions

The preceding example showed calculations of settlement associated with the serviceability limit state. In the case of settlement, the unfactored dead load, the unfactored permanent live load, and the unfactored downdrag are included in the settlement calculation, but the transient live load is not. The transient live load is included when checking the ultimate limit state at the top of the pile, but not when the

ultimate limit state is checked at the NP. The reason is that the transient live load does not last long enough to reverse the downdrag load.

Briaud and Tucker (1997) proposed to check the ultimate limit state at two locations along the pile: the pile top and the NP.

$$\text{At the pile top } 1.25DL + 1.75PLL + 1.75TLL < 0.5R_u \tag{18.161}$$

$$\text{At the NP } 1.25DL + 1.75PLL + 1.75F_n < 0.75(Q_{pu} + F_{pu}) \tag{18.162}$$

where DL is the dead load, PLL is the permanent live load, TLL is the transient live load, R_u is the ultimate capacity of the pile, F_n is the downdrag load, Q_{pu} is the ultimate point resistance, and F_{pu} is the friction resistance below the NP.

The resistance factors (0.5 and 0.75 on the right side of the equations) are for a high-quality static method of computing the resistances; they should be adjusted for other cases. Note that at the pile top the ultimate limit state is the same as the case of no downdrag, because the ultimate capacity of the pile is the same whether or not there is downdrag. The use of a higher resistance factor at the neutral point, 0.75, compared to 0.5 at the top, means that the consequence of exceeding the ultimate load below the neutral point is not as drastic as that of exceeding the ultimate load at the pile top. Indeed, if the ultimate capacity of the pile below the neutral point is exceeded, some settlement will take place, the neutral point will move up and the pile will find a new equilibrium; as long as the top load is less than the ultimate capacity, downdrag by itself cannot create plunging failure. In contrast, if the top load reaches the ultimate capacity of the pile, the pile will plunge, as there is no reserve in this case. AASHTO (2010) recommends checking the ultimate limit state at the neutral point as follows:

$$\text{If } F_n > F_{pu} \quad 1.25DL + 1.75PLL + 1.75(F_n - F_{pu}) < 0.5Q_{pu} \tag{18.163}$$

$$\text{If } F_n < F_{pu} \quad 1.25DL + 1.75PLL < 0.5(Q_{pu} + F_{pu} - F_n) \tag{18.164}$$

Going back to the example of section 18.6.3, case 4a, and assuming that the dead load is 300 kN and the permanent live load is 50 kN, then Eq. 18.162 gives:

$$1.25 \times 300 + 1.75 \times 50 + 1.75 \times 88.5 < 0.75(1000 + 15) \tag{18.165}$$

or $617.4 < 761.2$

This Briaud-Tucker ultimate limit state at the NP is satisfied. The AASHTO guidelines give (Eq. 18.158):

$$1.25 \times 300 + 1.75 \times 50 + 1.75(88.5 - 15) < 0.5 \times 1000 \tag{18.166}$$

or $591.1 < 500$

This AASHTO limit state would not be satisfied.

18.6.5 Downdrag on a Group of Piles

The downdrag force on a group of n closely spaced piles is less than n times the downdrag force on an isolated single pile. The reason is that the soil tends to settle on the outside of the pile group but does not settle as much between piles inside the group, as illustrated in Figure 18.55. The full-scale case history by Okabe (1977) demonstrates the impact of this observation very clearly. Figure 18.56 shows the pile group configuration together with the load distribution for different piles in the group compared to a single pile. The center-to-center spacing for the piles in the group is approximately 2.1 diameters. It can be seen that the single pile experiences a large downdrag load (7000 kN), that the outer piles in the group carry about one-half of the single pile downdrag load (3500 kN), and that the interior piles in the group are subjected to only about 500 to 1000 kN of downdrag, or 7% to 14% of the single-pile downdrag load. The reduction of downdrag on the interior piles in the group is dramatic. After calibrating their three-dimensional nonlinear finite element simulation against Okabe's result, Jeong and Briaud (1994) performed a large parametric study to investigate the downdrag reduction in pile groups. Based on those results and other measurements,

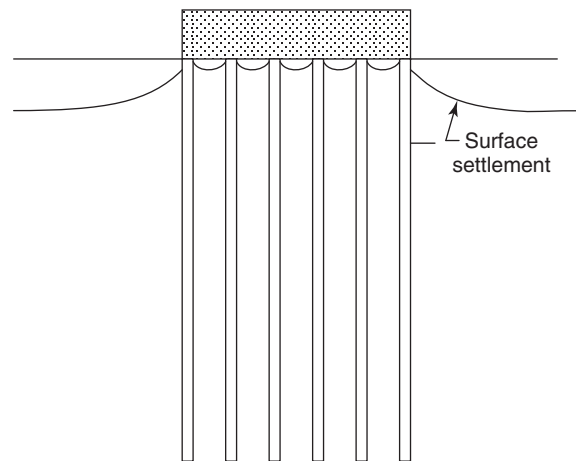


Figure 18.55 Soil settlement pattern around a pile group.

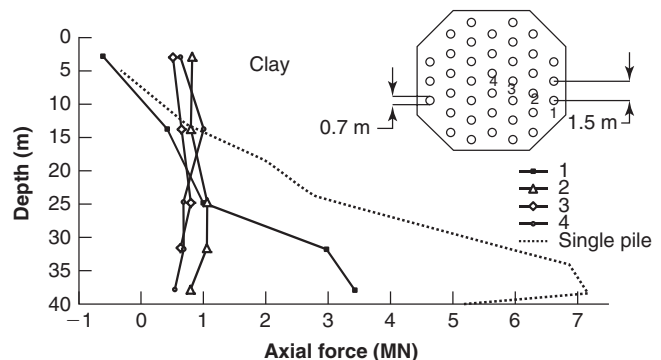
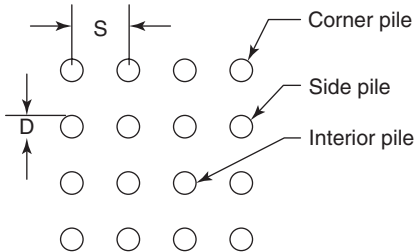


Figure 18.56 Okabe (1977) case history results.

Table 18.18 Downdrag Reduction Factors for Groups of Piles

| $S/D = 5$ |  | $S/D = 2.5$ |
|---|--|--|
| $F_{n(\text{corner})} = 0.9 F_{n(\text{single})}$ | | $F_{n(\text{corner})} = 0.5 F_{n(\text{single})}$ |
| $F_{n(\text{side})} = 0.8 F_{n(\text{single})}$ | | $F_{n(\text{side})} = 0.4 F_{n(\text{single})}$ |
| $F_{n(\text{interior})} = 0.5 F_{n(\text{single})}$ | | $F_{n(\text{interior})} = 0.15 F_{n(\text{single})}$ |

Definitions:

S = center-to-center spacing

D = pile diameter

$F_{n(\text{single})}$ = downdrag force on the single pile

$F_{n(\text{corner})}$ = downdrag force on a corner pile in the group

$F_{n(\text{side})}$ = downdrag force on a side pile in the group

$F_{n(\text{interior})}$ = downdrag force on an interior pile in the group

(Briaud and Tucker 1997)

Briaud and Tucker (1997) recommended the reduction factors listed in Table 18.18. Most often the piles in the groups are embedded into a rigid pile cap. The fact that the outside piles undergo more downdrag than the inside piles means that the outside piles pull down on the pile cap while the inside piles push up on it. This is the case of pile 1 in Okabe's experiment (Figure 18.56). Therefore, the connection between the pile cap and the outside piles should be designed for tension. The best way to simulate downdrag of a pile group is with the finite element method.

18.7 PILES IN SHRINK-SWELL SOILS

Piles in shrink-swell soils are subjected to soil movements that may increase or decrease the compression load in the pile (Figure 18.57). These vertical soil movements take place during the year as the top part of the soil deposit changes water content from one season to another. The depth of the zone influenced by these movements, called the *active zone*, seems to be on the order of 3 to 5 m. If the soil shrinks, the soil moves down with respect to the pile; this is a case similar to downdrag, where excessive settlement and excessive load in the pile are the design issues. If the soil swells, the soil moves up with respect to the pile and could create excessive upward movement of the foundation if the pile is not deep enough.

18.7.1 The Soil Shrinks

The case in which the soil shrinks is very similar to the case of downdrag, except that the neutral point is found at the bottom of the soil shrinkage zone. If the soil is uniform and

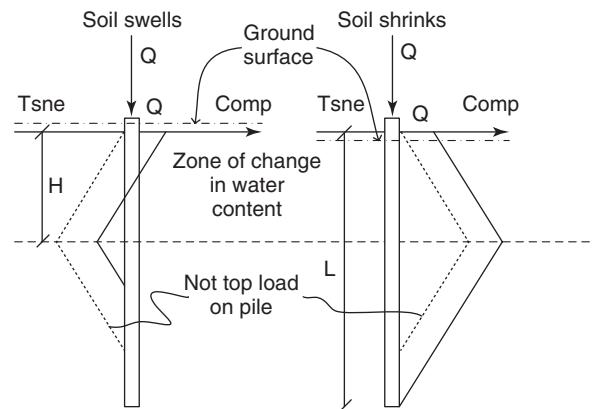


Figure 18.57 Load distribution in piles in shrink-swell soils.

the depth of the active zone is H , a pile length equal to $2.5 H$ must be ignored in the calculation of load carrying capacity. This minimum pile length is used to ensure that the shrinkage of the soil pulling down on the pile does not create downward movement of the structure. The downward load is applied over the top H of the pile, the next H resists that movement, and the next $0.5 H$ is there as a safety factor. An additional length of pile beyond $2.5 H$ and/or the point resistance is necessary to safely carry the compressive structural load in friction and/or point resistance. Note that there is some uncertainty as to whether the shrinking soil can truly load the pile downward; indeed, the shrinkage is usually in all directions, including away from the pile in the radial direction. At the same time, the shrinking soil can be much stronger than the soil below the active zone, which does not shrink.

18.7.2 The Soil Swells

In the case of swelling soil, the soil swells against the pile and pulls it upward over the depth H of the active zone. If the soil is uniform and the depth of the active zone is H , again the minimum length of pile must be $2.5 H$, excluding other loads. This minimum pile length is used to ensure that the swelling of the soil pulling up on the pile does not create upward movement of the structure. The uplift load is applied by the swelling soil over the top H , the next H resists that movement, and the next $0.5 H$ is there as a safety factor. If the structure applies a compressive load, this will counteract to some extent the uplift created by the soil. In this instance there is no need to lengthen the pile, unless the structural load is so large that the movement of the soil is overcome and the pile moves downward with respect to the soil over its entire length. In this extreme case, the swelling of the soil can be ignored and the pile is designed as an ordinary pile.

The friction load created by swelling $F_{u(swell)}$ or shrinking $F_{u(shrink)}$ of the soil over the depth of the active zone is calculated as:

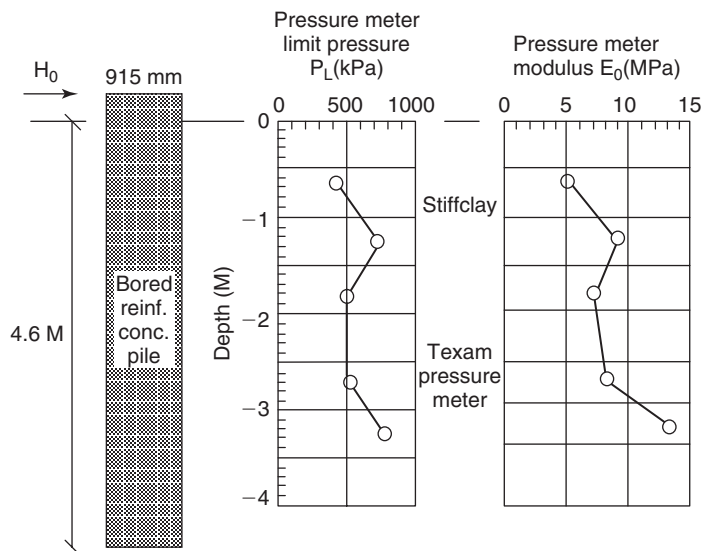
$$F_{u(swell)} = F_{u(shrink)} = f_u PH \tag{18.167}$$

where f_u is the ultimate friction, P is the pile perimeter, and H is the depth of the active zone. Reese et al. (1976) give some limiting values for the parameter f_u .

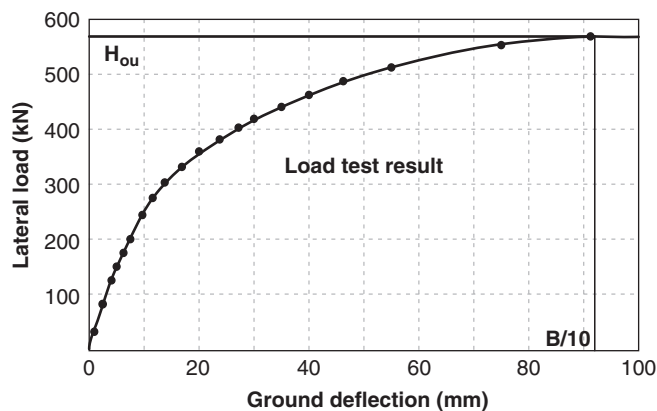
18.8 HORIZONTAL LOAD AND MOMENT: SINGLE PILE

18.8.1 Definitions and Behavior

This section deals with piles subjected to horizontal loads and overturning moments. Examples of such loading on pile foundations include wire tension at corner towers of power lines,



(a)



(b)

Figure 18.58 Example load test result. (Briaud 1997)

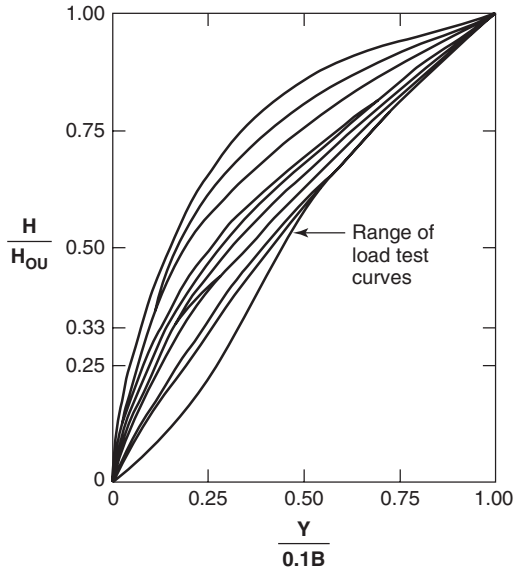


Figure 18.59 Normalized horizontal load test curves. (Briaud 1997)

hurricane waves on offshore platforms, ship impact on bridge piers, and earthquake shaking of a building and walls. A horizontal load test on a pile often consists of placing two piles at some distance from each other and either pulling them toward each other or pushing them apart. The resulting load displacement curve for one pile gives the horizontal load H_o versus the horizontal displacement y_o (Figure 18.58). From this curve, an ultimate load H_{ou} can be defined as the horizontal load H_o corresponding to a displacement equal to one-tenth of the pile diameter ($B/10$). With such a definition, the load test curve can be normalized as H_o/H_{ou} as a function of $y_o/0.1B$. Using a database of 20 piles, Briaud (1997) generated such normalized horizontal load test curves (Figure 18.59). It was found that the curves with the least amount of curvature came from steel piles, whereas the curves with the largest amount of curvature came from concrete piles. The reason is that concrete piles gradually crack as they are bent; steel piles do not. The bending stiffness EI (E modulus of elasticity of the pile material, I moment of inertia around the bending axis) of concrete piles decreases due to cracking as the pile bends, inducing more and more curvature; by comparison, the EI of the steel piles does not change measurably within the elastic range.

18.8.2 Ultimate Capacity

The ultimate capacity H_{ou} can be determined by using the free-body diagram of the upper part of the pile from the ground surface down to the point of zero shear force or maximum bending moment (Figure 18.60). By writing horizontal equilibrium, we get:

$$H_{ou} = pBz_{\max} \quad (18.168)$$

where p is the mean pressure against the pile within that depth, B is the pile width, and z_{\max} is the depth to zero shear

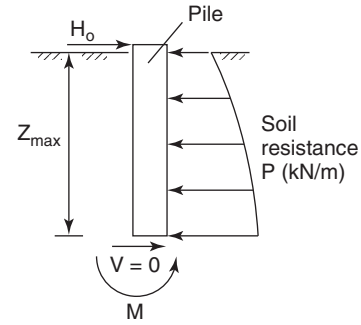


Figure 18.60 Free-body diagram of upper part of horizontally loaded pile.

force (maximum bending moment). By using the database of pile load tests and the associated pressuremeter data, Briaud found that p was equal to $0.75 p_L$ (pressuremeter limit pressure). Therefore, the ultimate load and the depth to zero shear are given by:

$$H_{ou} = \frac{3}{4} p_L B z_{\max} \begin{cases} z_{\max} = \left(\frac{\pi}{4}\right) l_o & \text{for } L > 3l_o \\ z_{\max} = \frac{L}{3} & \text{for } L < l_o \\ l_o = \left(\frac{4E_p I}{K}\right)^{1/4} \\ K = 2.3E_o \end{cases} \quad (18.169)$$

where H_{ou} is the ultimate horizontal load (the load that “breaks” the soil around the pile, not the load that “breaks” the pile), p_L is the average limit pressure from pressuremeter tests within the depth z_{\max} , z_{\max} is the depth to zero shear (maximum bending moment), B is the projected pile width, E_p is the modulus of the pile material, I is the pile moment of inertia, K is the soil stiffness, L is the length of the pile, l_o is the transfer length, and E_o is the pressuremeter first load modulus.

A comparison between predicted H_{ou} and measured H_{ou} is shown in Figure 18.61. The success of this methodology is attributed to the close analogy between the pressuremeter test and the lateral loading of the soil around the pile. It reminds us that when there is a close analogy between the test and the loading of the prototype, there is a very good chance for close predictions. Note that all piles in the database were pushed horizontally with no moment or very small moments applied at the ground surface. If a sizeable moment is applied, the value of z_{\max} can change significantly (sections 18.8.3 and 18.8.4).

18.8.3 Displacement and Maximum Moment: Long Flexible Pile

The problem of predicting the behavior of a laterally loaded pile is solved in section 11.4.4 for a long flexible pile. A long

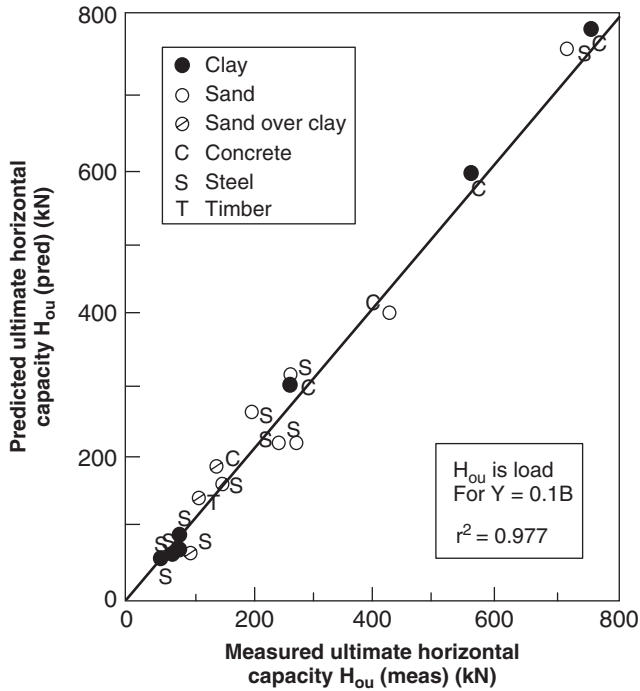


Figure 18.61 Predicted vs. measured ultimate horizontal capacity.

flexible pile corresponds to the case where:

$$L > 3l_o \quad \text{with} \quad l_o = \left(\frac{4E_p I}{K} \right)^{1/4} \quad (18.170)$$

where L is the length of the pile, l_o is the transfer length, E_p is the modulus of the pile material, I is the pile moment of inertia, and K is the soil stiffness. The soil stiffness K is taken as equal to $2.3 E_o$ where E_o is the pressuremeter first load modulus. The equations for the displacement $y(z)$, slope $y'(z)$, bending moment $M(z)$, shear $V(z)$, and line load $P(z)$ as a function of depth z are repeated here for convenience (Figure 18.62):

$$y(z) = \frac{2H_o}{l_o K} e^{-\frac{z}{l_o}} \cos \frac{z}{l_o} + \frac{2M_o}{l_o^2 K} e^{-\frac{z}{l_o}} \left(\cos \frac{z}{l_o} - \sin \frac{z}{l_o} \right) \quad (18.171)$$

$$y'(z) = -\frac{2H_o}{l_o^2 K} e^{-\frac{z}{l_o}} \left(\cos \frac{z}{l_o} + \sin \frac{z}{l_o} \right) - \frac{4M_o}{l_o^3 K} e^{-\frac{z}{l_o}} \cos \frac{z}{l_o} \quad (18.172)$$

$$M(z) = H_o l_o e^{-\frac{z}{l_o}} \sin \frac{z}{l_o} + M_o e^{-\frac{z}{l_o}} \left(\cos \frac{z}{l_o} + \sin \frac{z}{l_o} \right) \quad (18.173)$$

$$V(z) = H_o e^{-\frac{z}{l_o}} \left(\cos \frac{z}{l_o} - \sin \frac{z}{l_o} \right) - \frac{2M_o}{l_o} e^{-\frac{z}{l_o}} \sin \frac{z}{l_o} \quad (18.174)$$

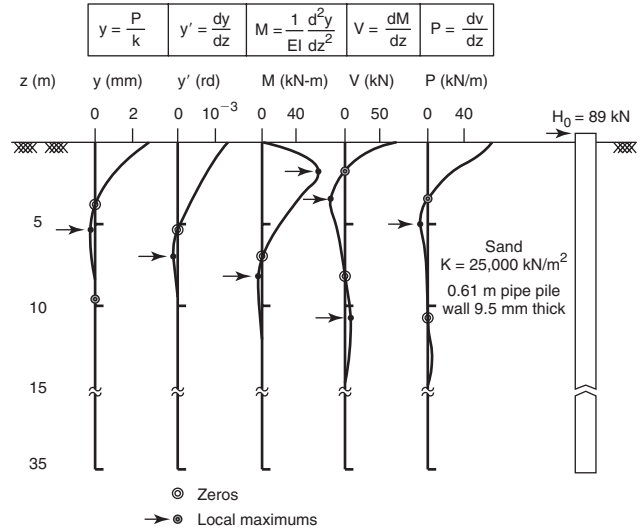


Figure 18.62 Displacement, slope, bending moment, shear, and line load profiles for a laterally loaded pile.

$$P(z) = -K y(z) \quad (18.175)$$

where H_o and M_o are the horizontal load and moment respectively applied at the ground surface, l_o is the transfer length given in Eq. 18.170, and K is the soil stiffness.

Using the same database of pile load tests and pressuremeter data as for the ultimate load equation, Briaud (1997) recommended that the soil stiffness K be taken as:

$$K = 2.3E_o \quad (18.176)$$

where E_o is the pressuremeter first load modulus. The important design quantities for the pile obtained from Eqs. 18.171 to 18.175 are the displacement at ground surface y_o , the pressure close to ground surface p_o , the slope at the ground surface y'_o , the depth to the maximum bending moment z_{max} , and the maximum bending moment M_{max} . The displacement at the ground surface comes from Eq. 18.171 for $z = 0$:

$$y_o = \frac{2H_o}{l_o K} + \frac{2M_o}{l_o^2 K} \quad (18.177)$$

The pressure close to the ground surface is:

$$p_o = -\frac{K y_o}{B} = -\frac{K}{B} \left(\frac{2H_o}{l_o K} + \frac{2M_o}{l_o^2 K} \right) \quad (18.178)$$

where B is the diameter or width of the pile. This pressure should be compared to the yield pressure of the soil close to the ground surface. For the pressuremeter, this yield pressure p_y is on the order of 50% of the limit pressure p_L in clays and 33% of the limit pressure p_L in sands. Alternatively, a factor

of safety can be applied to the limit pressure to ensure that the pressure p_o is acceptable:

$$p_o < \frac{PL}{F} \quad \text{or} \quad p_o < p_y \quad (18.179)$$

The slope at the ground surface comes from Eq. 18.172 for $z = 0$:

$$y'_o = -\frac{2H_o}{l_o^2 K} - \frac{4M_o}{l_o^3 K} \quad (18.180)$$

The depth z_{\max} to the location of the maximum bending moment M_{\max} is found by setting the expression for the shear force (derivative of M) equal to zero and solving for z_{\max} . This gives:

$$z_{\max} = l_o \tan^{-1} \left(\frac{l_o H_o}{l_o H_o + 2M_o} \right) \quad (18.181)$$

Note that z_{\max} must be calculated in radians; any other unit for angles, such as degrees or grades, will not give the right answer. Then M_{\max} is calculated by using Eq. 18.173 and the calculated value of z_{\max} .

Equation 18.177 was evaluated against the 20-pile database by comparing predicted versus measured values of y_o (Figure 18.63). As can be seen, the scatter is much larger than in the case of the ultimate load. This is in part due to the fact that the precision on the modulus is usually lower than the precision on the limit pressure or strength in general. Most of the piles in the database were flexible, but some were rigid. The case of a rigid pile is addressed in section 18.8.4.

18.8.4 Displacement and Maximum Moment: Short Rigid Pile

The case of a short rigid pile corresponds to:

$$L < l_o \quad \text{with} \quad l_o = \left(\frac{4E_p I}{K} \right)^{1/4} \quad (18.182)$$

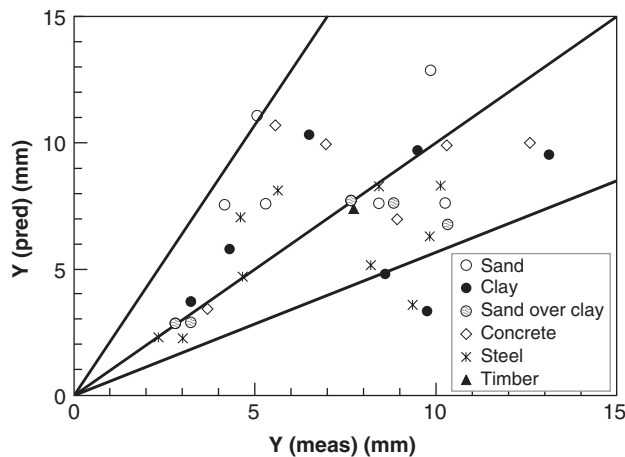


Figure 18.63 Predicted vs. measured horizontal displacements.

where L is the length of the pile, l_o is the transfer length, E_p is the modulus of the pile material, I is the pile moment of inertia, and K is the soil stiffness. In this case the constitutive law for the pile is no longer the relationship between the bending moment and the curvature of the pile, as the pile does not bend (rigid). Instead, the constitutive law for the pile expresses that the deflected shape is a straight line:

$$y = az + b \quad (18.183)$$

where y is the horizontal displacement of the pile and z is depth. The parameter a represents the first derivative of y with respect to z , which is the slope of the pile (y'_o), while b represents the horizontal displacement at the ground surface (y_o at $z = 0$). The solution is much like the solution for the case of the flexible pile.

The constitutive law for the soil is assumed to be a linear relationship between the line load on the pile and the horizontal displacement:

$$P = -Ky \quad (18.184)$$

where P is the line load on the pile, K is the soil stiffness (Eq. 18.176), and y is the horizontal displacement of the pile.

The shear force V at a depth z on the pile can be calculated by integration of the line load P as follows:

$$V = H_o - \int_0^z P d\zeta = H_o + Ka \frac{z^2}{2} + Kbz \quad (18.185)$$

where H_o is the horizontal load applied to the pile at the ground surface, z is the depth where V is calculated, and ζ is the running variable varying between 0 and z .

The bending moment at a depth z in the pile can be obtained by integration of the shear force as follows:

$$\begin{aligned} M &= M_o + H_o z - \int_0^z P(z - \zeta) d\zeta \\ &= M_o + H_o z + Ka \frac{z^3}{6} + Kb \frac{z^2}{2} \end{aligned} \quad (18.186)$$

We use the boundary conditions to find the values of a and b that represent the slope y'_o and the horizontal displacement y_o at the ground surface respectively:

$$\text{for } z = 0, \quad V = H_o, \quad M = M_o \quad (18.187)$$

$$\text{for } z = L, \quad V = 0, \quad M = 0 \quad (18.188)$$

The condition at $z = 0$ is already satisfied and the condition at $z = L$ leads to:

$$y'_o = + \frac{6(H_o L + 2M_o)}{KL^3} = a \quad (18.189)$$

$$y_o = - \frac{2(2H_o L + 3M_o)}{KL^2} = b \quad (18.190)$$

The pressure close to the ground surface is:

$$p_o = -\frac{Ky_o}{B} = 2\frac{K}{B} \left(\frac{2H_oL + 3M_o}{KL^2} \right) \quad (18.191)$$

where B is the diameter or width of the pile. This pressure should be compared to the yield pressure of the soil close to the ground surface. For the pressuremeter, this yield pressure p_y is about 50% of the limit pressure p_L in clays and 33% of the limit pressure p_L in sands. Alternatively, a factor of safety can be applied to the limit pressure to ensure that the pressure p_o is acceptable:

$$p_o < \frac{p_L}{F} \quad \text{or} \quad p_o < p_y \quad (18.192)$$

The depth z_{\max} to the location of the maximum bending moment M_{\max} is found by setting the expression for the shear force (derivative of M) equal to zero and solving for z_{\max} . This gives:

$$z_{\max} = \frac{H_oL^2}{3(H_oL + 2M_o)} \quad (18.193)$$

Then M_{\max} is calculated by using Eq. 18 and the calculated value of z_{\max} .

18.8.5 Modulus of Subgrade Reaction

There are three types of soil stiffness, as shown in the following equations 18.194 to 18.196:

Spring constant:

$$K_1 (\text{kN/m}) = \frac{H (\text{kN})}{y (\text{m})} \quad (18.194)$$

Soil stiffness:

$$K_2 (\text{kN/m}^2) = \frac{P (\text{kN/m})}{y (\text{m})} \quad (18.195)$$

Modulus of horizontal subgrade reaction:

$$K_3 (\text{kN/m}^3) = \frac{p (\text{kN/m}^2)}{y (\text{m})} \quad (18.196)$$

where H is the resultant force on the side of a given length of pile, y is the horizontal displacement of the pile, P is the line load on the pile, and p is the average pressure on the side of a given length of pile.

K_1 and K_3 contain foundation and soil properties, but K_2 is a soil property only. This can be illustrated by using the equation for the settlement of a square plate on an elastic soil:

$$y = I \frac{pB}{E_s} = I \frac{H}{BE_s} \quad (18.197)$$

where y is the settlement of the plate, I is an influence factor, p is the mean pressure under the plate, B is the width of the plate, E_s is the soil modulus, and H is the load on the

plate. Using Eq. 18.197, the values of K_1 , K_2 , and K_3 can be obtained as:

Spring constant:

$$K_1 = \frac{BE_s}{I} \quad (18.198)$$

Soil stiffness:

$$K_2 = \frac{E_s}{I} \quad (18.199)$$

Modulus of horizontal subgrade reaction:

$$K_3 = \frac{E_s}{IB} \quad (18.200)$$

As can be seen, K_1 and K_3 have the width of the plate and the soil modulus in their expression, whereas K_2 only has the soil modulus. Therefore, one should use K_2 and not K_1 and K_3 , especially if K_1 and K_3 are derived from tests performed at a scale very different from the field application.

18.8.6 Free-Head and Fixed-Head Conditions

A free-head condition exists when the loading at the top of the pile consists only of a horizontal load (no moment) (Figure 18.64):

$$M_o = 0 \quad (18.201)$$

A fixed-head condition exists when the loading at the top of the pile is such that the top of the pile remains vertical during the horizontal displacement:

$$y'_o = 0 \quad (18.202)$$

For the same horizontal load H_o , the displacement of the free-head pile will be larger than the displacement of the fixed-head pile. However, the fixed-head pile will develop a significant moment at the ground surface in the process. This moment is given in Eqs. 18.203 and 18.204 for a flexible pile and a rigid pile:

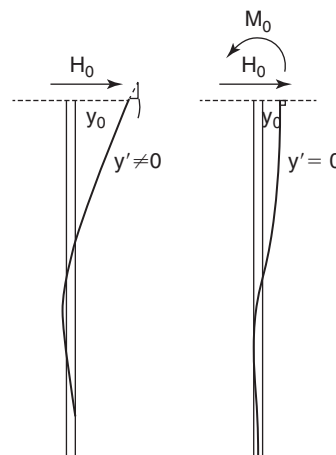


Figure 18.64 Free-head and fixed-head piles.

Table 18.19 Ground Surface Displacement for Horizontally Loaded Piles

| | Free head | Fixed head |
|--------------------|---|--|
| Long flexible pile | $y_o = \frac{2H_o}{l_o K}$ for $L > 3l_o$ | $y_o = \frac{H_o}{l_o K}$ for $L > 3l_o$ |
| Short rigid pile | $y_o = -\frac{4H_o}{LK}$ for $L < l_o$ | $y_o = -\frac{H_o}{KL}$ for $L < l_o$ |

Fixed-head flexible pile:

$$M_o = -\frac{H_o l_o}{2} \quad (18.203)$$

Fixed-head rigid pile:

$$M_o = -\frac{H_o L}{2} \quad (18.204)$$

These moments also happen to be the maximum bending moments in the pile. Table 18.19 summarizes the equation giving the ground surface displacement y_o for flexible and rigid piles in free-head and fixed-head conditions.

18.8.7 Rate of Loading Effect

The rate of loading has an effect on the ultimate horizontal load and on the horizontal displacement at the ground surface. The model proposed by Briaud and Garland (1985) leads to the following relationships:

$$\frac{H_{ou}(t)}{H_{ou}(t_o)} = \left(\frac{t}{t_o}\right)^{-n} \quad (18.205)$$

$$\frac{y_o(t)}{y_o(t_o)} = \left(\frac{t}{t_o}\right)^n \quad (18.206)$$

where $H_{ou}(t)$ and $H_{ou}(t_o)$ are the ultimate horizontal load reached in a time t and t_o respectively, $y_o(t)$ and $y_o(t_o)$ are the horizontal displacements reached in a time t and t_o respectively, and n is the viscous exponent for the soil.

The value of n varies between 0.01 to 0.03 for sand and from 0.02 to 0.05 for clays, with values up to 0.08 or even 0.1 being reached for very soft, high-plasticity clays (see Figure 15.18). For example, if a retaining wall is founded on bored piles in stiff clay and is designed for 50 years of life, then the load $H_{ou}(t_o)$ obtained from Eq. 18.161 must be altered, because of the long-term sustained load. The reference time t_o is associated with the load tests used to calibrate the method. These tests are typically done in a few hours. If we say that t_o is equal to 2 hours, then Eq. 18.205 gives:

$$\begin{aligned} n = 0.02 \quad H_{ou}(50\text{yrs}) &= H_{ou}(2\text{hrs}) \left(\frac{50 \times 365 \times 24}{2}\right)^{-0.02} \\ &= 0.78 H_{ou}(2\text{hrs}) \end{aligned} \quad (18.207)$$

$$\begin{aligned} n = 0.06 \quad H_{ou}(50\text{yrs}) &= H_{ou}(2\text{hrs}) \left(\frac{50 \times 365 \times 24}{2}\right)^{-0.06} \\ &= 0.48 H_{ou}(2\text{hrs}) \end{aligned} \quad (18.208)$$

In contrast, if the pile is hit by a truck and the impact lasts 50 milliseconds, the results are:

$$\begin{aligned} n = 0.02 \quad H_{ou}(50\text{ms}) &= H_{ou}(2\text{hrs}) \left(\frac{0.050}{2 \times 3600}\right)^{-0.02} \\ &= 1.27 H_{ou}(2\text{hrs}) \end{aligned} \quad (18.209)$$

$$\begin{aligned} n = 0.06 \quad H_{ou}(50\text{ms}) &= H_{ou}(2\text{hrs}) \left(\frac{0.050}{2 \times 3600}\right)^{-0.06} \\ &= 2.04 H_{ou}(2\text{hrs}) \end{aligned} \quad (18.210)$$

The same model can be applied to the horizontal displacement $y_o(t)$. Note that the viscous exponent n can be measured directly and on a site-specific basis with a pressuremeter test. The PMT consists of holding the pressure in the probe for a chosen amount of time and recording the increase in radius as a function of time (Figure 18.65). Then n is given by the following equations:

$$\frac{E(t)}{E(t_o)} = \left(\frac{t}{t_o}\right)^{-n} \quad \text{or} \quad n = \frac{-\log\left(\frac{E(t)}{E(t_o)}\right)}{\log\left(\frac{t}{t_o}\right)} \quad (18.211)$$

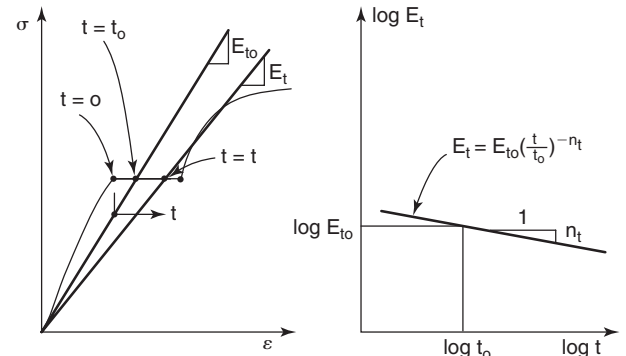


Figure 18.65 Obtaining the viscous exponent from a pressuremeter test.

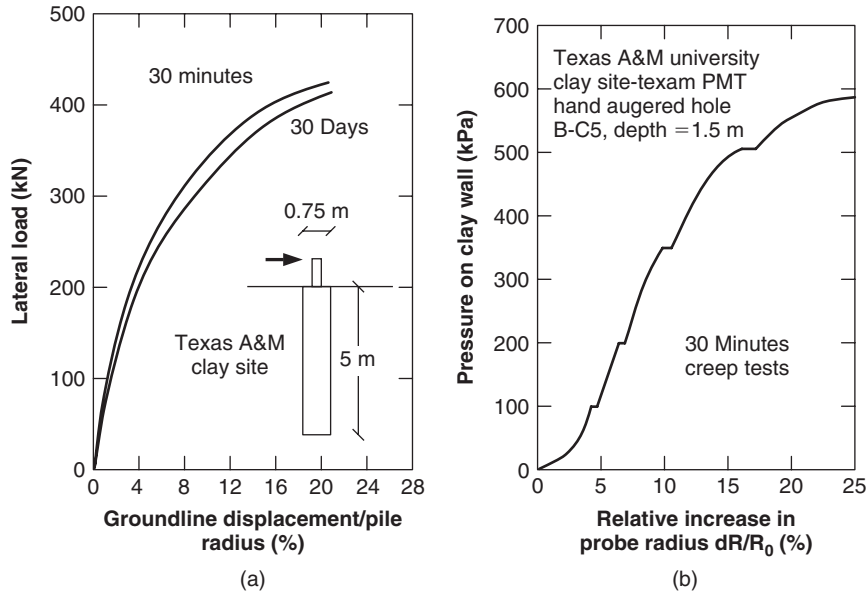


Figure 18.66 Horizontal pile load test and pressuremeter test with long loading steps: (a) Horizontal pile load test, 30-min and 30-day load steps. (b) Pressuremeter test, 30-min pressure steps.

where $E(t)$ and $E(t_o)$ are the first load PMT moduli at time t and t_o respectively. They are obtained from the slopes as shown in Figure 18.65.

Usually t_o is chosen as the reading at 1 minute after the start of the pressure holding step that lasts 10 minutes. The viscous exponent n should be obtained from a pressure holding step in the pressuremeter performed at a ratio p/p_L equal to the ratio H_o/H_{ou} .

Figure 18.66 shows the results of a horizontal pile load test in a stiff clay which was performed with 30-minute and 30-day-long load steps and a pressuremeter test that was performed next to the pile with 30-minute-long pressure steps. The parallel is striking.

18.8.8 Cyclic Loading Effect

The effect of cycles on the behavior of laterally loaded piles can be modeled as follows:

$$y_N = y_1 N^a \tag{18.212}$$

where y_1 and y_N are the ground surface horizontal displacement at the top of the first and the n th cycle respectively, N is the number of cycles, and a is the cyclic exponent.

A major distinction should be made between one-way cyclic loading and two-way cyclic loading (Figure 18.67). In one-way cyclic loading, the direction of the load is not reversed, whereas in the case of two-way cyclic loading the direction of the load is reversed. This distinction makes a difference in the response of the pile depending on the type of soil loaded. If the soil behaves in such a way that pushing the pile in one direction does not affect the behavior of the soil in

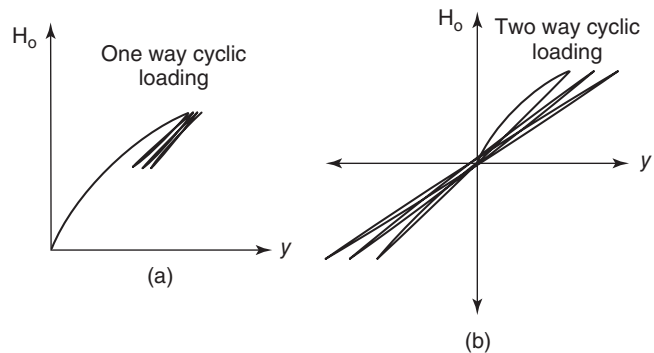


Figure 18.67 Difference between one-way and two-way cyclic loading: (a) One-way cyclic loading. (b) Two-way cyclic loading.

the opposite direction, then there is little difference between one-way and two-way cyclic loading. This is typically the case in clay. There are cases, such as in dry sands, for example, where pushing the pile in one direction opens a gap behind the pile which fills up when the sand falls into it. Then, when the pile is pushed in the opposite direction, the pile is stiffer than it would have been had the sand not fallen into the open gap. This phenomenon can stiffen the pile during two-way cyclic loading and make two-way loading less detrimental to accumulation of displacement than one-way cyclic loading. The cyclic exponent a was collected from cyclic lateral load tests (Briaud 1992) and found to vary in the ranges shown in Table 18.20.

The pressuremeter test can be performed by including cycles of loading (Figure 18.68). The cyclic exponent can be

Table 18.20 Range of Measured Cyclic Exponent for Piles Subjected to Cyclic Horizontal Loads

| Cyclic Loading Type | Soil Types | Range of Values of Cyclic Exponent a | Average |
|---------------------|------------|--------------------------------------|---------|
| One-way and two-way | Clay | 0.01 to 0.35 | 0.094 |
| One-way | Sand | 0.005 to 0.26 | 0.076 |
| Two-way | Sand | -0.14 to 0.06 | 0.002 |

(Briaud 1992)

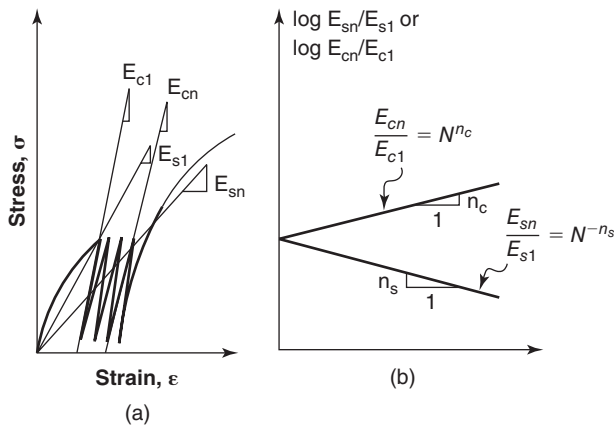


Figure 18.68 Obtaining the cyclic exponent from a cyclic PMT test.

obtained from the cyclic PMT. The cyclic exponent is given by the following equations:

$$\frac{E(N)}{E(1)} = \left(\frac{N}{1}\right)^a \quad \text{or} \quad a = \frac{\log\left(\frac{E(N)}{E(1)}\right)}{\log\left(\frac{N}{1}\right)} \quad (18.213)$$

where $E(N)$ and $E(1)$ are the first load PMT moduli corresponding to the n th cycle and the first cycle respectively. They are obtained from the slopes as shown in Figure 18.68.

The cycles should be performed by matching the anticipated cycles for the pile as closely as possible. In that respect, it is important to realize that the cyclic loading in a PMT can only be one-way cyclic loading. Indeed, in the pressuremeter test the soil is always in radial compression. Therefore, a cyclic pressuremeter test can be used for one-way and two-way cyclic loading for piles in clay where there does not seem to be any difference. However, it can only be used for one-way cyclic loading of sands. If the PMT is used for predicting the accumulation of movement as a function of the number of cycles for two-way cyclic loading in sand, the amount of movement will likely be overestimated. Figure 18.69 shows the results of a one-way horizontal cyclic loading test on a pile in sand. Figure 18.70 shows the results of a cyclic pressuremeter test in the same sand.

18.8.9 P-y Curve Approach

The previous approaches assume that the soil is uniform and that the pile has a constant cross section. In many cases, the actual soil is stratified with layers of different strength and stiffness. Also, sometimes the pile cross section varies as a

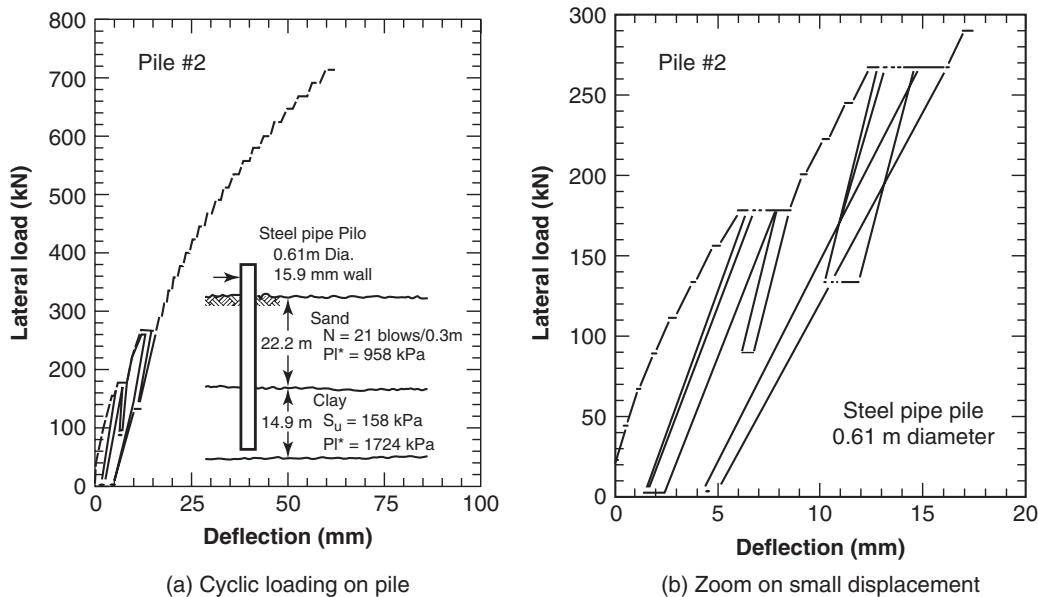


Figure 18.69 Cyclic lateral load test.

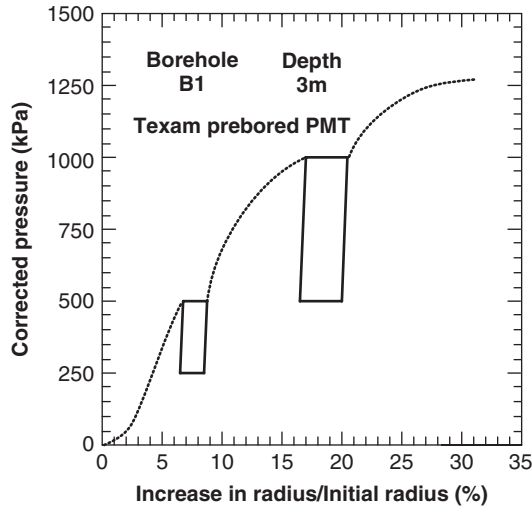


Figure 18.70 Cyclic pressuremeter test.

function of depth. In this case, one of the solutions is the *P*-*y* curve approach. In this approach, the soil resistance is described at any given depth by a nonlinear curve linking the line load *P* on the pile to the pile deflection into the soil *y*. Much of the early work on *P*-*y* curves was done by Matlock and Reese, who recommended a set of curves based on large-scale load tests, analytical developments, and software calibration. These curves are well documented in the offshore recommended practice API-RP 2A (2000), which includes the effect of cyclic loading. Briaud (1992) recommended *P*-*y* curves based on the pressuremeter curve. Frank (2013) and Norme Francaise AFNOR P94-262 (2012)

also have recommendations as to how to construct *p*-*y* curves on the basis of pressuremeter data. The general solution for the *P*-*y* curve approach is the finite difference solution which is described in detail in Section 11.5.1 with a complete example in Section 11.5.2.

18.8.10 Horizontal Loading Next to a Trench

Sometimes there is a need to dig a trench in front of a laterally loaded pile. In this situation one often needs to know how far and how deep the trench can be dug and, if the trench is constructed within the zone of influence of the loading, how much the ultimate capacity will be reduced. If $H_{ou(no\ trench)}$ is the ultimate capacity when there is no nearby trench, and if $H_{ou(trench)}$ is the ultimate capacity when there is a trench, then the reduction factor λ is:

$$H_{ou(trench)} = \lambda H_{ou(no\ trench)} \tag{18.214}$$

Pressuremeter tests were conducted closer and closer to a trench in sand and then to a trench in clay (Briaud and Tucker 1987). The results, shown in Figure 18.71, indicate the weakening of the PMT curve as the distance from the PMT to the edge of the trench is decreased. These data were used to generate the reduction factor λ chart shown in Figure 18.72. Of course, before this chart can be used, one should first check that the trench is stable.

18.9 HORIZONTAL LOAD AND MOMENT: PILE GROUP

The resistance of pile groups to horizontal loading (Figure 18.73) includes several topics: resistance to overturning moments, ultimate loads, and movements at working loads.

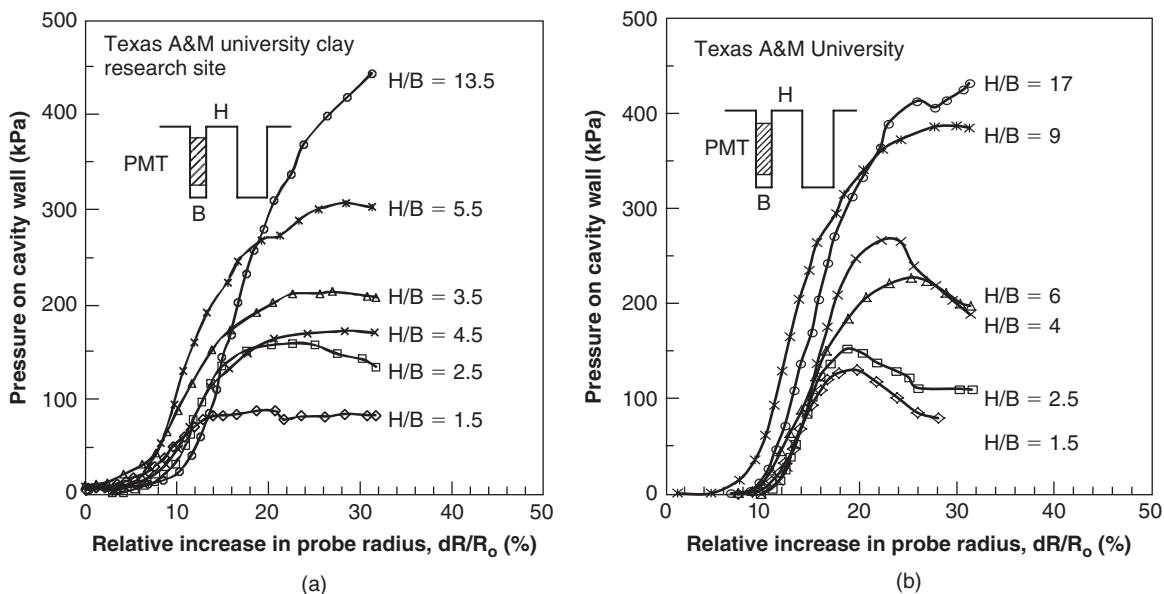


Figure 18.71 Pressuremeter tests near a trench: (a) PMT tests near a trench in clay. (b) PMT tests near a trench in sand.

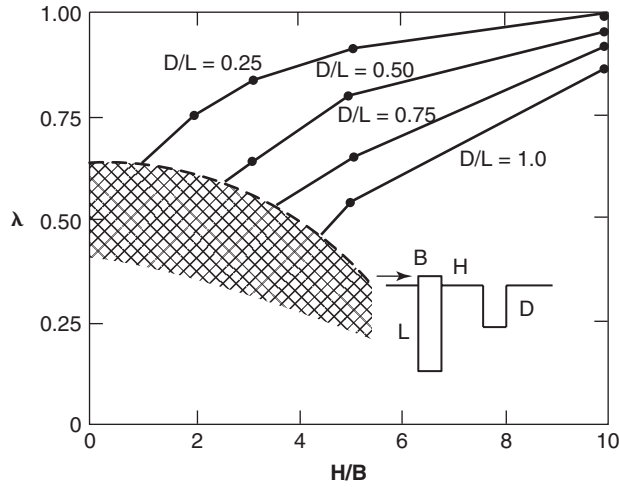


Figure 18.72 Horizontal capacity reduction factor for the presence of a trench.

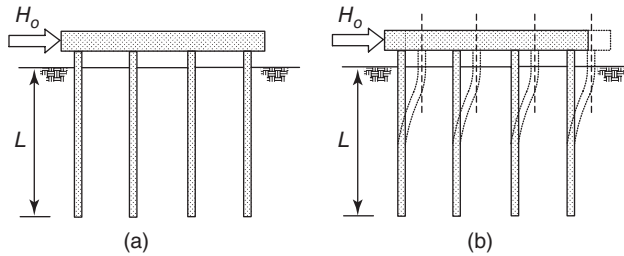


Figure 18.73 Horizontal loading of a pile group (cross section).

18.9.1 Overturning Moment

The resistance to overturning moment is usually taken through an increase in axial compression for the piles on one side of the group and a corresponding decrease in axial compression or possibly tension for the piles on the other side of the group (Figure 18.74).

Consider a rectangular group of piles with n piles in one direction and m piles in the other. The horizontal distances between the center of the group and individual piles in the group are a_i (Figure 18.74). The width of the group is B and the length is L . In this case, the change in load ΔQ_i in each pile due to the moment M is given by:

$$\Delta Q_i = \frac{a_i}{B/2} \Delta Q_{\max} \quad (18.215)$$

where ΔQ_{\max} is the change in axial load in the pile located at the largest distance away from the center of the group ($B/2$). Then the resisting moment provided by the pile group is given by:

$$\Delta Q_{\max} = \frac{MB}{2m \sum_{i=1}^n a_i^2} \quad (18.216)$$

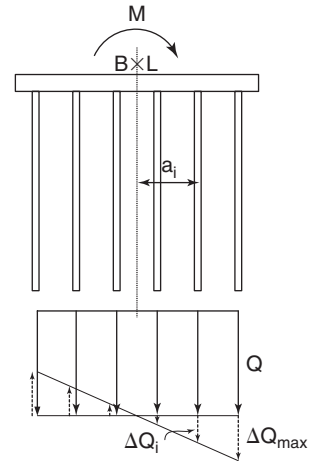


Figure 18.74 Overturning of a pile group.

where ΔQ_{\max} is the change in load in the piles at the edge of the group, M is the global moment applied, B is the width of the group, m is the number of piles in the length direction, n is the number of piles in the width direction, and a_i is the distance between pile i and the center axis around which the moment is applied. Once the value of ΔQ_i is known for each pile, the problem reverts to being a vertical load problem.

18.9.2 Ultimate Capacity

The ultimate horizontal load that can be applied to a pile group can be estimated as:

$$H_{ou(group)} = enH_{ou(single)} \quad (18.217)$$

where $H_{ou(group)}$ and $H_{ou(single)}$ are the ultimate horizontal load for the group and for the single pile respectively, n is the number of piles in the group, and e is the efficiency of the group.

The load resisted by each pile in the group is not the same for all piles. The piles in the front of the group (leading piles) will develop more resistance than the piles behind them (trailing piles) (Figure 18.75).

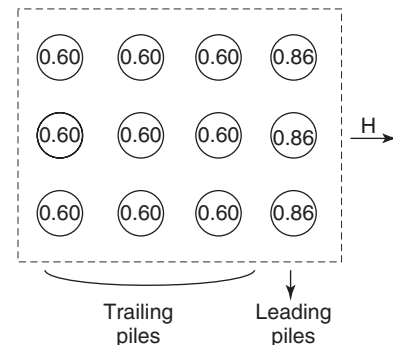


Figure 18.75 Horizontal load on a pile group (plan view).

One reasonable assumption is that all leading piles carry the same load and that all trailing piles carry the same load. Then the following influence factors can be defined for a leading pile and a trailing pile:

$$H_{ou(leading\ pile)} = e_{lp} H_{ou(single)} \quad (18.218)$$

$$H_{ou(trailing\ pile)} = e_{tp} H_{ou(single)} \quad (18.219)$$

where $H_{ou(leading\ pile)}$ and $H_{ou(trailing\ pile)}$ are the ultimate horizontal capacity of the leading pile and trailing pile respectively, and e_{lp} and e_{tp} are the efficiency factors for the leading pile and trailing pile respectively. The group ultimate capacity can then be assembled as:

$$H_{ou(group)} = (n_{lp} e_{lp} + n_{tp} e_{tp}) H_{ou(single)} \quad (18.220)$$

where n_{lp} and n_{tp} are the number of leading piles and trailing piles respectively.

Cox et al. (1983) measured the behavior of groups of in-line piles. They loaded these lines of piles in the direction of the line (in-line loading) and perpendicularly to that line (side-by-side loading). Their measurements were used to develop the global efficiency factors for line groups shown in Figure 18.76. The global efficiency factor is the ratio of the group ultimate capacity $H_{ou(group)}$ divided by n times the ultimate capacity of a single pile $H_{ou(single)}$ where n is the total number of piles in the group.

The measurements by Cox et al. (1983) also showed that all the trailing piles carry approximately the same load and that the leading pile carries more than the trailing piles. The ratio of the ultimate load of the leading pile over the ultimate load of the trailing pile depends on the spacing:

$$H_{ou(leading\ pile)} = \lambda H_{ou(trailing\ pile)} \quad (18.221)$$

The values of λ are shown in Figure 18.77. Therefore, another way to express the group capacity is:

$$H_{ou(group)} = \left(n_{lp} e_{lp} + n_{tp} \frac{e_{lp}}{\lambda} \right) H_{ou(single)} \quad (18.222)$$

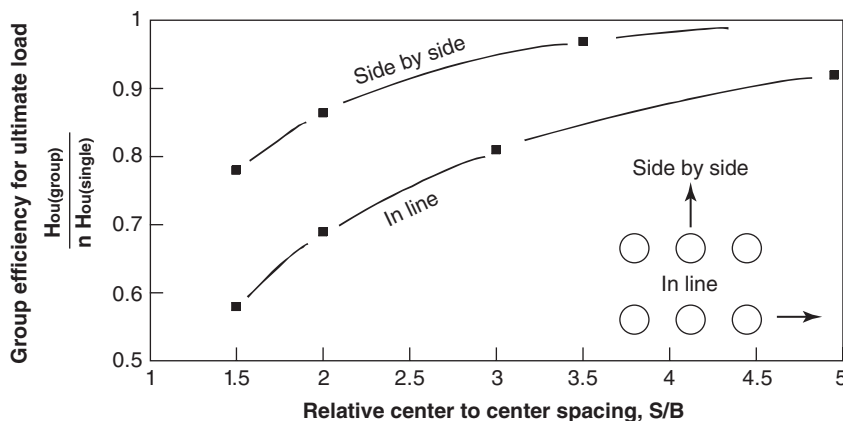


Figure 18.76 Efficiency for side-by-side and in-line groups (After Cox et al. 1983).

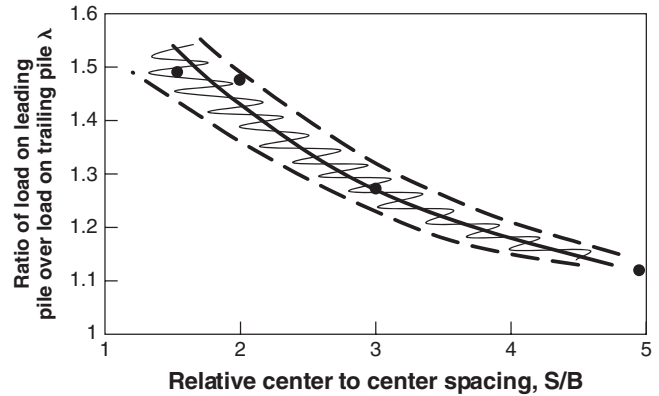


Figure 18.77 Ratio of load on leading pile over trailing pile.

As an example, consider the 3 by 4 pile group of Figure 18.75. The center-to-center spacing is equal to two times the pile diameter. The single-pile ultimate horizontal load $H_{ou(single)}$ has been calculated to be 100 kN. We now wish to obtain the group ultimate capacity if the horizontal load is applied in the direction perpendicular to the three-pile side as shown in Figure 18.75.

1. The leading-pile efficiency e_{lp} is obtained from Figure 18.76 for a pile spacing of 2. The value is 0.86. Therefore, because there are 3 leading piles, the contribution to the group capacity is $3 \times 0.86 = 2.58$.
2. The ratio λ between the capacity of the leading pile and the trailing pile is given by Figure 18.77. The value is 1.43 for a spacing of 2; therefore, the efficiency of the trailing piles is $0.86/1.43 = 0.60$. Because there are 9 trailing piles, the contribution to the group capacity is $9 \times 0.60 = 5.40$.
3. The contribution of the leading piles plus the trailing piles is then $2.58 + 5.40 = 7.98$. If the group was 100% efficient, it would carry 12 times the single-pile capacity, but in fact it carries 7.98 times the single-pile capacity. Therefore, the global efficiency of the group

is $7.98/12 = 0.665$. The ultimate horizontal capacity of the group is $0.665 \times 100 \times 12 = 798$ kN.

18.9.3 Movement

The movement of a pile group is difficult to estimate by simple calculations. One way is to consider that the pile cap prevents any rotation of the individual piles, so that the displacement is the one associated with the case of fixed-head piles (Figure 18.73). The results in this case are given here and detailed in section 18.8.6. A moment M_o must develop between the pile and the pile cap to prevent rotation of the pile at the ground line. For flexible and rigid piles, this moment is given by:

$$\text{Fixed-head flexible pile } M_o = -\frac{H_o l_o}{2} \quad (18.223)$$

$$\text{Fixed-head rigid pile } M_o = -\frac{H_o L}{2} \quad (18.224)$$

where H_o is the horizontal load, l_o is the transfer length (Eq. 18.170), and L is the length of the pile.

These moments also happen to be the maximum bending moments in the pile. The displacement y_o at the ground surface in this case will be:

$$\text{Fixed-head flexible pile } y_o = \frac{H_o}{l_o K} \quad (18.225)$$

$$\text{Fixed-head rigid pile } y_o = \frac{H_o}{LK} \quad (18.226)$$

where K is the soil stiffness. This stiffness is recommended to be taken as $2.3 E_o$ for single piles, where E_o is the pressuremeter first load modulus.

In the case of pile groups, and because of the overlapping of soil stresses around the piles in the group, this number must be decreased by a factor indicative of the interaction between piles in the group.

A second approach for predicting the response of pile groups is to use the P-y curve approach (section 18.8.9) and soften the P-y curves to take into account the effect of overlapping stresses among piles. Given the P_s -y curve for a single pile, the P_g -y curve for the group is obtained simply by writing that for a given value of y (Figure 18.78):

$$P_g = m P_s \quad (18.227)$$

where m is called the multiplier. Brown et al. (2010) gave recommendations for the values of m as shown in Figure 18.79.

The softened P-y curves are then used to simulate each pile in the group as a single pile while using a finite difference program to predict the deflection and maximum bending moment. Alternatively, programs such as FLPIER, which simulate the entire group on the basis of P-y curves, can be used. Ultimately, the finite element method in three dimensions is the best tool to predict the behavior of horizontally loaded pile groups, using programs such as ABAQUS or PLAXIS, but the computing time required is much larger.

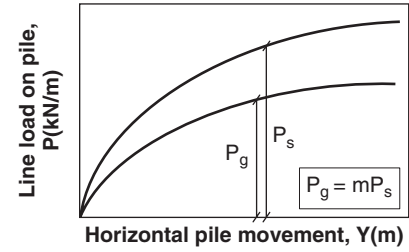


Figure 18.78 P-y curve for piles in groups.

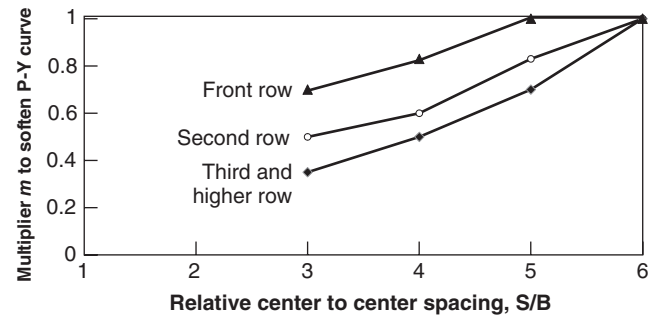


Figure 18.79 Multiplier to soften P-y curves. (After Brown et al. 2010)

18.10 COMBINED PILED RAFT FOUNDATION

A *combined piled raft foundation* (CPRF) is composed of a mat foundation with a number of piles underneath the mat. It is an intermediate between a mat foundation and a pile-group foundation (Figure 18.80). Guidelines for CPRF have been proposed by the ISSMGE technical Committee on Deep Foundations (Katzenbach, 2012). The difference between a CPRF and a pile-group foundation is twofold:

1. In the calculations of the pile-group foundation, the contribution of the pile cap or mat is ignored, whereas it is an integral part of the carrying capacity of the CPRF.
2. The CPRF has fewer piles and the piles are typically longer under the center of the mat than at the edges. The reason is that the mat foundation settles in the shape of a dish; the settlement tends to be larger under the center

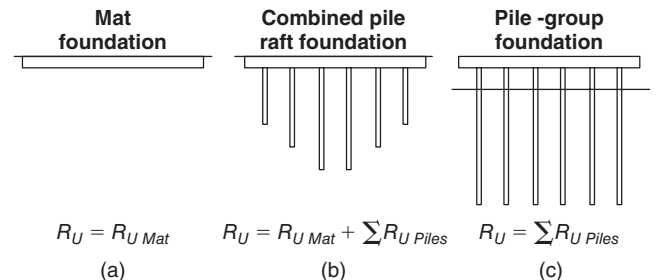


Figure 18.80 Difference between mat foundation, pile-group foundation, and combined piled raft foundation.

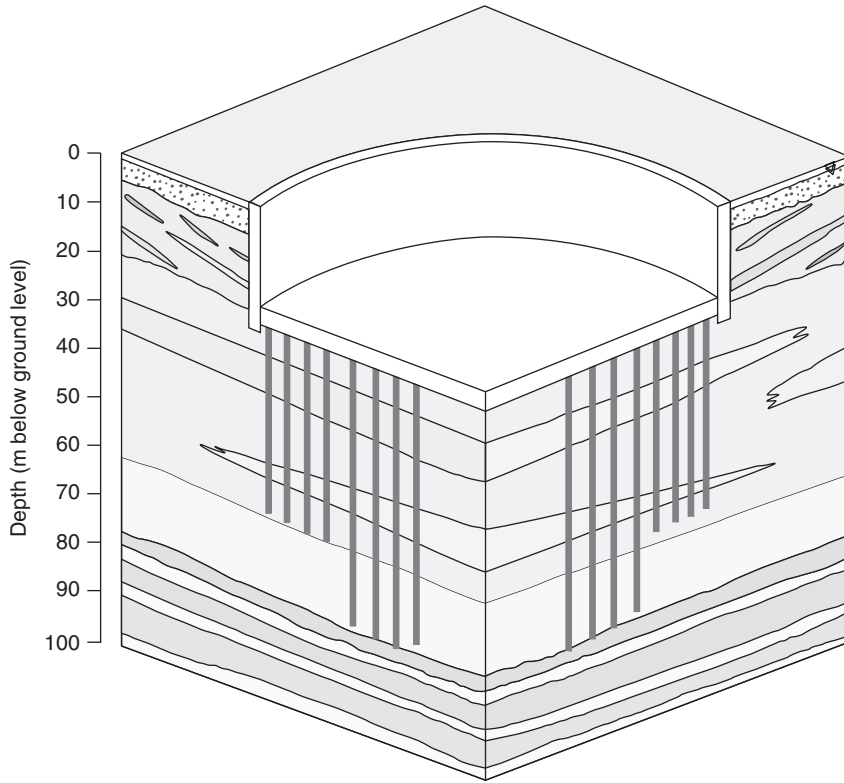


Figure 18.81 CPRF for a very high building in Dubai. (Courtesy of Chris Haberfield, Golder and Associates)

than under the edges. Thus, placing more piles under the center and fewer around the edges counterbalances the dishing tendency and reduces the bending moment in the mat.

An example of a CPRF for a very high building in Dubai is shown in Figure 18.81.

The CPRF offers a combined resistance to the building loads that comes from the pile point resistance (R_{pi}), pile friction resistance (R_{fi}), and raft or mat resistance (R_{ri}). The subscript i refers to pile i and to the raft resistance tributary to pile i (Figure 18.82). The CPRF ratio α is defined as the ratio of the load carried by the n piles divided by the total load R_t carried by the CPRF (Katzenbach 2012):

$$\alpha = \frac{\sum_{i=1}^n (R_{pi}(s) + R_{fi}(s))}{R_t(s)} \quad (18.228)$$

where s is the settlement of the CPRF. Values of the CPRF ratio around 0.5 are common.

At the ultimate limit state, the ultimate pile capacity can be estimated according to the guidelines presented in section 18.4 for single piles and section 18.5 for pile groups. The resistance R_{ri} contributed by the raft around pile i is given by:

$$R_{ri} = \iint_A \sigma(s, x, y) dx dy \quad (18.229)$$

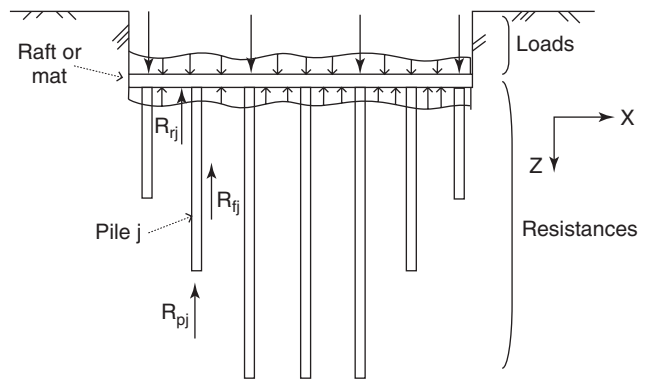


Figure 18.82 Free-body diagram of a CPRF. (After Katzenbach 2012)

where $\sigma(s, x, y)$ is the vertical and upward normal stress on the bottom of the raft around pile i , s is settlement, x and y are the coordinates in the horizontal plane, and A is the area domain of integration corresponding to the portion of the raft tributary to pile i .

It is very difficult to estimate the values of R_{pj} , R_{fj} , and R_{rj} by simple means because they all depend on the movement that takes place around the piles and under the mat. For this reason, the best way to predict the behavior of a CPRF is

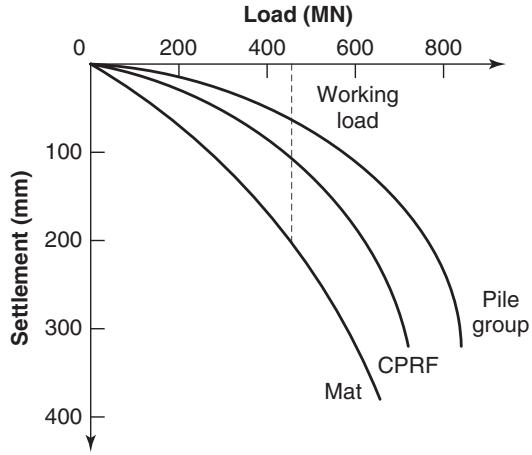


Figure 18.83 Load settlement curves of the structure for three types of foundations. (After Katzenbach, 2012)

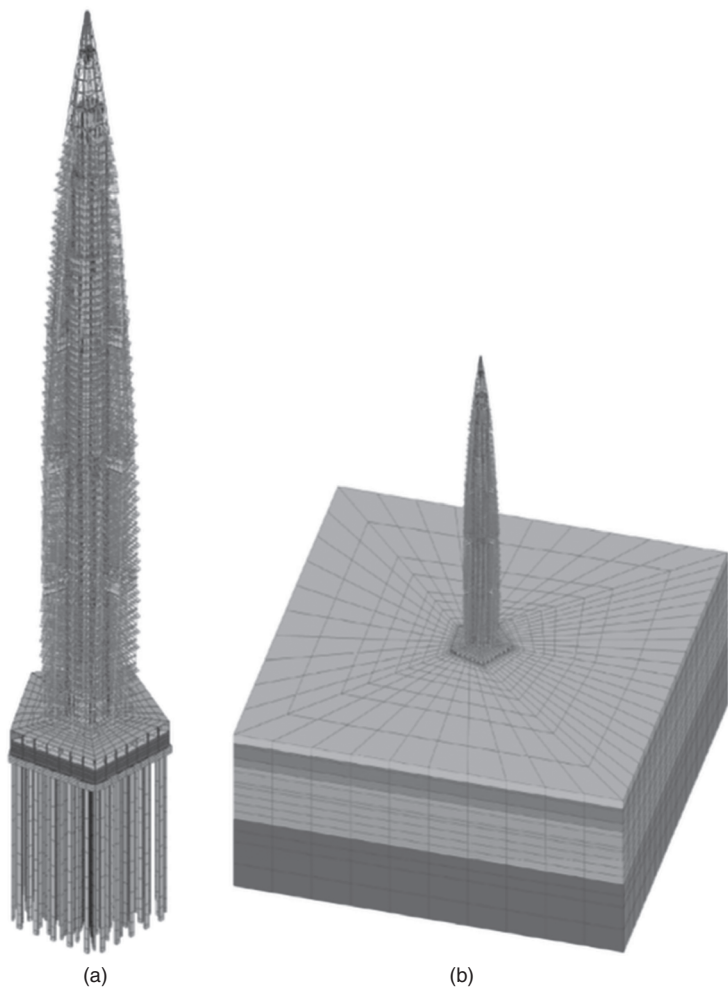


Figure 18.84 Complete soil-foundation-structure simulation: (a) Tower and foundation. (b) Tower, foundation, and mass. (Courtesy of Lisyuk and Ulitsky 2012)

through the finite element method. A typical approach for very large structures consists of the following steps:

1. Carry out load tests with group effect if possible.
2. Calibrate the FEM model to match the load test results.
3. Use the calibrated model to predict the behavior of the complete CPRF.
4. Monitor the construction of the structure to verify predictions and if needed make adjustments.

The result of such an approach appears in Figure 18.83, which shows the load settlement curve of the structure for three different foundation alternatives: mat, pile group, and CPRF. A parallel economic study can be used along with tolerable movements to decide which solution is both economical and safe.

The future of foundation engineering is in the use of the FEM with the goal of modeling the soil, the foundation, and the structure all in one model. An example of such approach is shown in Figure 18.84. Note that the unit weight of a building typically ranges between 2.5 and 5 kN/m³ and is therefore a small fraction of the soil unit weight. As such, buildings are much lighter than soil for a given volume. This is why it is very advantageous to place basements in a building, as the weight of soil excavated for one story is equal to 5 to 10 stories of building. For example, a 20-story building with 3 levels of underground parking garages could well be as heavy as the soil removed to create the underground parking garages. In this case the settlement is limited to the recompression of the soil that expanded upon excavation.

PROBLEMS

- 18.1 In cross hole logging of a bored pile, the speed v of the compression wave is measured.
 - a. If $v = 4000$ m/s how good is the concrete?
 - b. If $v = 3500$ m/s how good is the concrete?
 - c. If $v = 3000$ m/s how good is the concrete?
- 18.2 Draw a typical and clean record of velocity signal in a sonic echo test on a bored pile with a necking defect. Repeat the question for a bored pile with a bulb defect.
- 18.3 Use the pile driving equation to obtain the rated energy of a diesel hammer necessary to drive a pile with an ultimate resistance at the time of driving of 1000 kN to a penetration rate of 4 mm/blow. Assume that the diesel hammer has an efficiency of 0.5.
- 18.4 Calculate in km/h how fast the compression wave generated by the hammer blow from problem 18.3 propagates in a steel pile, in a concrete pile, and in a timber pile. If the pile is 20 m long, how much time does it take for the wave to go down to the bottom of the pile and back up to the top?
- 18.5 A hammer impacts a concrete pile with a 0.25 m² cross section and generates a particle velocity at the top of the pile equal to 3 m/s. Calculate the force and then the compressive stress in the concrete at the pile head.
- 18.6 The ultimate static soil resistance of a short, relatively rigid pile in silt is 800 kN with 500 kN of friction and 300 kN of point resistance. Calculate the ultimate dynamic soil resistance if the pile velocity is 4 m/s.
- 18.7 Show all calculations leading to the wave equation numbers populating Table 18.5.
- 18.8 Develop the theoretical expression of the residual load in a driven pile for the following conditions. The initial condition is the stress and load distribution in the pile at failure. The ultimate skin friction is f_u and the ultimate point pressure is p_u . The ultimate load at the top of the pile is R_u and the ultimate load at the point is R_{pu} . The unloading of the friction and point transfer curve is assumed to obey the linear elastic model shown in Figure 18.1s.

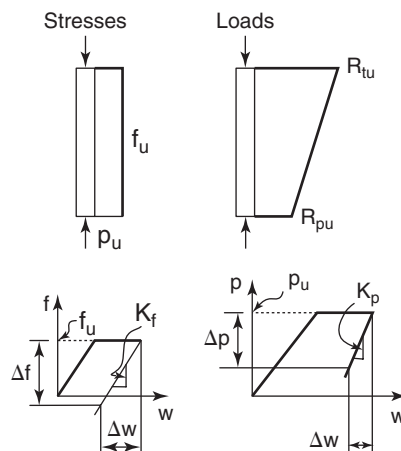


Figure 18.1s Initial conditions and models for residual loads.

- 18.9 Explain Figures 18.21 and 18.22 in your own words.
- 18.10 A pile is driven and the force (F) and particle velocity time impedance ($v \times EA/c$) at the top of the pile are measured as shown in Figure 18.2s. Calculate the dynamic resistance of the pile using the observations at times t_1 and t_2 separated by the down and up travel time of the wave ($2L/c$) and the Case method.

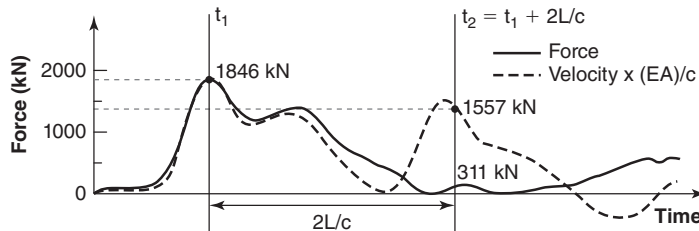


Figure 18.2s Force and velocity signal.

- 18.11 Calculate the static resistance of the pile in problem 18.10 by the Case method.
- 18.12 Is it possible to break a concrete pile in tension by driving it in the ground? If yes, explain how.
- 18.13 A suction caisson is 20 m long and 2 m by 2 m in cross section with a wall thickness of 20 mm. It is made of steel and is to be installed in a soft clay with an undrained shear strength of 20 kPa. Calculate the ultimate capacity of the caisson and the underpressure required to install it to full penetration. Check that this underpressure does not create inverse bearing capacity failure.

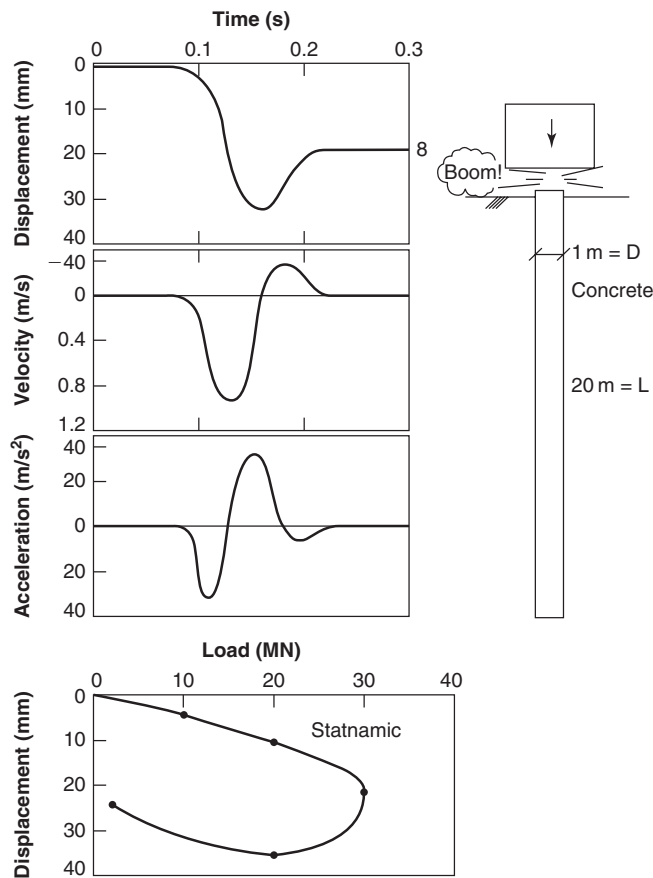


Figure 18.3s Statnamic test results.

- 18.14 Calculate the strain, the stress, and the friction on each segment of the pile shown in Figure 18.29 for the maximum load applied. How would you measure such values? The pile is a bored pile 1 m in diameter and made of concrete.

- 18.15 Calculate the slope of the load transfer curves for the axially loaded pile discussed in section 18.4.3 and verify the value of the movement necessary to reach the maximum friction and point resistance shown in Figure 18.43. Generate a spreadsheet to develop the complete load settlement curve of this axially loaded pile.
- 18.16 Calculate the ultimate static capacity of the pile subjected to the Statnamic test. The pile is a 1 m diameter, 20 m long bored concrete pile. The test results are summarized in Figure 18.3s.
- 18.17 Calculate the ultimate capacity of the two piles shown in Figure 18.4s by all possible methods. The pile in clay is a circular bored pile and the pile in sand is a square driven pile. At what depth along the pile would you place the Osterberg load cell to balance the load on both sides of the pile at ultimate load?

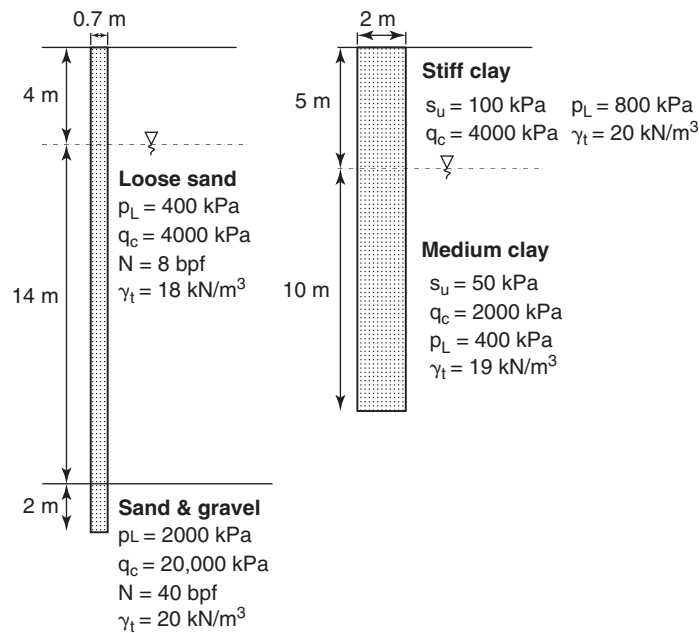


Figure 18.4s Ultimate capacity of two piles.

- 18.18 For the pile of Figure 18.43, find the top movement and the load distribution in the pile for a point movement of 5 mm.
- 18.19 A 16-story hospital weighs 1500 MN, and its imprint is 75 m by 75 m. The building rests on 10,000 timber piles, each 15 m long, 0.3 m in average diameter, and driven with a spacing of 0.75 m center to center. The soil is made of a clay layer down to 14.5 m ($s_u = 20 \text{ kN/m}^2$, $e_o = 0.8$, and $C_c = 0.1$), then a sand layer down to 16.5 m ($N = 30 \text{ bpf}$), and then clay again down to a depth of 100 m ($s_u = 30 \text{ kN/m}^2$, $e_o = 0.7$, and $C_c = 0.06$). The water table is at the ground surface and the total unit weight of all soils is 20 kN/m^3 . Calculate:
- The capacity of one timber pile
 - The capacity of the pile group
 - The settlement of the hospital
 - Comment on this design.
- 18.20 Calculate the group efficiency for settlement using Poulos interaction factors for the case of a flexible pile cap (all piles carry the same load). The group is 4 by 4 with a 3-pile diameter center-to-center spacing.
- 18.21 If the uncoated pile subjected to downdrag in Figure 18.54 was pushed into the ground 100 mm at the pile top, what would be:
- The new position of the neutral point?
 - The load at the top of the pile?
 - The load distribution in the pile?
- 18.22 A bored pile foundation is used for a house on a shrink-swell soil. The piles are 0.5 m in diameter, the load per pile is 50 kN, and the zone of active movement from one season to the next extends from the ground surface to a depth of 3 m. The soil is a very stiff clay with an undrained shear strength of 120 kPa and a total unit weight of 20 kN/m^3 . The groundwater level is at a depth of 10 m. How deep should each bored pile be to minimize the potential uneven movement of the house?

18.23 For the long flexible pile shown in Figure 18.5s, calculate:

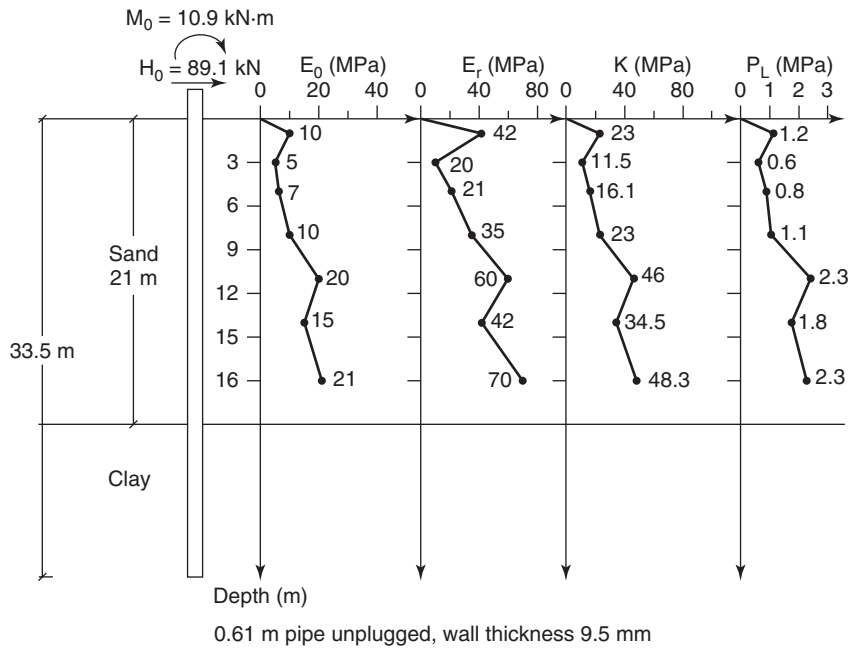


Figure 18.5s Long flexible pile loaded horizontally.

- The ultimate load H_{ou}
- The deflection and slope at the ground surface under the working load
- The maximum bending moment under the working load
- The factor of safety against yielding of the soil near the ground surface under the working load

18.24 For the short rigid pile shown in Figure 18.6s, calculate:

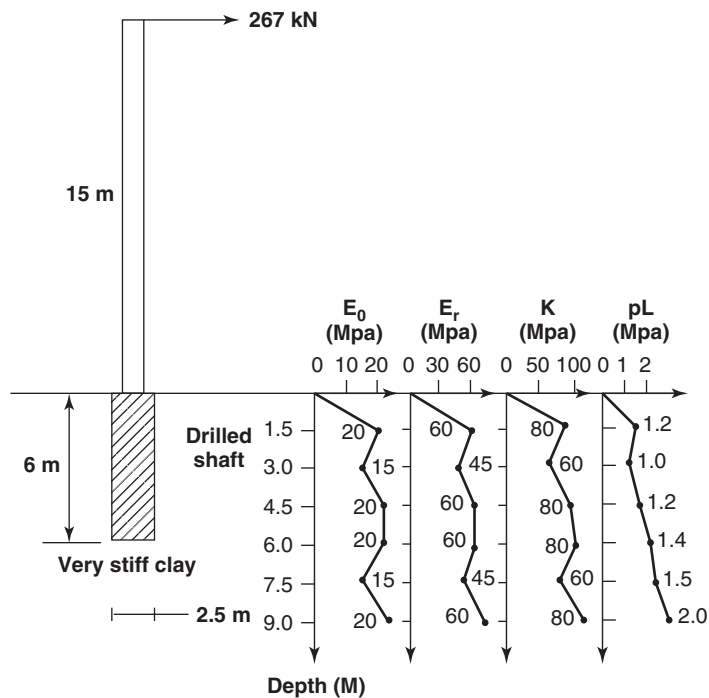


Figure 18.6s Short rigid pile loaded horizontally.

- a. The ultimate load H_{ou}
 - b. The deflection and slope at the ground surface under the working load
 - c. The maximum bending moment under the working load
 - d. The factor of safety against yielding of the soil near the ground surface under the working load
- 18.25 Calculate z_{\max} for a flexible pile and a rigid pile if the pile is subjected to a horizontal load only (H_o different from 0 but M_o equal to 0).
- 18.26 Calculate the ratio between the ground surface displacement for a free-head condition and for a fixed-head condition. Do the calculation first for a flexible pile and then for a rigid pile.
- 18.27 For the pile group shown in Figure 18.75, calculate the efficiency of the group if it is loaded horizontally in a direction perpendicular to the four-pile line.
- 18.28 The pile group of Figure 18.75 is subjected to an overturning moment of 10 MN.m in the direction of largest resistance to overturning of the group. The piles are 0.4 by 0.4 square concrete driven piles embedded 25 m in a loose sand with a blow count of 6 bpf. What will be the ratio between the applied tension load and the ultimate tension capacity of the most loaded pile in the group?
- 18.29 A steel pipe pile has a diameter D equal to 0.61 m and a wall thickness t equal to 9.5 mm. The pile is 33.5 m long and the steel has a modulus E equal to 200 GPa. The pile is loaded horizontally with a load H_o of 89 kN in fixed-head condition. The soil is characterized by stiffness coefficient K from pressuremeter tests equal to 25,000 kPa. Plot the profiles versus depth of the deflection, slope, shear, bending moment, and line load in the pile.

Problems and Solutions

Problem 18.1

In cross hole logging of a bored pile, the speed v of the compression wave is measured.

- a. If $v = 4000$ m/s, how good is the concrete?
- b. If $v = 3500$ m/s, how good is the concrete?
- c. If $v = 3000$ m/s, how good is the concrete?

Solution 18.1

- a. If $v = 4000$ m/s, the concrete is good.
- b. If $v = 3500$ m/s, the concrete is questionable.
- c. If $v = 3000$ m/s, the concrete is poor or there is a defect in the pile.

Problem 18.2

Draw a typical and clean record of velocity signal in a sonic echo test on a bored pile with a necking defect. Repeat the question for a bored pile with a bulb defect.

Solution 18.2

- a. Necking defect

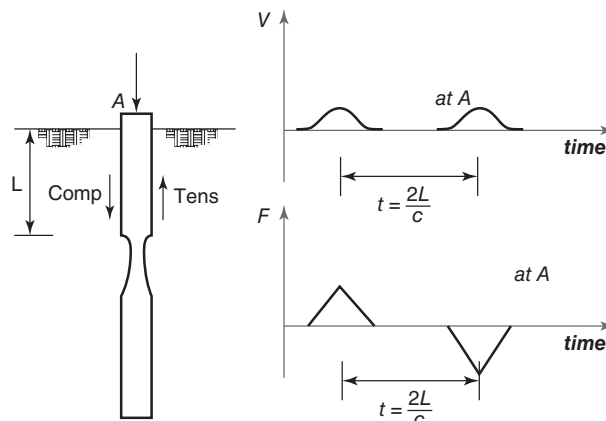


Figure 18.7s Necking defect.

b. Bulb defect

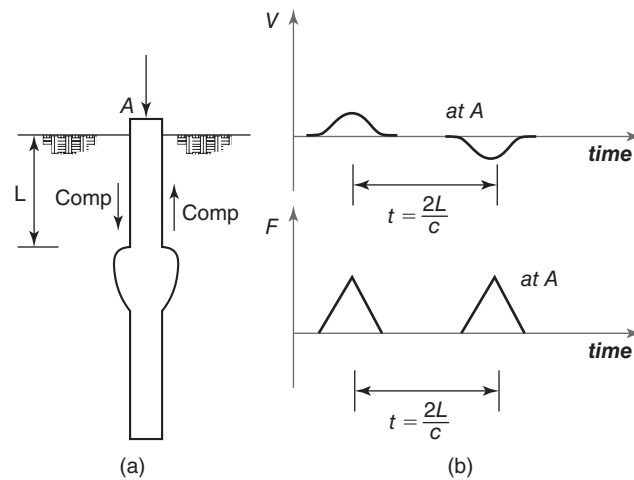


Figure 18.8s Bulb defect.

Problem 18.3

Use the pile driving equation to obtain the rated energy of a diesel hammer necessary to drive a pile with an ultimate resistance at the time of driving of 1000 kN to a penetration rate of 4 mm/blow. Assume that the diesel hammer has an efficiency of 0.5.

Solution 18.3

$$R_{ud} = \frac{eWh}{s + \frac{c}{2}} = \frac{eWh}{s + 2.5}$$

$$Wh = \frac{R_{ud} \times (s + 2.5)}{e}$$

$$Wh = \frac{1000 \times (4 + 2.5)}{0.5}$$

$$Wh = \frac{1000 \times (4 + 2.5)}{0.5}$$

$$Wh = 13000 \text{ kN.m} = 13000 \text{ kJ}$$

Problem 18.4

Calculate in km/h how fast the compression wave generated by a hammer blow propagates in a steel pile, in a concrete pile, and in a timber pile. If the pile is 20 m long, how much time does it take for the wave to go down to the bottom of the pile and back up to the top?

Solution 18.4

The wave speed for a given material can be calculated using the following formula:

$$c = \sqrt{\frac{E}{\rho}}$$

For steel : $E = 2 \times 10^8$ kPa and $\rho = 7850$ kg/m³

For concrete : $E = 2 \times 10^7$ kPa and $\rho = 2400$ kg/m³

For wood : $E = 1 \times 10^7$ kPa and $\rho = 800$ kg/m³

$$c_{steel} = \sqrt{\frac{2 \times 10^{11}}{7850}} = 5047.5 \text{ m/sec.} \quad \therefore \quad 18171.2 \text{ km/hr.}$$

$$c_{concrete} = \sqrt{\frac{2 \times 10^{10}}{2400}} = 2886.8 \text{ m/sec.} \quad \therefore \quad 10392.3 \text{ km/hr.}$$

$$c_{timber} = \sqrt{\frac{1 \times 10^{10}}{800}} = 3535.5 \text{ m/sec.} \quad \therefore \quad 12727.9 \text{ km/hr.}$$

The time it takes for the wave to go down to the bottom of the pile and back up to the top can be calculated as:

$$t = \frac{2L}{c}$$

$$t_{steel} = \frac{2 \times 20}{5047.5} = 0.00792 \text{ sec.}$$

$$t_{concrete} = \frac{2 \times 20}{2886.8} = 0.01386 \text{ sec.}$$

$$t_{timber} = \frac{2 \times 20}{3535.5} = 0.01131 \text{ sec.}$$

Problem 18.5

A hammer impacts a concrete pile with a 0.25 m² cross section and generates a particle velocity at the top of the pile equal to 3 m/s. Calculate the force and then the compressive stress in the concrete at the pile head.

Solution 18.5

Using the results of $c = 2886$ m/sec. computed in problem 18.4 for a concrete pile, the force can be estimated using the following formula:

$$F = \frac{EA}{c}v$$

$$F = \frac{2 \times 10^7 \text{ kPa} \times 0.25 \text{ m}^2}{2886 \text{ m/sec.}} \times 3 \text{ m/sec.} = 5198 \text{ kN}$$

The compressive stress in the pile head is:

$$\sigma = \frac{F}{A} = \frac{5198 \text{ kN}}{0.25 \text{ m}^2} = 20792 \text{ kPa}$$

Problem 18.6

The ultimate static soil resistance of a short, relatively rigid pile in silt is 800 kN with 500 kN of friction and 300 kN of point resistance. Calculate the ultimate dynamic soil resistance if the pile velocity is 4 m/s.

Solution 18.6

The dynamic soil resistance of the soil is obtained using Eq. 18.30 and assuming rigid body motion of the pile:

$$R_{DYN} = R_{STA_p}(1 + J_p v) + R_{STA_f}(1 + J_f v)$$

where R_{STA} is 800 kN, v is 4 m/s, J is 0.65 m/s for fine-grained soils and side damping, and J is 0.50 m/s for fine-grained soils and point damping (from Table 18.2). The ultimate dynamic soil resistance is:

$$R_{DYN} = 500(1 + 0.65 \times 4) + 300(1 + 0.50 \times 4) = 2700 \text{ kN}$$

Problem 18.7

Show all calculations leading to the wave equation numbers populating Table 18.5.

Solution 18.7

Figure 18.18 gives the pile details. The calculations for all the numbers in Table 18.1s (Table 18.5 earlier in the chapter) are shown in this solution. Some conditions that must be satisfied for all calculations are:

- $F(1, t)$ is always ≥ 0 , because no tension can be developed between the hammer and the pile head
- $F(3, t)_s$ is always ≤ 500 , because of the maximum point resistance

Table 18.1s Wave Equation Calculations

| | 1 | 2 | 3 | 4 | 5 | 6 | 7 |
|---|-------------|------|----------|----------|----------|----------|----------|
| A | Time | s | 0.0000 | 0.0005 | 0.0010 | 0.0015 | 0.0020 |
| B | $D(1, t)$ | mm | 0.000 | 1.500 | 2.834 | 3.897 | 4.672 |
| C | $D(2, t)$ | mm | 0.000 | 0.000 | 0.368 | 1.296 | 2.708 |
| D | $D(3, t)$ | mm | 0.000 | 0.000 | 0.000 | 0.045 | 0.241 |
| E | $C(1, t)$ | mm | 0.000 | 1.500 | 2.467 | 2.601 | 1.964 |
| F | $C(2, t)$ | mm | 0.000 | 0.000 | 0.368 | 1.250 | 2.467 |
| G | $F(1, t)$ | kN | 0.000 | 1350.000 | 2219.923 | 2341.013 | 1767.614 |
| H | $F(2, t)$ | kN | 0.000 | 0.000 | 165.544 | 562.706 | 1110.058 |
| I | $R(3, t)_s$ | kN | 0.000 | 0.000 | 0.000 | 9.022 | 48.211 |
| J | $R(3, t)_d$ | kN | 0.000 | 0.000 | 0.000 | 9.185 | 51.990 |
| K | $V(1, t)$ | mm/s | 3000.000 | 2668.913 | 2124.476 | 1550.343 | 1116.836 |
| L | $V(2, t)$ | mm/s | 0.000 | 735.750 | 1855.387 | 2824.564 | 3182.932 |
| M | $V(3, t)$ | mm/s | 0.000 | 0.000 | 90.221 | 391.890 | 968.537 |

At $t = 0$ s:

$$V(1, 0) = 3000 \text{ mm/s}$$

At $t = 0.0005$ s:

$$D(1, 0.0005) = D(1, 0) + V(1, 0)\Delta t = 0 + 3000 \times 0.0005 = 1.50 \text{ mm}$$

$$D(2, 0.0005) = D(2, 0) + V(2, 0)\Delta t = 0 \text{ mm}$$

$$D(3, 0.0005) = D(3, 0) + V(3, 0)\Delta t = 0 \text{ mm}$$

$$C(1, 0.0005) = D(1, 0.0005) - D(2, 0.0005) = 1.50 \text{ mm}$$

$$C(2, 0.0005) = D(2, 0.0005) - D(3, 0.0005) = 0.00 \text{ mm}$$

$$F(1, 0.0005) = K_1 \times C(1, 0.0005) = 900 (1.50) = 1350 \text{ kN}$$

$$F(2, 0.0005) = K_2 \times C(2, 0.0005) = 450 (0) = 0 \text{ kN}$$

$$F(3, 0.0005)_s = K'_s \times D(3, 0.0005) = 200 (0) = 0 \text{ kN}$$

$$F(3, 0.0005)_d = F(3, 0.0005)_s \times (1 + J_s \times V(3, 0)) = 0 \times (1 + 0.0002 (0)) = 0 \text{ kN}$$

$$\begin{aligned}
 V(1, 0.0005) &= V(1, 0) + (0 - F(1, 0.0005)) \frac{g\Delta t}{W_H} \\
 &= 3000 + \left((0 - 1350) \times \frac{9.81 \times 0.0005}{20} \times 1000 \right) = 2668.913 \text{ mm/s}
 \end{aligned}$$

$$\begin{aligned}
 V(2, 0.0005) &= V(2, 0) + (F(1, 0.0005) - F(2, 0.0005)) \frac{g\Delta t}{W_1} \\
 &= 0 + \left((1350 - 0) \times \frac{9.81 \times 0.0005}{9} \times 1000 \right) = 735.750 \text{ mm/s} \\
 &= 0 + \left((0 - 0) \times \frac{9.81 \times 0.0005}{9} \times 1000 \right) = 0 \text{ mm/s}
 \end{aligned}$$

At $t = 0.0010$ s:

$$D(1, 0.0010) = D(1, 0.0005) + V(1, 0.0005)\Delta t = 1.50 + 2668.9 \times 0.0005 = 2.834 \text{ mm}$$

$$D(2, 0.0010) = D(2, 0.0005) + V(2, 0.0005)\Delta t = 0 + 735.75 \times 0.0005 = 0.368 \text{ mm}$$

$$D(3, 0.0010) = D(3, 0.0005) + V(3, 0.0005)\Delta t = 0 \text{ mm}$$

$$C(1, 0.0010) = D(1, 0.0010) - D(2, 0.0010) = 2.83 - 0.37 = 2.467 \text{ mm}$$

$$C(2, 0.0010) = D(2, 0.0010) - D(3, 0.0010) = 0.368 \text{ mm}$$

$$F(1, 0.0010) = K_1 \times C(1, 0.0010) = 900 (2.467) = 2219.923 \text{ kN}$$

$$F(2, 0.0010) = K_2 \times C(2, 0.0010) = 450 (0.368) = 165.544 \text{ kN}$$

$$F(3, 0.0010)_s = K' \times D(3, 0.0010) = 200 (0) = 0 \text{ kN}$$

$$F(3, 0.0010)_d = F(3, 0.0010)_s \times (1 + J_s \times V(3, 0.0005)) = 0 \times (1 + 0.0002 (0)) = 0 \text{ kN}$$

$$\begin{aligned}
 V(1, 0.0010) &= V(1, 0.0005) + (0 - F(1, 0.0010)) \frac{g\Delta t}{W_H} \\
 &= 2668.913 + \left((0 - 2219.923) \times \frac{9.81 \times 0.0005}{20} \times 1000 \right) = 2124.476 \text{ mm/s}
 \end{aligned}$$

$$\begin{aligned}
 V(2, 0.0010) &= V(2, 0.0005) + (F(1, 0.0010) - F(2, 0.0010)) \frac{g\Delta t}{W_1} \\
 &= 735.750 + \left((2219.923 - 165.544) \times \frac{9.81 \times 0.0005}{9} \times 1000 \right) = 1855.387 \text{ mm/s}
 \end{aligned}$$

$$\begin{aligned}
 V(3, 0.0010) &= V(3, 0.0005) + (F(2, 0.0010) - F(3, 0.0010)) \frac{g\Delta t}{W_2} \\
 &= 0 + \left((165.544 - 0) \times \frac{9.81 \times 0.0005}{9} \times 1000 \right) = 90.221 \text{ mm/s}
 \end{aligned}$$

At $t = 0.0015$ s:

$$D(1, 0.0015) = D(1, 0.0010) + V(1, 0.0010)\Delta t = 2.834 + 2124.476 \times 0.0005 = 3.897 \text{ mm}$$

$$D(2, 0.0015) = D(2, 0.0010) + V(2, 0.0010)\Delta t = 0.368 + 1855.387 \times 0.0005 = 1.296 \text{ mm}$$

$$D(3, 0.0015) = D(3, 0.0010) + V(3, 0.0010)\Delta t = 0 + 90.221 \times 0.0005 = 0.045 \text{ mm}$$

$$C(1, 0.0015) = D(1, 0.0015) - D(2, 0.0015) = 3.896 - 1.296 = 2.601 \text{ mm}$$

$$C(2, 0.0015) = D(2, 0.0015) - D(3, 0.0015) = 1.296 - 0.045 = 1.250 \text{ mm}$$

$$F(1, 0.0015) = K_1 \times C(1, 0.0015) = 900 (2.601) = 2341.013 \text{ kN}$$

$$F(2, 0.0015) = K_2 \times C(2, 0.0015) = 450 (1.251) = 562.706 \text{ kN}$$

$$F(3, 0.0015)_s = K' \times D(3, 0.0015) = 200 (0.045) = 9.022 \text{ kN}$$

$$\begin{aligned} F(3, 0.0015)_d &= F(3, 0.0015)_s \times (1 + J_s \times V(3, 0.0010)) \\ &= 9.022 \times (1 + 0.0002 (90.221)) = 9.185 \text{ kN} \end{aligned}$$

$$\begin{aligned} V(1, 0.0015) &= V(1, 0.0010) + (0 - F(1, 0.0015)) \frac{g\Delta t}{W_H} \\ &= 2124.476 + \left((0 - 2341.013) \times \frac{9.81 \times 0.0005}{20} \times 1000 \right) = 1550.343 \text{ mm/s} \end{aligned}$$

$$\begin{aligned} V(2, 0.0015) &= V(2, 0.0010) + (F(1, 0.0015) - F(2, 0.0015)) \frac{g\Delta t}{W_1} \\ &= 1855.387 + \left((2341.013 - 562.706) \times \frac{9.81 \times 0.0005}{9} \times 1000 \right) = 2824.564 \text{ mm/s} \end{aligned}$$

$$\begin{aligned} V(3, 0.0015) &= V(3, 0.0010) + (F(2, 0.0015) - F(3, 0.0015)) \frac{g\Delta t}{W_2} \\ &= 90.221 + \left((562.706 - 9.185) \times \frac{9.81 \times 0.0005}{9} \times 1000 \right) = 391.890 \text{ mm/s} \end{aligned}$$

At $t = 0.0020$ s:

$$D(1, 0.0020) = D(1, 0.0015) + V(1, 0.0015)\Delta t = 3.897 + 1550.343 \times 0.0005 = 4.672 \text{ mm}$$

$$D(2, 0.0020) = D(2, 0.0015) + V(2, 0.0015)\Delta t = 1.296 + 2824.564 \times 0.0005 = 2.708 \text{ mm}$$

$$D(3, 0.0020) = D(3, 0.0015) + V(3, 0.0015)\Delta t = 0.045 + 391.890 \times 0.0005 = 0.241 \text{ mm}$$

$$C(1, 0.0020) = D(1, 0.0020) - D(2, 0.0020) = 4.672 - 2.708 = 1.964 \text{ mm}$$

$$C(2, 0.0020) = D(2, 0.0020) - D(3, 0.0020) = 2.708 - 0.241 = 2.467 \text{ mm}$$

$$F(1, 0.0020) = K_1 \times C(1, 0.0020) = 900 (1.964) = 1767.614 \text{ kN}$$

$$F(2, 0.0020) = K_2 \times C(2, 0.0020) = 450 (2.467) = 1110.058 \text{ kN}$$

$$F(3, 0.0020)_s = K' \times D(3, 0.0020) = 200 (0.241) = 48.211 \text{ kN}$$

$$\begin{aligned} F(3, 0.0020)_d &= F(3, 0.0020)_s \times (1 + J_s \times V(3, 0.0015)) \\ &= 48.211 \times (1 + 0.0002 (391.890)) = 51.990 \text{ kN} \end{aligned}$$

$$\begin{aligned} V(1, 0.0020) &= V(1, 0.0015) + (0 - F(1, 0.0020)) \frac{g\Delta t}{W_H} \\ &= 1550.343 + \left((0 - 1767.614) \times \frac{9.81 \times 0.0005}{20} \times 1000 \right) = 1116.836 \text{ mm/s} \end{aligned}$$

$$\begin{aligned} V(2, 0.0020) &= V(2, 0.0015) + (F(1, 0.0020) - F(2, 0.0020)) \frac{g\Delta t}{W_1} \\ &= 2824.564 + \left((1767.614 - 1110.058) \times \frac{9.81 \times 0.0005}{9} \times 1000 \right) = 3182.932 \text{ mm/s} \end{aligned}$$

$$\begin{aligned} V(3, 0.0020) &= V(3, 0.0015) + (F(2, 0.0020) - F(3, 0.0020)) \frac{g\Delta t}{W_2} \\ &= 391.890 + \left((1110.058 - 51.990) \times \frac{9.81 \times 0.0005}{9} \times 1000 \right) = 968.537 \text{ mm/s} \end{aligned}$$

Problem 18.8

Develop the theoretical expression of the residual load in a driven pile for the following conditions. The initial condition is the stress and load distribution in the pile at failure. The ultimate skin friction is f_u and the ultimate point pressure is p_u . The ultimate load at the top of the pile is R_u and the ultimate load at the pile point is R_{pu} . The unloading of the friction and point transfer curve is assumed to obey the linear elastic model shown in Figure 18.1s.

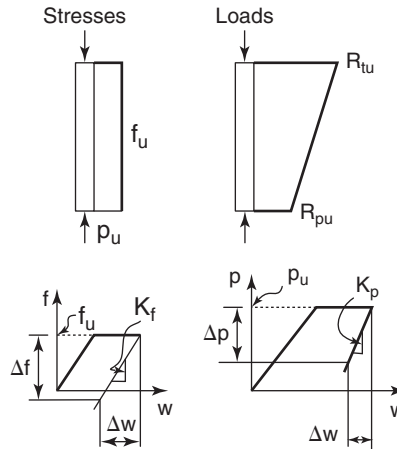


Figure 18.1s Initial conditions and models for residual loads.

Solution 18.8

Residual loads are loads that are locked in upon unloading after the pile has been brought to the ultimate soil resistance during driving or load testing. Therefore, the theoretical analysis takes, as an initial condition, the stress and load distribution in the pile at failure. The ultimate skin friction is f_u and the ultimate point resistance is p_u . The ultimate load at the pile head is R_{tu} and the ultimate load at the pile point is R_{pu} . The load anywhere in the pile is R_u . The unloading of the friction is assumed to obey the linear elastic model, which gives the following equation:

$$\Delta f = K_f \Delta w$$

in which Δf = decrease in pile-soil friction stress at depth z ; K_f' = unloading stiffness in friction; and Δw = upward movement of the pile upon unloading at depth z . Similarly, the unloading of the point follows the equation:

$$\Delta p = K_p' \Delta w_p$$

in which Δp = decrease in point resistance; K_p' = unloading stiffness for the point; and Δw_p = upward movement of the pile at the point upon unloading. The equilibrium equation of the elementary pile element can be written as follows:

$$-\frac{\partial \Delta \sigma}{\partial z} - \frac{P}{A} \Delta \tau = 0$$

in which $\Delta \sigma$ = normal stress decrease in the pile at depth z ; A = cross-sectional area of the pile; and P = perimeter of the pile. The constitutive equation for the pile is:

$$\Delta \sigma = E_p \Delta \varepsilon = -E_p \frac{\partial \Delta w}{\partial z}$$

in which E_p = pile modulus of elasticity and $\Delta \varepsilon$ = change in normal strain at depth z due to stress change. The solution to the previous equation gives the residual load, R_r , in the pile at a depth z :

$$R_r = R_u - R_{tu} \left[\frac{(E_p \Omega + K_p') e^{\Omega(L-z)} - (E_p \Omega - K_p') e^{-\Omega(L-z)}}{(E_p \Omega + K_p') e^{\Omega L} - (E_p \Omega - K_p') e^{-\Omega L}} \right]$$

in which L = length of the pile, z = depth at which R_r exists, and $\Omega = \sqrt{K_f' P / E_p A}$.

The residual point load, R_{pr} , is:

$$R_{pr} = R_{pu} - \frac{2R_{tu}}{\left(1 + \frac{E_p \Omega}{K'_p}\right) e^{\Omega L} + \left(1 - \frac{E_p \Omega}{K'_p}\right) e^{-\Omega L}}$$

Problem 18.9

Explain Figures 18.21 and 18.22 in your own words.

Solution 18.9

Imagine a pile suspended horizontally from the ceiling and hit at one end (Figure 18.21). There is no soil surrounding it and the end of the pile is free. In this case the compression force in the pile will be proportional to the particle velocity ($F = Iv$, from Eq. 18.23). Now the wave is racing along the pile at the wave speed c . When it gets to the end of the pile, the compression force F finds no resistance and reflects as a tension force, but the magnitude of the particle velocity doubles while the wave speed is unchanged (see Eqs. 18.24 to 18.26). This is similar to a case of easy driving with very little point resistance.

Now let's say that the pile is still suspended from the ceiling, but the other end is against a strong wall (Figure 18.22) and the pile is hit at one end. When the compression wave gets to the wall, it cannot displace it. As a result, the compression force doubles, the velocity vanishes, and the F and Iv signals are as shown in Figure 18.22. Equations 18.24 to 18.26 give the mathematical reason. This approximates hard driving into a strong bearing layer.

Problem 18.10

A pile is driven and the force (F) and particle velocity time impedance ($v \times EA/c$) at the top of the pile are measured as shown in Figure 18.2s. Calculate the dynamic resistance of the pile using the observations at times t_1 and t_2 separated by the down and up travel time of the wave ($2L/c$) and the Case method.

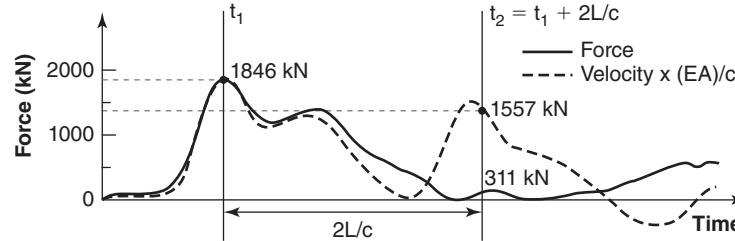


Figure 18.2s Force and velocity signal.

Solution 18.10

From the plot shown in Figure 18.2s:

$$t_1 = t_1$$

$$t_2 = t_1 + 2L/c$$

$$F_{(t_1)} = 1846 \text{ kN}$$

$$F_{(t_1+2L/c)} = 311 \text{ kN}$$

$$V_{(t_1)} \times \frac{EA}{c} = 1846 \text{ kN}$$

$$V_{(t_1+2L/c)} \times \frac{EA}{c} = 1557 \text{ kN}$$

The dynamic resistance of the pile can be computed as:

$$R_D = \frac{1}{2}(F_{(t_1)} + F_{(t_1+2L/c)}) + I(v_{(t_1)} - v_{(t_1+2L/c)})$$

$$R_D = \frac{1}{2}(F_{(t_1)} + F_{(t_1+2L/c)}) + \frac{EA}{c}(v_{(t_1)} - v_{(t_1+2L/c)})$$

$$R_D = \frac{1}{2} \left(F_{(t_1)} + F_{(t_1+2L/c)} + \frac{EA}{c} v_{(t_1)} - \frac{EA}{c} v_{(t_1+2L/c)} \right)$$

$$R_D = \frac{1}{2} (1846 + 311 + 1846 - 1557) = 1223 \text{ kN}$$

Problem 18.11

Calculate the static resistance of the pile in problem 18.10 by the Case method.

Solution 18.11

The static capacity of the pile can be computed as:

$$R_S = R_D - J_c I v$$

$$R_S = R_D - J_c I \left(\frac{F_{(t_1)} + I v_{(t_1)} - R_D}{I} \right)$$

$$R_S = R_D - J_c (F_{(t_1)} + I v_{(t_1)} - R_D)$$

$$R_S = R_D - J_c \left(F_{(t_1)} + \frac{EA}{c} v_{(t_1)} - R_D \right)$$

$$R_S = 1223 - 0.3(1846 + 1846 - 1223) = 482 \text{ kN}$$

Problem 18.12

Is it possible to break a concrete pile in tension by driving it in the ground? If yes, explain how.

Solution 18.12

Yes, it is possible to break a concrete pile in tension if it is not reinforced properly. Driving through a hard layer into a soft layer will generate tension in the pile when the pile point has very little resistance. The compression wave coming down the pile will turn back into a tension wave. The tension stresses created by the tension wave can be large enough to break the pile in tension. This condition should be considered during the design of the pile.

Problem 18.13

A suction caisson is 20 m long and 2 m by 2 m in cross section with a wall thickness of 20 mm. It is made of steel and is to be installed in a soft clay with an undrained shear strength of 20 kPa and an effective unit weight of 10 kN/m³. Calculate the ultimate capacity of the caisson and the underpressure required to install it to full penetration. Check that this underpressure does not create inverse bearing capacity failure.

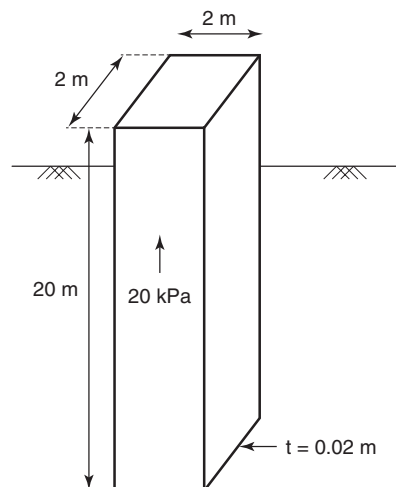
Solution 18.13

Figure 18.9s Suction caisson.

$$R_u = 4 \times 2 \times 20 \times 20 \times 2 + 4 \times 2 \times 0.02 \times (9 \times 20 + 10 \times 20) = 6460.8 \text{ kN}$$

$$W = 4 \times 2 \times 0.02 \times 20 \times 75 = 240 \text{ kN}$$

$$W' = 240 - 4 \times 2 \times 0.02 \times 20 \times 10 = 208 \text{ kN}$$

$$A_{in} = (2 - 0.04)^2 = 3.84 \text{ m}^2$$

$$\Delta u_{rq} = \frac{6460.8 - 208}{3.84} = 1628.33 \text{ kPa}$$

$$\Delta u_{crit} = N_c s_u + \frac{\alpha s_u A_{wall}}{A_{in}} = 9 \times 20 + \frac{1 \times 20 \times 8 \times 20}{3.84} = 1013.3 \text{ kPa}$$

Therefore it is unlikely that the suction caisson can be installed to the required depth of 20 m without some risk of inward bearing capacity failure

Problem 18.14

Calculate the strain, the stress, and the friction on each segment of the pile shown in Figure 18.29 for the maximum load applied. How would you measure such values? The pile is a bored pile 1 m in diameter and made of concrete. Solution 18.14

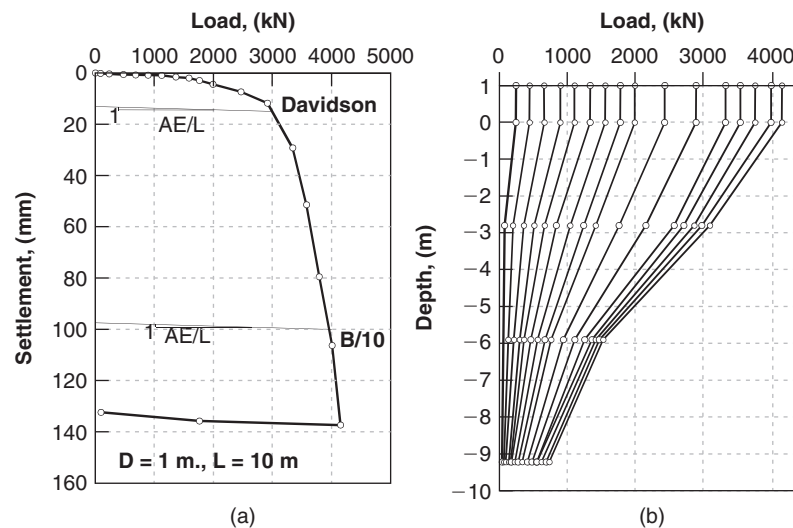


Figure 18.10s Results of an instrumented load test on a bored pile: (a) Load settlement curve. (b) Load versus depth profiles (Briaud et.al. 2000)

$$Area = \pi \frac{D^2}{4} = 0.785 \text{ m}^2$$

- Top load = 4200 kN
- Depth = 0 to 2.8 m, Average load = 3700 kN

$$\sigma_1 = \frac{F}{A} = \frac{3700}{0.785} = 4713 \left(\frac{\text{kN}}{\text{m}^2} \right)$$

$$\varepsilon_1 = \frac{\sigma}{E_{conc}} = \frac{4713}{2.5 \times 10^7} = 0.189 \times 10^{-3}$$

$$f_{u1} = \frac{F_{top} - F_{bot}}{P \times \Delta L} = \frac{4200 - 3200}{3.14 \times 1 \times 2.8} = 114 \left(\frac{\text{kN}}{\text{m}^2} \right)$$

- Depth = 2.8 to 5.8 m, Average load = 2400 kN

$$\sigma_2 = \frac{F}{A} = \frac{2400}{0.785} = 3057 \left(\frac{\text{kN}}{\text{m}^2} \right)$$

$$\varepsilon_2 = \frac{\sigma}{E_{conc}} = \frac{3057}{2.5 \times 10^7} = 0.122 \times 10^{-3}$$

$$f_{u1} = \frac{F_{top} - F_{top}}{P \times \Delta L} = \frac{3200 - 1600}{3.14 \times 1 \times 3} = 167 \left(\frac{\text{kN}}{\text{m}^2} \right)$$

- Depth = 5.8 to 9.2 m, Average load = 1175 kN

$$\sigma_3 = \frac{F}{A} = \frac{1175}{0.785} = 1497 \left(\frac{\text{kN}}{\text{m}^2} \right)$$

$$\varepsilon_3 = \frac{\sigma}{E_{conc}} = \frac{1497}{2.5 \times 10^7} = 0.060 \times 10^{-3}$$

$$f_{u1} = \frac{F_{top} - F_{top}}{P \times \Delta L} = \frac{1600 - 750}{3.14 \times 1 \times 3} = 79.6 \left(\frac{\text{kN}}{\text{m}^2} \right)$$

- Point load = 750 kN. Point pressure:

$$p_u = \frac{F_{point}}{\pi D^2/4} = \frac{750}{3.14 \times 1^2/4} = 955 \left(\frac{\text{kN}}{\text{m}^2} \right)$$

Problem 18.15

Calculate the slope of the load transfer curves for the axially loaded pile discussed in section 18.4.3 and verify the value of the movement necessary to reach the maximum friction and point resistance shown in Figure 18.43. Generate a spreadsheet to develop the complete load settlement curve of this axially loaded pile.

Solution 18.15

The slope of the point load transfer curve is:

$$P_{point} = \frac{4E_s}{\pi D(1 - \nu^2)} s_{point}$$

For the pile of Figure 18.43, $D = 0.3$ m, $E_s = 100,000$ kPa, and $\nu = 0.35$, so the equation becomes:

$$P_{point} = \frac{4 \times 100,000}{\pi \times 0.3(1 - 0.35^2)} s_{point} = 483910 \times s_{point}$$

Because the ultimate point load is 706 kN, the ultimate pressure p_u is:

$$p_u = \frac{706}{\pi \times 0.3^2/4} = 9993 \text{ kPa}$$

Then the displacement necessary to mobilize p_u will be:

$$s_{point} = \frac{p_u}{483910} = 21 \text{ mm}$$

The slope of the friction load transfer curve is:

$$f = \frac{E_s}{(1 + \nu)(1 + \ln(L/D))D} s_{friction}$$

For the pile of Figure 18.43, $D = 0.3$ m, $L = 10$ m, $E_s = 100,000$ kPa for the dense sand layer, and $\nu = 0.35$, so the equation becomes:

$$f = \frac{100,000}{(1 + 0.35)(1 + Ln(10/0.3))0.3} s_{friction} = 54790 \times s_{friction}$$

Because the ultimate friction load over the 1 m of pile in the dense sand layer is 75.4 kN, the ultimate friction f_u is:

$$f_u = \frac{75.4}{\pi \times 0.3 \times 1} = 80 \text{ kPa}$$

Then the displacement necessary to mobilize f_u will be:

$$s_{friction} = \frac{80}{54790} = 1.5 \text{ mm}$$

The same calculations apply to the two locations in the soft clay:

$$f = \frac{5000}{(1 + 0.35)(1 + Ln(10/0.3))0.3} s_{friction} = 2739 \times s_{friction}$$

$$f_u = \frac{84.8}{\pi \times 0.3 \times 4.5} = 20 \text{ kPa}$$

$$s_{friction} = \frac{20}{2739} = 7.3 \text{ mm}$$

The results from an Excel spreadsheet for the load settlement curve are shown in Table 18.2s.

Table 18.2s Load Settlement Curve Results

| Bottom Settlement (mm) | Top Settlement (mm) | Q_{top} (kN) |
|------------------------|---------------------|----------------|
| 0.000 | 0.000 | 0.000 |
| 1.000 | 2.013 | 115.647 |
| 2.000 | 3.696 | 196.891 |
| 3.000 | 5.179 | 257.389 |
| 4.000 | 6.662 | 317.888 |
| 5.000 | 8.145 | 378.387 |
| 8.000 | 12.594 | 559.883 |
| 10.000 | 15.560 | 680.880 |
| 12.000 | 18.526 | 801.877 |
| 15.000 | 22.976 | 983.373 |
| 18.000 | 27.425 | 1164.869 |
| 20.000 | 30.391 | 1285.867 |
| 21.000 | 31.744 | 1333.455 |
| 25.000 | 36.191 | 1427.693 |
| 28.000 | 39.461 | 1471.174 |
| 30.000 | 41.628 | 1494.412 |
| 35.000 | 46.642 | 1496.362 |
| 38.000 | 49.642 | 1496.362 |
| 40.000 | 51.642 | 1496.362 |

The load settlement curve is shown in Figure 18.11s. You can note a slight bend in the load settlement curve when the friction is completely mobilized, at around 270 kN. This is often observed on the load settlement curve in load tests.

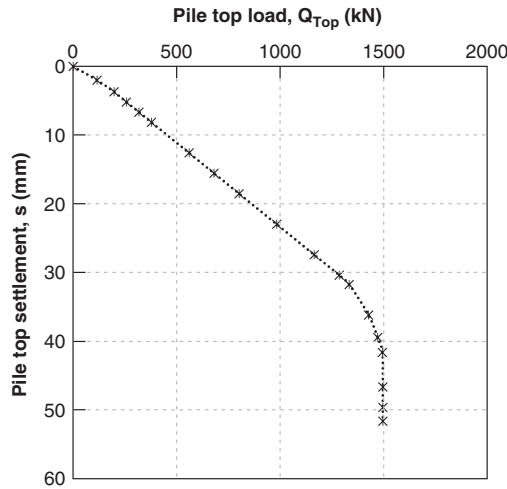


Figure 18.11s Load settlement curve.

Problem 18.16

Calculate the ultimate static capacity of the pile subjected to the Statnamic test. The pile is a 1 m diameter, 20 m long bored concrete pile. The test results are summarized in Figure 18.3s.

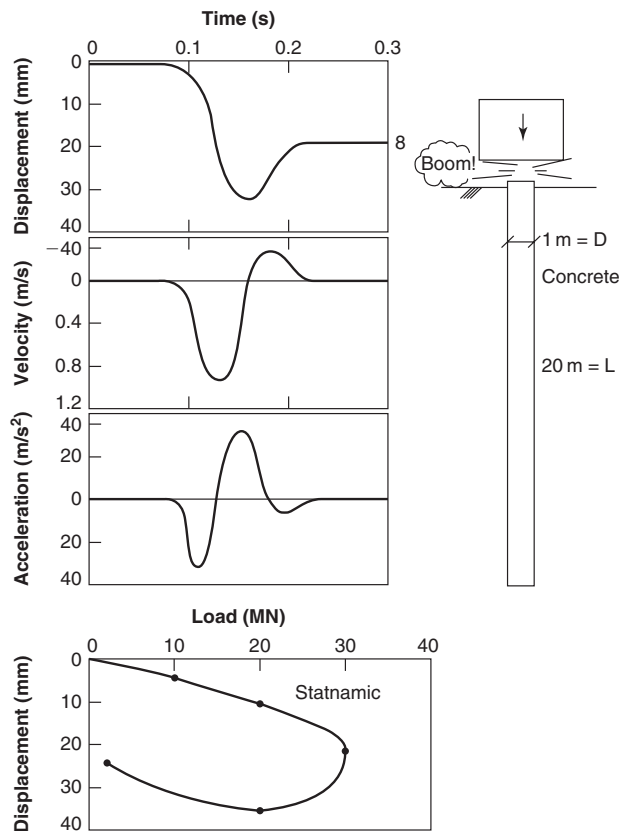


Figure 18.3s Statnamic test results.

Solution 18.16

$$F_{su}(t) = F_{stn}(t) - Ma(t)$$

From Figure 18.3s, the largest displacement during the Statnamic test is 35 mm occurring at time t equal to 0.16 s. At that point the velocity is zero, the acceleration is 33 m/s^2 , and the force is:

$$F_{stn}(t) = 20 \text{ MN}$$

$$a(t) = 33 \text{ m/s}^2$$

$$M = \rho_{conc} V = 2450 \times 20 \times \pi \times (0.5)^2 = 38465 \text{ kg}$$

$$F_{su}(t) = 20000000 - 38465 \times 33 = 18.73 \text{ MN}$$

Problem 18.17

Calculate the ultimate capacity of the two piles shown in Figure 18.4s by all possible methods. The pile in clay is a circular bored pile and the pile in sand is a square driven pile. At what depth along the pile would you place the Osterberg load cell to balance the load on both sides of the pile at ultimate load?

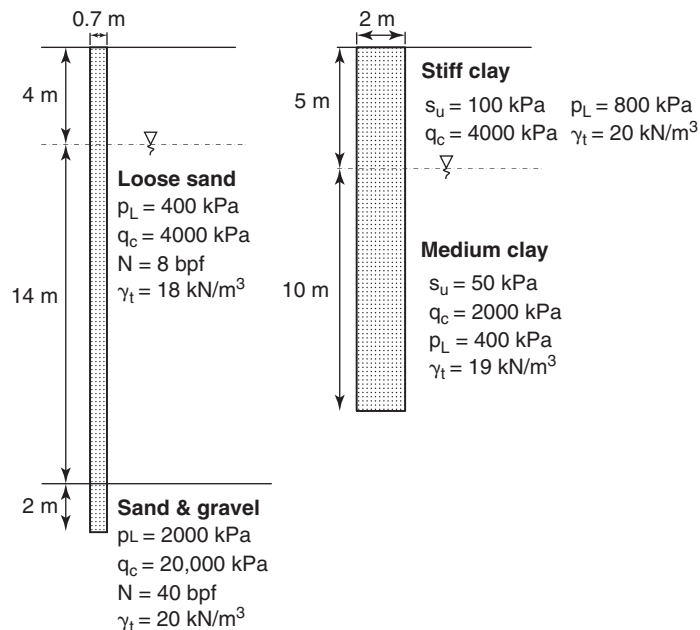


Figure 18.4s Ultimate capacity of two piles.

Solution 18.17**Case #1. Driven square concrete pile in sandy soil**

Pile tip area: $0.7 \text{ m} \times 0.7 \text{ m}$

Layer 1: Loose sand / Layer 2: Sand & gravel

1. Briaud-Tucker SPT method:
 - a. Calculate f_u :

$$f_{u1} = f_{u2} = 5(N)^{0.7} = 5(8)^{0.7} = 21.44 \text{ kPa}$$

$$f_{u3} = 5(N)^{0.7} = 5(40)^{0.7} = 66.1 \text{ kPa}$$

b. Calculate p_u :

$$p_u = 1000(N)^{0.5} = 1000(40)^{0.5} = 6324.6 \text{ kPa}$$

c. Ultimate bearing capacity calculation:

$$\begin{aligned} Q_u &= f_{u1}A_{s1} + f_{u2}A_{s2} + f_{u3}A_{s3} + p_{u2}A_p \\ &= (21.44)(4 \times 0.7 \times 4) + (21.44)(4 \times 0.7 \times 14) + (66.1)(4 \times 0.7 \times 2) + (6324.6)(0.7^2) \\ &= 4548 \text{ (kN)} \end{aligned}$$

2. LPC-PMT method:

a. Classify the soil (Table 18.8):

Layer 1, 2: Sand: loose

Layer 3: Sand and gravel: dense to very dense

b. Pile type being used (Table 18.9): Driven concrete pile, Curve Q2, $\alpha = 1.4$ and $f_{lim} = 130 \text{ kPa}$ for layers 1, 2, and 3.

c. Calculations of f_u :

Layer 1, 2 (Q2, $p_L = 400 \text{ kPa}$): $f_u = \alpha f_{soil} = 1.4 \times 25 = 35 \text{ kPa}$

Layer 3 (Q2, $p_L = 2000 \text{ kPa}$): $f_u = \alpha f_{soil} = 1.4 \times 74 = 103.6 \text{ kPa}$

d. The value of p_u :

k_p value (Table 18.10): 3.1

$$p_u = k_p p_L = 3.1 \times 2000 = 6200 \text{ kPa}$$

e. Ultimate bearing capacity calculation:

$$\begin{aligned} Q_u &= f_{u1}A_{s1} + f_{u2}A_{s2} + f_{u3}A_{s3} + p_{u2}A_p \\ &= (35)(4 \times 0.7 \times 4) + (35)(4 \times 0.7 \times 14) + (103.6)(4 \times 0.7 \times 2) + (6200)(0.7^2) \\ &= 5384 \text{ (kN)} \end{aligned}$$

3. LPC-CPT method:

a. Classify the soil (Table 18.8):

Layer 1, 2: Sand loose

Layer 3: Sand and gravel dense to very dense

b. Pile type being used (Table 18.11): Driven concrete, Curve Q2, $\alpha = 1.0$, and $f_{lim} = 130 \text{ kPa}$ for layers 1, 2, and 3.

c. Calculations of f_u :

Layer 1, 2 (Q3, $q_c = 4000 \text{ kPa}$): $f_u = \alpha f_{soil} = 1.0 \times 47 = 47 \text{ kPa}$ Layer 3 (Q3, $q_c = 20000 \text{ kPa}$): $f_u = \alpha f_{soil} = 1.0 \times 118 = 118 \text{ kPa}$

d. Calculate P_u :

k_c value: 0.4 (Table 18.12)

$$p_u = k_c q_c = 0.4 \times 20000 = 8000 \text{ kPa}$$

e. Ultimate bearing capacity calculation:

$$\begin{aligned} Q_u &= f_{u1}A_{s1} + f_{u2}A_{s2} + f_{u3}A_{s3} + p_{u2}A_p \\ &= (47)(4 \times 0.7 \times 4) + (47)(4 \times 0.7 \times 14) + (118)(4 \times 0.7 \times 2) + (8000)(0.7^2) \\ &= 6950 \text{ (kN)} \end{aligned}$$

4. API-RP2A method for driven piles in coarse-grained soils:

| | σ'_{0v} (kPa) | k | δ | N_q | f_{\max} (kPa) | f_u (kPa) | P_u (kPa) |
|---------|----------------------|-----|----------|-------|------------------|-------------|-------------|
| Layer 1 | 36.0 | 0.8 | 15 | 8 | 48 | 7.7 | |
| Layer 2 | 128.0 | 0.8 | 15 | 8 | 48 | 27.4 | |
| Layer 3 | 194.0 | 0.8 | 25 | 20 | 81 | 72.4 | |
| | 204.0 | | | | | | 4080.0 |

Ultimate bearing capacity calculation:

$$\begin{aligned}
 Q_u &= f_{u1}A_{s1} + f_{u2}A_{s2} + f_{u3}A_{s3} + p_{u2}A_p \\
 &= (7.7)(4 \times 0.7 \times 4) + (27.4)(4 \times 0.7 \times 14) + (72.4)(4 \times 0.7 \times 2) + (4080)(0.7^2) \\
 &= 3565.0 \text{ (kN)}
 \end{aligned}$$

Comparison of bearing capacity:

| Estimation method | f_{u1} (kPa) | f_{u2} (kPa) | Q_{fu12} (kN) | f_{u3} (kPa) | Q_{fu3} (kN) | P_u (kPa) | Q_{pu} (kN) | Q_u (kN) |
|-------------------|----------------|----------------|-----------------|----------------|----------------|-------------|---------------|------------|
| LPC-PMT | 35 | 35 | 1764 | 104 | 582 | 6200 | 3038 | 5384 |
| LPC-CPT | 47 | 47 | 2369 | 118 | 661 | 8000 | 3920 | 6950 |
| Briaud-Tucker | 21.4 | 21.4 | 1079 | 66.1 | 370 | 6325 | 3099 | 4548 |
| API-RP2A | 7.7 | 27.4 | 1160 | 72.4 | 405 | 4080.0 | 1999 | 3564 |
| Average | | | 1593 | | 505 | | 3014 | 5112 |

The average ultimate capacity is 5112kN. Because the average friction capacity is $1593 + 505 = 2098$ kN and the point capacity is 3014 kN, we have to place the O-cell at the bottom of the pile and will be limited to pushing the point capacity to the extent of the friction capacity. Nevertheless, we will be able to push the pile to 82% of its total capacity ($2 \times 2098/5112 = 0.82$).

Case #2. Bored concrete pile in clayey soil

Pile diameter, $d = 2$ m

Bored by dry method

Layer 1: Stiff clay / Layer 2: Medium clay

1. LPC-PMT method:

a. Classify the soil (Table 18.8):

Layer 1: Clay firm

Layer 2: Clay soft to firm

b. Pile type being used (Table 18.9): Bored pile in the dry, Curve Q1, $\alpha = 1.1$, $f_{lim} = 90$ kPa

c. Calculation of f_u :

Layer 1 (Q1, $p_L = 800$ kPa): $f_u = \alpha f_{soil} = 1.1 \times 40 = 44$ kPa

Layer 2 (Q1, $p_L = 400$ kPa): $f_u = \alpha f_{soil} = 1.1 \times 32 = 35.2$ kPa

d. The value of P_u :

k_p value (Table 18.10): 1.1

$$p_u = k_p p_L = 1.15 \times 400 = 460 \text{ kPa}$$

e. Ultimate bearing capacity calculation:

$$Q_u = f_{u1}A_{s1} + f_{u2}A_{s2} + p_{u2}A_p = (44)(\pi \times 2 \times 5) + (35.2)(\pi \times 2 \times 10) + 460 \left(\frac{\pi}{4} \times 2^2 \right) = 5036 \text{ (kN)}$$

2. LPC-CPT method:

a. Classify the soil (Table 18.8):

Layer 1: Clay firm

Layer 2: Clay soft to firm

b. Pile type being used (Table 18.11): Bored pile in the dry, Curve Q1, $\alpha = 0.55$, $f_{im} = 90$ kPa.

c. Calculation of f_u :

Layer 1 (Q1, $q_c = 4000$ kPa): $f_u = \alpha f_{soil} = 0.55 \times 87 = 47.8$ kPa

Layer 2 (Q1, $q_c = 2000$ kPa): $f_u = \alpha f_{soil} = 0.55 \times 55 = 30.2$ kPa

d. Calculate P_u :

k_c value: 0.4 (Table 18.12)

$$p_u = k_c q_c = 0.4 \times 2000 = 800 \text{ kPa}$$

e. Ultimate bearing capacity calculation:

$$Q_u = f_{u1}A_{s1} + f_{u2}A_{s2} + p_{u2}A_p = (47.8)(\pi \times 2 \times 5) + (30.2)(\pi \times 2 \times 10) + 800 \left(\frac{\pi}{4} \times 2^2 \right) = 5910 \text{ (kN)}$$

3. FHWA method for bored piles in fine-grained soils:

a. Calculate f_u and p_u :

Layer 1: $f_u = 0.55s_u = 0.55 \times 100 = 55$ kPa

Layer 2: $f_u = 0.55s_u = 0.55 \times 50 = 27.5$ kPa

$$p_u = N_c s_u = 9 \times 50 = 450 \text{ kPa}$$

(According to bearing capacity factors for clays, after Skempton)

b. Ultimate bearing capacity calculation:

$$Q_u = f_{u1}A_{s1} + f_{u2}A_{s2} + p_{u2}A_p = (55)(\pi \times 2 \times 5) + (27.5)(\pi \times 2 \times 10) + 450 \left(\frac{\pi}{4} \times 2^2 \right) = 4869.5 \text{ (kN)}$$

c. Comparison of bearing capacity:

| Estimation method | f_{u1} (kPa) | Q_{fu1} (kN) | f_{u2} (kPa) | Q_{fu2} (kN) | p_u (kPa) | Q_{pu} (kN) | Q_u (kN) |
|-------------------|-------------------|-------------------|-------------------|-------------------|----------------|------------------|---------------|
| LPC-PMT | 44 | 1381 | 35.2 | 2211 | 460 | 1444 | 5036 |
| LPC-CPT | 47.8 | 1501 | 30.2 | 1897 | 800 | 2512 | 5910 |
| FHWA | 55 | 1727 | 27.5 | 1727 | 450 | 1413 | 4867 |
| Average | | 1536 | 30.9 | 1945 | | 1789 | 5271 |

The average ultimate capacity is 5271 kN. The average friction capacity is $1536 + 1945 = 3481$ kN and the average point capacity is 1789 kN. Therefore, because we have more friction capacity than point capacity, we can place the O-cell along the pile shaft to balance the loads. The position should be such that the point capacity plus some friction is equal to one-half of the total capacity:

$$1769 + 30.9 \times \pi \times 2 \times L_o = \frac{5271}{2} \quad \text{or} \quad L_o = 4.52\text{m}$$

Thus, we should place the O-cell 4.52 meters above the pile point to optimize our chances of reaching failure above and below the O-cell at the same time, thereby testing the pile to its full capacity.

Problem 18.18

For the pile of Figure 18.43, find the top movement and the load distribution in the pile for a point movement of 5 mm.

Solution 18.18

The point load for a point movement of 5 mm is is (Eq. 18.100):

$$Q_{point} = \left(\frac{0.3 \times 10^5}{1 - 0.35^2} \right) \times 0.005 = 170.9 \text{ KN}$$

The friction mobilized in element 1 (from Eq. 18.102) is:

$$f_1 = \frac{10^5}{(1 + 0.35)(1 + \ln(16.3/0.3)) \times 0.3} \times 0.005 = 247.2 \text{ KPa} > 80 \text{ KPa}$$

$$\rightarrow f_1 = 80 \text{ KPa}$$

The load carried in element 1 is:

$$Q_{f1} = f_1 \pi D \Delta L_1 = 80 \times \pi \times 0.3 \times 4 = 301.4 \text{ KN}$$

The movement at the bottom of element 2 is:

$$s_2 = s_p + \frac{\left(Q_p + \frac{Q_{f1}}{2} \right) \Delta L_1}{A_{cs} E_p} = 0.005 + \frac{\left(170.9 + \frac{301.4}{2} \right) 4}{\pi \times 0.3 \times 0.005 \times 2 \times 10^8} = 0.00637 \text{ m} = 6.37 \text{ mm}$$

The friction mobilized in element 2 is:

$$f_2 = \frac{5000}{(1 + 0.35)(1 + \ln(16.3/0.3)) \times 0.3} \times 0.00637 = 4.72 \text{ KPa} < 20 \text{ KPa}$$

The load carried in element 2 is:

$$Q_{f2} = f_2 \pi D \Delta L_2 = 4.72 \times \pi \times 0.3 \times 7.3 = 32.46 \text{ KN}$$

The movement at the bottom of element 3 is:

$$s_3 = s_2 + \frac{\left(Q_p + Q_{f1} + \frac{Q_{f2}}{2} \right) \Delta L_2}{A_{cs} E_p} = 0.00637 + \frac{\left(170.9 + 301.4 + \frac{32.46}{2} \right) 7.3}{\pi \times 0.3 \times 0.005 \times 2 \times 10^8} = 0.01016 \text{ m} = 10.16 \text{ mm}$$

The friction mobilized in element 3 is:

$$f_3 = \frac{5000}{(1 + 0.35)(1 + \ln(16.3/0.3)) \times 0.3} \times 0.01016 = 7.53 \text{ KPa} < 20 \text{ KPa}$$

The load carried in element 3 is:

$$Q_{f3} = f_3 \pi D \Delta L_3 = 7.53 \times \pi \times 0.3 \times 7 = 49.65 \text{ kN}$$

The top movement is:

$$s_t = s_3 + \frac{\left(Q_p + Q_{f1} + Q_{f2} + \frac{Q_{f3}}{2} \right) \Delta L_3}{A_{cs} E_p}$$

$$= 0.01016 + \frac{\left(170.9 + 301.4 + 32.46 + \frac{49.65}{2} \right) 7}{\pi \times 0.3 \times 0.005 \times 2 \times 10^8} = 0.0141 \text{ m} = 14.1 \text{ mm}$$

The load at the top of the pile is:

$$Q_{top} = Q_p + Q_{f1} + Q_{f2} + Q_{f3} = 170.9 + 301.4 + 32.46 + 49.65 = 554.41 \text{ kN}$$

Problem 18.19

A 16-story hospital weighs 1500 MN, and its imprint is 75 m by 75 m. The building rests on 10,000 timber piles, each 15 m long, 0.3 m in average diameter, and driven with a spacing of 0.75 m center to center. The soil is made of a clay layer down to 14.5 m ($s_u = 20 \text{ kN/m}^2$, $e_o = 0.8$, and $C_c = 0.1$), then a sand layer down to 16.5 m ($N = 30 \text{ bpf}$), and then clay again down to a depth of 100 m ($s_u = 30 \text{ kN/m}^2$, $e_o = 0.7$, and $C_c = 0.06$). The water table is at the ground surface and the total unit weight of all soils is 20 kN/m^3 . Calculate:

- The capacity of one timber pile
- The capacity of the pile group
- The settlement of the hospital
- Comment on this design.

Solution 18.19

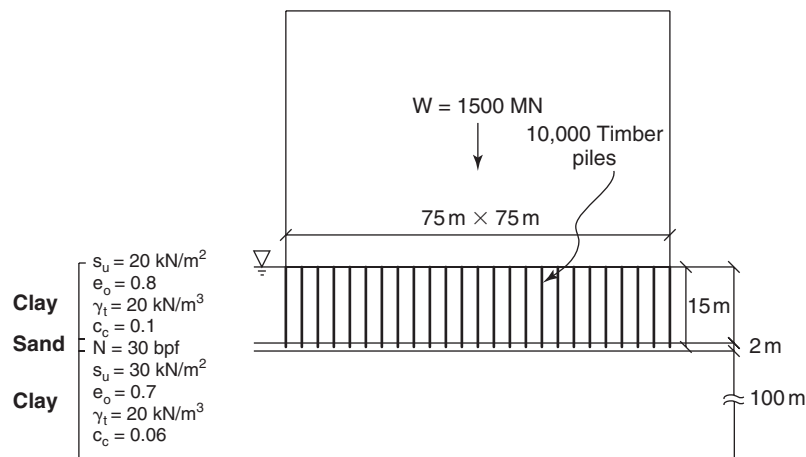


Figure 18.12s Building geometry and soil profile.

- Bearing capacity of single pile

Side resistance with API-RP2A method

$$\text{if } \sigma'_{ov} = s_u \rightarrow z = \frac{20}{(18 - 9.8)} \approx 2.5 \text{ m}$$

$$f_u = \begin{cases} 0.5 \left(\frac{s_u}{\sigma'_{ov}} \right)^{-0.5} & s_u \text{ for } z \leq 2.5 \text{ m} \\ 0.5 \left(\frac{s_u}{\sigma'_{ov}} \right)^{-0.25} & s_u \text{ for } 2.5 \text{ m} < z < 14.5 \text{ m} \end{cases}$$

$$\rightarrow f_u = \begin{cases} 0.5 \left(\frac{20}{(18 - 9.8) \times 1.25} \right)^{-0.5} & 20 = 7.2 \text{ kPa} & z \leq 2.5 \text{ m} \\ 0.5 \left(\frac{20}{(18 - 9.8) \times 8.5} \right)^{-0.25} & 20 = 13.7 \text{ kPa} & 2.5 \text{ m} < z < 14.5 \text{ m} \end{cases}$$

$$R_{uf} = (7.2 \times 2.5 + 13.7 \times 12) \times 0.3\pi = 171.8 \text{ kN}$$

Point bearing capacity with Briaud-Tucker method:

$$p_u = 1000 \times (30)^{0.5} = 5477 \text{ kPa}$$

$$R_{up} = 5477 \times \frac{0.3^2 \pi}{4} = 387 \text{ kN}$$

The capacity of one timber pile:

$$R_u = 171.8 + 387 = 558.8 \text{ kN}$$

b. Bearing capacity considering group effect:

Bearing capacity of 10,000 single piles

$$R_{u\text{-group}} = 558.8 \times 10000 = 5588 \times 10^3 \text{ kN} = 5588 \text{ MN}$$

Bearing capacity considering block failure:

$$R_{u\text{-block}} = 2(75 + 75) \times 14.5 \times 20 + 75 \times 75 \times (N_c \times 30)$$

The relative depth of embedment is $D/B = 15/75 = 0.2$

Skempton chart for $D/B = 0.2$ gives $N_c = 6.6$

$$R_{u\text{-block}} = 2(75 + 75) \times 14.5 \times 20 + 75 \times 75 \times (N_c \times 30)$$

$$R_{ug} = \text{Min}(5588, 1201) = 1201 \text{ MN}$$

c. Settlement calculations (Figure 18.13s)

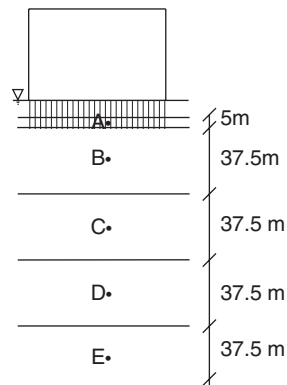


Figure 18.13s Settlement calculation points.

The average pressure under the building is:

$$p = \frac{F}{A} = \frac{1500000}{75 \times 75} = 267 \text{ kPa}$$

For settlement calculations, the large pile group is considered to be equivalent to a large footing located at 2/3 of the pile depth or 10 m below the ground surface. The depth of influence is considered to be 2 times the width of the foundation or 150 m. The thin sand layer is neglected; the layers involved are a 5 m layer of the upper clay and four layers of the lower clay each 37.5 m thick. The pressure factors are obtained from the bulb of pressure for a square foundation (see Figure 17.31). The settlement equation is:

$$\Delta H = \sum \frac{H_{oi}}{1 + e_o} C_c \log \left(\frac{\sigma'_{ovi} + \Delta \sigma_{vi}}{\sigma'_{ovi}} \right) = \frac{C_c}{1 + e_o} \sum H_{oi} \log \left(\frac{\sigma'_{ovi} + \Delta \sigma_{vi}}{\sigma'_{ovi}} \right)$$

| Point | Depth (m) | H_o (m) | e_o | C_c | σ'_{ov} (kPa) | Pressure factor | $\Delta \sigma_v$ (kPa) | σ'_v (kPa) | ΔH (m) |
|-------|-----------|-----------|-------|-------|----------------------|-----------------|-------------------------|-------------------|----------------|
| A | 12.5 | 5 | 0.8 | 0.1 | 125 | 1 | 267 | 392 | 0.138 |
| B | 33.75 | 37.5 | 0.7 | 0.06 | 337.5 | 0.8 | 213.6 | 551.1 | 0.282 |
| C | 71.25 | 37.5 | 0.7 | 0.06 | 712.5 | 0.45 | 120.1 | 832.6 | 0.090 |
| D | 108.75 | 37.5 | 0.7 | 0.06 | 1087.5 | 0.23 | 61.4 | 1148.9 | 0.032 |
| E | 146.25 | 37.5 | 0.7 | 0.06 | 1462.5 | 0.14 | 37.4 | 1499.9 | 0.015 |
| | | | | | | | | | 0.557 |

d. Comment

As can be seen, the ultimate load of the pile group is smaller than the weight of the building; therefore, the foundation is insufficient to carry the building weight safely. The settlement is also a great concern, because more than half a meter of settlement could lead to serious problems. This problem is actually close to the case of the New Orleans Charity Hospital built in 1939.

Problem 18.20

Calculate the group efficiency for settlement using Poulos interaction factors for the case of a flexible pile cap (all piles carry the same load). The group is 4 by 4 with a 3-pile diameter center-to-center spacing.

Solution 18.20

Because we have symmetry in piles location, we calculate the interaction factor only for three piles (a, b, and c in Figure 18.14s).

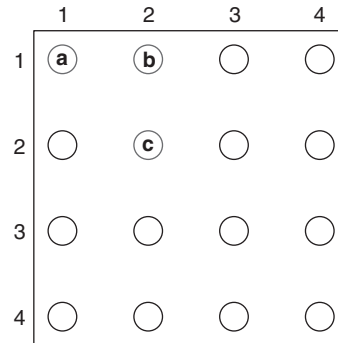


Figure 18.14s Piles location.

$$\rho_k = \rho_1 \sum_{\substack{j=1 \\ j \neq k}}^n (P_j \alpha_{kj}) + \rho_1 P_k$$

Flexible pile cap $\rightarrow P_i = P$

$$\rho_i = P \rho_1 \left(\sum_{\substack{j=1 \\ j \neq k}}^n (\alpha_{kj}) + 1 \right)$$

$$\alpha_{kj} = f \left(\frac{s}{d} \right) \rightarrow \text{Fig. 18.50}$$

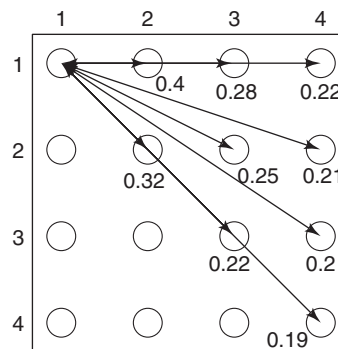


Figure 18.15s α values for pile a.

$$\rho_a = P \rho_1 [2(0.4 + 0.28 + 0.22 + 0.25 + 0.21 + 0.2) + 0.32 + 0.22 + 0.19] = 3.85 P \rho_1$$

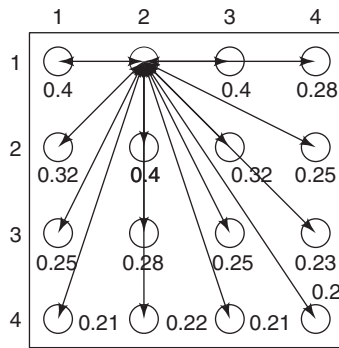


Figure 18.16s α values for pile *b*.

$$\rho_b = P\rho_1[3 \times 0.4 + 2 \times 0.32 + 2 \times 0.28 + 3 \times 0.25 + 0.23 + 2 \times 0.21 + 0.22 + 0.2] = 4.2P\rho_1$$

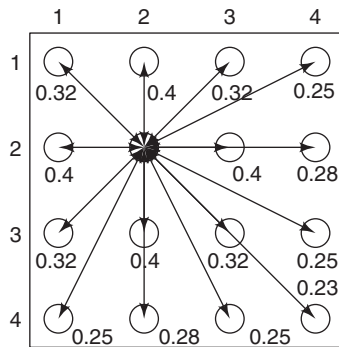


Figure 18.17s α values for pile *c*.

$$\rho_c = P\rho_1[4 \times 0.4 + 4 \times 0.32 + 2 \times 0.28 + 4 \times 0.25 + 0.23] = 4.67P\rho_1$$

| | | | |
|------|------|------|------|
| ○ | ○ | ○ | ○ |
| 3.85 | 4.2 | 4.2 | 3.85 |
| ○ | ○ | ○ | ○ |
| 4.2 | 4.67 | 4.67 | 4.2 |
| ○ | ○ | ○ | ○ |
| 4.2 | 4.67 | 4.67 | 4.2 |
| ○ | ○ | ○ | ○ |
| 3.85 | 4.2 | 4.2 | 3.85 |

Figure 18.18s α values settlement factor for each pile in the group.

This gives an average of a group settlement equal to 4.23 times the settlement of one pile. The rule of thumb $\sqrt{B_G/B}$ would give $\sqrt{10/1} = 3.16$.

Problem 18.21

If the uncoated pile subjected to downdrag in Figure 18.54 was pushed into the ground 100 mm at the pile top, what would be:

- The new position of the neutral point?
- The load at the top of the pile?
- The load distribution in the pile?

Solution 18.21

Initial assumption: $w_p > 5 \text{ mm} \Rightarrow Q_p = 1000 \text{ kN}$

$$w_{NP(soil)} = w_{NP(pile)} = w_{NP}$$

$$w_t = w_{NP} + \frac{(Q_{NP} + Q_t) z_{NP}}{2 EA} = 100 \text{ mm} = 0.1 \text{ m}$$

$$w_{NP(soil)} = \frac{0.2}{30} (30 - z_{NP})$$

$$Q_{NP} = Q_p + (L - z_{NP}) \times f \times A_p = 1000 + (30 - z_{NP}) \times 25 \times 1.2 = 1900 - 30z_{NP}$$

$$Q_t = Q_{NP} - z_{NP} \times f \times A_p = 1900 - 30z_{NP} - 25 \times 1.2 \times z_{NP} = 1900 - 60z_{NP}$$

$$w_t = \frac{0.2}{30} (30 - z_{NP}) + \frac{(1900 - 30z_{NP} + 1900 - 60z_{NP}) z_{NP}}{2 \times 0.3 \times 0.3 \times 2 \times 10^7} = 0.1 \text{ m}$$

$$z_{NP} = 16.6 \text{ m}$$

Check the initial assumption:

$$\begin{aligned} w_p &= w_{NP} - \frac{(Q_{NP} + Q_p) (30 - z_{NP})}{2 EA} \\ &= \frac{0.2}{30} (30 - 16.6) - \frac{(1900 - 30 \times 16.6 + 1000) (30 - 16.6)}{2 \times 0.3 \times 0.3 \times 2 \times 10^7} = 0.08 > 0.005 \end{aligned}$$

$$Q_t = 1900 - 60z_{NP} = 904 \text{ kN}$$

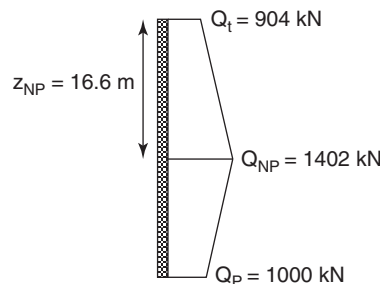
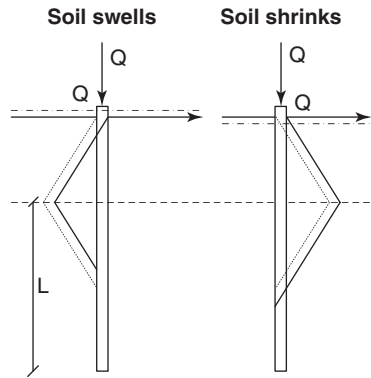


Figure 18.19s Load profile on pile.

Problem 18.22

A bored pile foundation is used for a house on a shrink-swell soil. The piles are 0.5 m in diameter, the load per pile is 50 kN, and the zone of active movement from one season to the next extends from the ground surface to a depth of 3 m. The soil is a very stiff clay with an undrained shear strength of 120 kPa and a total unit weight of 20 kN/m³. The groundwater level is at a depth of 10 m. How deep should each bored pile be to minimize the uneven movement of the house?

Solution 18.22**Figure 18.20s** Load profile due to soil swelling and shrinking.**Swelling**

Swelling and uplift load:

$$F_{sw} = \alpha s_u \pi D L_{sw} = 0.5 \times 120 \times \pi \times 0.5 \times 3 = 282.6 \text{ kN}$$

Maximum resisting load:

$$F_r = \alpha s_u \pi D L_r + Q = 0.5 \times 120 \times \pi \times 0.5 \times L_r + 50 = 94.2 L_r + 50 \text{ kN}$$

$$\frac{F_r}{F_{sw}} = SF = 2 \Rightarrow L = 5.47 \text{ m}$$

Shrinking

Shrinkage and downward load:

$$: F_{sh} = \alpha s_u \pi D L_{sh} + Q = 0.5 \times 120 \times \pi \times 0.5 \times 3 + 50 = 332.6 \text{ kN}$$

Maximum resisting load:

$$F_r = \alpha s_u \pi D L_r + 9 s_u A_p = 0.5 \times 120 \times \pi \times 0.5 \times L_r + 9 \times 120 \times \frac{0.5^2 \pi}{4} = 94.2 L_r + 212 \text{ kN}$$

$$\frac{F_r}{F_{sh}} = SF = 2 \Rightarrow L = 4.81 \text{ m}$$

$$L_r = \text{Max}(5.47, 4.81) = 5.47 \text{ m}$$

Total length of the pile = 8.47 m

Problem 18.23

For the long flexible pile shown in Figure 18.5s, calculate:

- The ultimate load H_{ou}
- The deflection and slope at the ground surface under the working load
- The maximum bending moment under the working load

d. The factor of safety against yielding of the soil near the ground surface under the working load

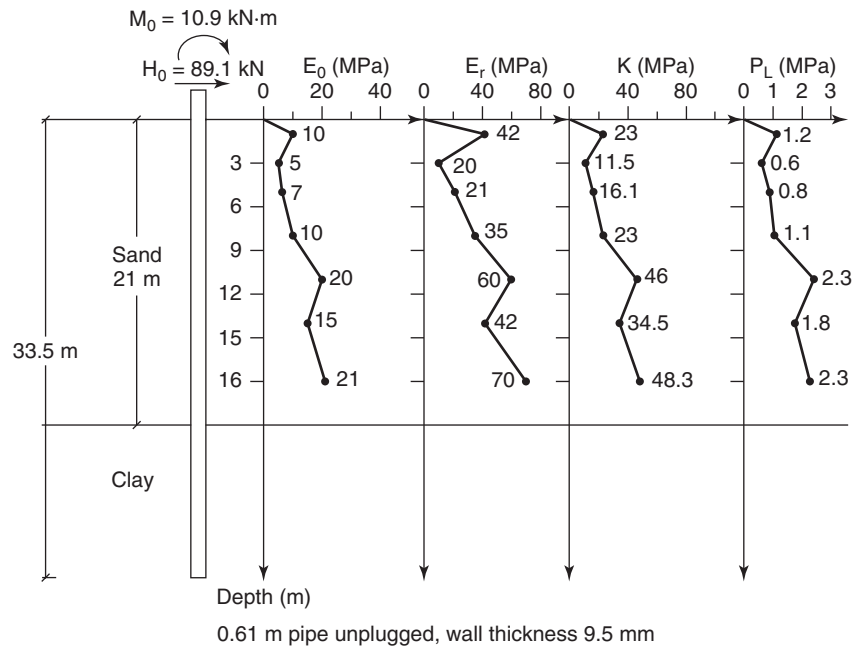


Figure 18.5s Long flexible pile loaded horizontally.

Solution 18.23

- a. Select horizontal spring constant K :
 - a. A value of $K = 15,000$ kPa is selected from the soil profile.
- b. Calculate the transfer length l_0 :

$$l_0 = \sqrt[4]{\frac{4EI}{K}}$$

$$I = \frac{\pi}{64}(D_0^4 - D_i^4) = \frac{\pi}{64}(0.61^4 - 0.591^4) = 8.08 \times 10^{-4} \text{ m}^4$$

$$E = 2 \times 10^8 \text{ kPa}$$

$$l_0 = \sqrt[4]{\frac{4 \times 2 \times 10^8 \times 8.08 \times 10^{-4}}{15000}} = 2.56 \text{ m}$$

- c. Check if pile is long and flexible or short and rigid:

$$\frac{L}{l_0} = \frac{33.5}{2.56} > 3, \text{ flexible pile}$$

- d. Deflection at the ground surface under the working load:

$$y_0 = \frac{2H_0}{l_0 K} + \frac{2M_0}{l_0^2 K} = \frac{2 \times 89.1}{2.56 \times 15000} + \frac{2 \times 10.9}{2.56^2 \times 15000} = 0.00464 + 0.00022 = 4.86 \text{ mm}$$

e. Slope at the ground surface under the working load:

$$\begin{aligned} y'_0 &= \frac{2H_0}{l_0^2 K} + \frac{4M_0}{l_0^3 K} \\ &= -\frac{2 \times 89.1}{2.56^2 \times 15000} - \frac{4 \times 10.9}{2.56^3 \times 15000} \\ &= -1.81 \times 10^{-3} - 0.17 \times 10^{-3} = -1.98 \text{ radians} \end{aligned}$$

f. Depth z_{\max} to maximum bending moment M_{\max} :

$$\begin{aligned} \tan \frac{z_{\max}}{l_0} &= \frac{1}{1 + \frac{2M_0}{l_0 H_0}} \\ &= \frac{1}{1 + \frac{2 \times 10.9}{2.56 \times 89.1}} = 0.913 \quad \text{and} \quad \frac{z_{\max}}{l_0} = 0.739 \\ z_{\max} &= 1.89 \text{ m} \end{aligned}$$

g. Maximum bending moment under the working load:

$$\begin{aligned} M_{\max} &= H_0 l_0 e^{-\frac{z_{\max}}{l_0}} \sin\left(\frac{z_{\max}}{l_0}\right) + M_0 e^{-\frac{z_{\max}}{l_0}} \left(\cos\left(\frac{z_{\max}}{l_0}\right) + \sin\left(\frac{z_{\max}}{l_0}\right)\right) \\ M_{\max} &= 89.1 \times 2.56 e^{-\frac{1.89}{2.56}} \sin\left(\frac{1.89}{2.56}\right) + 10.9 e^{-\frac{1.89}{2.56}} \left(\cos\left(\frac{1.89}{2.56}\right) + \sin\left(\frac{1.89}{2.56}\right)\right) \\ &= 73.4 + 7.4 = 80.8 \text{ kN.m} \end{aligned}$$

h. Factor of safety against yielding of the soil near the ground surface under the working load:

$$\begin{aligned} P &= Ky = 15000 \times 0.00486 = 72.9 \text{ kN/m} \\ p_a &= \frac{P}{B} = \frac{72.9}{0.61} = 119.5 \text{ kPa} \end{aligned}$$

p_L within the loaded depth is at least 0.6 MPa = 600 kPa

Safety factor:

$$F = \frac{p_L}{p_a} = \frac{600}{119.5} = 5.02$$

i. Ultimate horizontal load:

$$H_{ou} = \frac{3}{4} p_L B z_{\max} = 0.75 \times 600 \times 0.61 \times 1.89 = 518.8 \text{ kN}$$

So the applied load of 89.1 kN is a safe load.

Problem 18.24

For the short rigid pile shown in Figure 18.6s, calculate:

- The ultimate load H_{ou}
- The deflection and slope at the ground surface under the working load
- The maximum bending moment under the working load
- The factor of safety against yielding of the soil near the ground surface under the working load

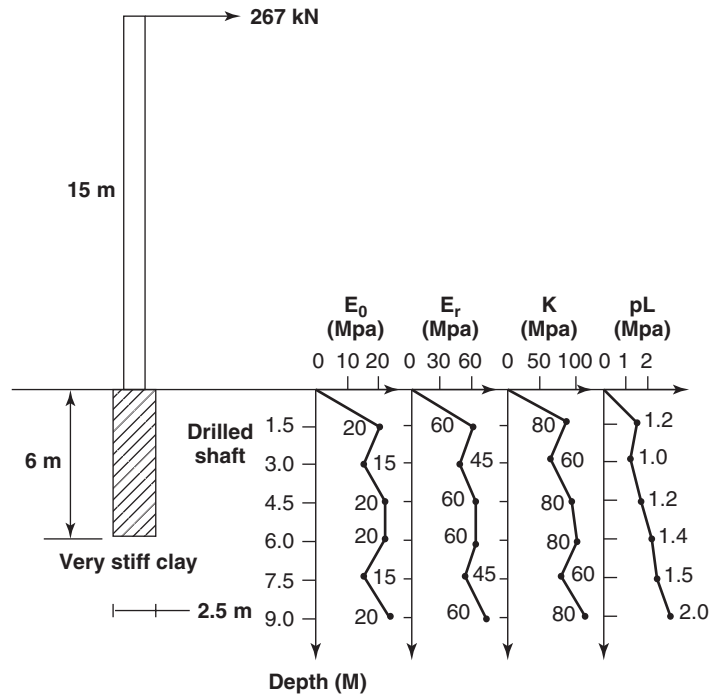


Figure 18.6s Short rigid pile loaded horizontally.

Solution 18.24

- a. Select horizontal spring constant K :
 - a. A value of $K = 60,000$ kPa is selected from the soil profile.
- b. Calculate the transfer length l_0 :

$$l_0 = \sqrt[4]{\frac{4EI}{K}}$$

$$I = \frac{\pi D^4}{64} = \frac{\pi 2.5^4}{64} = 1.92 \text{ m}^4$$

$$E = 2 \times 10^7 \text{ kPa}$$

$$l_0 = \sqrt[4]{\frac{4 \times 2 \times 10^7 \times 1.92}{60000}} = 7.1 \text{ m}$$

- c. Check if the pile is long and flexible or short and rigid:
 - a. $L = 6 \text{ m} < l_0 = 7.1 \text{ m}$; therefore, the pile is rigid and short.
- d. Deflection at the ground surface under the working load:

$$H_o = 267 \text{ kN}$$

$$M_o = 267 \times 15 = 4005 \text{ kN}$$

$$\begin{aligned} y_o &= -\frac{2(2H_oL + 3M_o)}{KL^2} \\ &= -\frac{2(2 \times 267 \times 6 + 3 \times 4005)}{60000 \times 6^2} \\ &= -0.014 \text{ m} \end{aligned}$$

e. Slope at the ground surface under the working load:

$$y'_o = \frac{6(H_0L + 2M_0)}{KL^3} = \frac{6(267 \times 6 + 2 \times 267 \times 15)}{60000 \times 6^3} = +0.0045 \text{ radians} = +0.26 \text{ degrees}$$

f. Depth z_{\max} to maximum bending moment M_{\max} :

$$z_{\max} = -\frac{2y'_o}{y''_o} - L = 0.22 \text{ m}$$

g. Maximum bending moment under the working load:

$$M_{\max} = M_0 + H_0z_{\max} - Ky'_o \frac{z_{\max}}{6} - Ky''_o \frac{z_{\max}^2}{6} = 4071.6 \text{ kN.m}$$

h. Factor of safety against yielding of the soil

The load in the soil near the ground surface is:

$$P = Ky = 60000 \times 0.14 = 840 \text{ kN/m}$$

$$p_a = \frac{P}{B} = \frac{840}{2.5} = 336 \text{ kPa}$$

p_L at the top soil is $\sim 1 \text{ MPa} = 1000 \text{ kPa}$

$$\text{Safety factor is } F = \frac{p_L}{p_a} = \frac{1000}{336} = 2.98 \approx 3$$

i. Ultimate horizontal load:

$$H_{ou} = \frac{3}{4} p_L B z_{\max} = 0.75 \times 1000 \times 2.5 \times 0.22 = 412.5 \text{ kN}$$

So, the applied load of 267 kN is safe, and the factor of safety is $412.5/267 = 1.54$. Note that the large overturning moment affects the horizontal capacity by inducing horizontal movement of its own. If no moment was applied at the top, the z_{\max} value would be $L/3$ and the ultimate horizontal load would be equal to $0.75 \times 1000 \times 2.5 \times 2 = 3750 \text{ kN}$.

Problem 18.25

Calculate z_{\max} for a flexible pile and a rigid pile if the pile is subjected to a horizontal load only (H_0 different from 0 but M_0 equal to 0).

Solution 18.25

Case 1: A flexible pile

The depth z_{\max} to maximum bending moment is the value of z that gives zero shear. Therefore:

$$V(z) = H_0 e^{-\frac{z}{l_0}} \left(\cos \frac{z}{l_0} - \sin \frac{z}{l_0} \right) - \frac{2M_0}{l_0} e^{-\frac{z}{l_0}} \sin \frac{z}{l_0} = 0$$

For $M_0 = 0$, the equation simplifies to:

$$H_0 e^{-\frac{z}{l_0}} \left(\cos \frac{z}{l_0} - \sin \frac{z}{l_0} \right) = 0 \quad \text{or} \quad \cos \frac{z}{l_0} = \sin \frac{z}{l_0}$$

This gives:

$$\frac{z_{\max}}{l_0} = \frac{\pi}{4} \quad \text{or} \quad z_{\max} = \frac{\pi}{4} \sqrt{\frac{4EI}{K}}$$

Case 2: A rigid pile

The depth z_{\max} to maximum bending moment is the value of z that gives zero shear. Therefore:

$$V = H_o + K \frac{6(H_o L + 2M_o)}{K L^3} \frac{z^2}{2} - K \frac{2(2H_o L + 3M_o)}{K L^2} z = 0$$

For $M_o = 0$, this equation simplifies to:

$$3z^2 - 4Lz + L^2 = 0$$

for which the positive root is $L/3$. Therefore:

$$z_{\max} = \frac{L}{3}$$

Problem 18.26

Calculate the ratio between the ground surface displacement for a free-head condition and for a fixed-head condition. Do the calculation first for a flexible pile and then for a rigid pile.

Solution 18.26**Case 1: A long flexible pile****Free-head condition**

The displacement at the ground surface is calculated as:

$$y_o(\text{free head}) = \frac{2H_o}{l_o K}$$

Fixed-head condition

The displacement at the ground surface is calculated as:

$$\begin{cases} y_o(\text{fixed head}) = \frac{2H_o}{l_o K} + \frac{2M_o}{l_o^2 K} \\ y'_o(\text{fixed head}) = -\frac{2H_o}{l_o^2 K} - \frac{4M_o}{l_o^3 K} = 0 \Rightarrow M_o = -\frac{H_o l_o}{2} \end{cases}$$

Therefore,

$$y_o(\text{fixed head}) = \frac{2H_o}{l_o K} + \frac{2M_o}{l_o^2 K} = \frac{2H_o}{l_o K} - \frac{H_o}{l_o K} = \frac{H_o}{l_o K}$$

Hence, for a long flexible pile, the ratio between the ground surface displacement for a free-head condition and for a fixed-head condition is:

$$\frac{y_o(\text{free head})}{y_o(\text{fixed head})} = \frac{\frac{2H_o}{l_o K}}{\frac{H_o}{l_o K}} = 2$$

Case 2: A short rigid pile**Free-head condition**

The displacement at the ground surface is calculated as:

$$y_o(\text{free head}) = \frac{-2(2H_o L)}{K L^2} = \frac{-4H_o}{K L}$$

Fixed-head condition

The displacement at the ground surface is calculated as:

$$\begin{cases} y_o(\text{fixed head}) = \frac{-2(2H_o L + 3M_o)}{K L^2} \\ y'_o(\text{fixed head}) = \frac{6(H_o L + 2M_o)}{K L^3} = 0 \Rightarrow M_o = -\frac{H_o L}{2} \end{cases}$$

Therefore,

$$y_o(\text{fixed head}) = \frac{-2(2H_oL + 3M_o)}{KL^2} = \frac{-2\left(2H_oL + 3\frac{-H_oL}{2}\right)}{KL^2} = \frac{-H_o}{KL}$$

Hence, for a short rigid pile, the ratio between the ground surface displacement for a free-head condition and for a fixed-head condition is:

$$\frac{y_o(\text{free head})}{y_o(\text{fixed head})} = \frac{\frac{-4H_o}{KL}}{\frac{-H_o}{KL}} = 4$$

Problem 18.27

For the pile group shown in Figure 18.75, calculate the efficiency of the group if it is loaded horizontally in a direction perpendicular to the four-pile line.

Solution 18.27

Figure 18.21s shows an illustration of the horizontal loading on the pile group. The center-to-center spacing S of the piles is two times the pile diameter B .

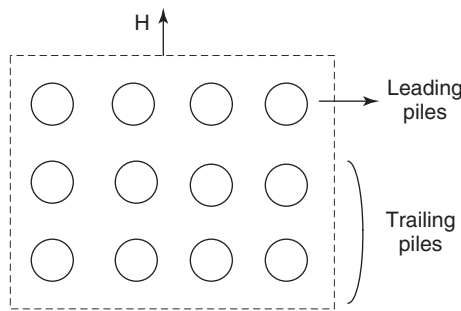


Figure 18.21s Horizontal loading of a pile group.

The leading pile efficiency e_{lp} is obtained from Figure 18.22s for a pile relative spacing of 2. The value is 0.86. Because there are 4 leading piles, the contribution to the group capacity is $4 \times 0.86 = 3.44$.

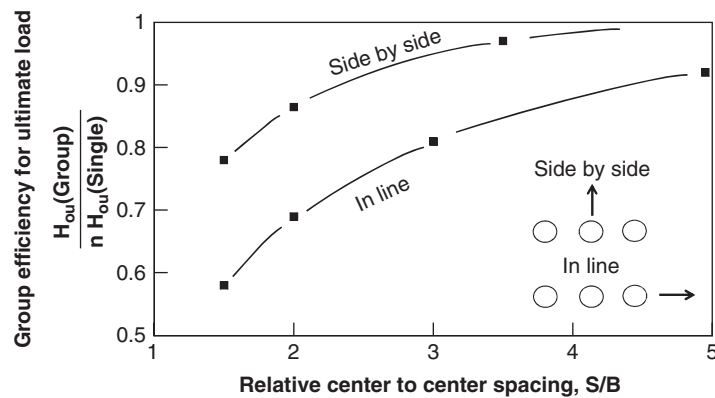


Figure 18.22s Efficiency for side-by-side and in-line groups.

The ratio λ between the capacity of the leading pile and the trailing pile is given by Figure 18.23s. The value is 1.43 for a relative spacing of 2. Therefore, the efficiency of each trailing pile is $e_{tp} = 0.86/1.43 = 0.60$. Because there are 8 trailing piles, the contribution to the group capacity is $8 \times 0.6 = 4.8$.

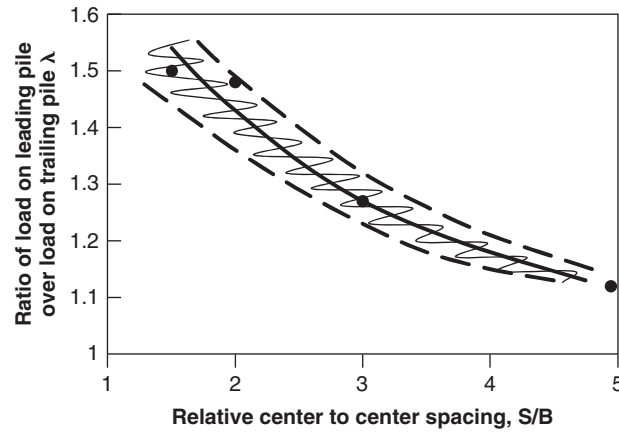


Figure 18.23s Ratio of load on leading pile over trailing pile.

The efficiency of the pile group is calculated as.

$$e = \frac{H_{ou(\text{group})}}{nH_{ou(\text{single})}} = \frac{n_{lp}e_{lp} + n_{tp}e_{tp}}{n} = \frac{4 \times 0.86 + 8 \times 0.6}{12} = 0.69$$

Problem 18.28

The pile group of Figure 18.75 is subjected to an overturning moment of 10 MN.m in the direction of largest resistance to overturning of the group. The piles are 0.4 by 0.4 square concrete driven piles embedded 25 m in a loose sand with a blow count of 6 bpf. What will be the ratio between the applied tension load and the ultimate tension capacity of the most loaded pile in the group?

Solution 18.28

The ultimate capacity of the piles in tension can be estimated by the Briaud-Tucker method:

$$Q_u = f_u PL = 5 \times 6^{0.7} \times 4 \times 0.4 \times 25 = 701 \text{ kN}$$

The maximum tension load on the outside of the group, in the absence of any compression load, is:

$$\Delta Q_{\max} = \frac{MB}{2m \sum_{i=1}^n a_i^2} = \frac{10000 \times 2.8}{2 \times 3((3 \times 0.4)^2 + (1 \times 0.4)^2 + (1 \times 0.4)^2 + (3 \times 0.4)^2)} = 1458 \text{ kN}$$

So, unless there is a significant compression load (coming from the structure deadweight, for example), the outside pile will fail.

Problem 18.29

A steel pipe pile has a diameter D equal to 0.61 m and a wall thickness t equal to 9.5 mm. The pile is 33.5 m long and the steel has a modulus E equal to 200 GPa. The pile is loaded horizontally with a load H_o of 89 kN in fixed-head condition. The soil is characterized by stiffness coefficient K from pressuremeter tests equal to 25 000 kPa. Plot the profiles versus depth of the deflection, slope, shear, bending moment, and line load in the pile.

Solution 18.29

Step 1: Define the type of pile

$$I = \frac{\pi(D^4 - d^4)}{64} = \frac{\pi(0.61^4 - (0.61 - 2 \times 9.5 \times 10^{-3})^4)}{64} = 8.08 \times 10^{-4} \text{ m}^4$$

Transfer length l_o is calculated as:

$$l_o = \sqrt[4]{\frac{4EI}{K}} = \sqrt[4]{\frac{4 \times 2 \times 10^{11} \times 8.08 \times 10^{-4}}{25 \times 10^6}} = 2.25 \text{ m}$$

Because $L > 3l_o$, the pile is defined as a long, flexible pile.

Step 2: Calculate the deflection, slope, shear, bending moment, and line load in the pile

The fixed-head flexible pile has a slope of zero at the top of the pile. Therefore,

$$y'_o(\text{fixed head}) = -\frac{2H_o}{l_o^2 K} - \frac{4M_o}{l_o^3 K} = 0$$

Hence, the bending moment at the ground surface can be calculated as:

$$M_o = -\frac{H_o l_o}{2} = -\frac{89 \times 2.25}{2} = -100 \text{ kN} \cdot \text{m}$$

With z as the depth along the pile, the deflection, slope, bending moment, shear, and line load in the pile can be calculated as:

$$\text{Deflection} \quad y(z) = \frac{2H_o}{l_o K} e^{-\frac{z}{l_o}} \cos \frac{z}{l_o} + \frac{2M_o}{l_o^2 K} e^{-\frac{z}{l_o}} \left(\cos \frac{z}{l_o} - \sin \frac{z}{l_o} \right)$$

$$\text{Slope} \quad y'(z) = -\frac{2H_o}{l_o^2 K} e^{-\frac{z}{l_o}} \left(\cos \frac{z}{l_o} + \sin \frac{z}{l_o} \right) - \frac{4M_o}{l_o^3 K} e^{-\frac{z}{l_o}} \cos \frac{z}{l_o}$$

$$\text{Bending moment} \quad M(z) = H_o l_o e^{-\frac{z}{l_o}} \sin \frac{z}{l_o} + M_o e^{-\frac{z}{l_o}} \left(\cos \frac{z}{l_o} + \sin \frac{z}{l_o} \right)$$

$$\text{Shear} \quad V(z) = H_o e^{-\frac{z}{l_o}} \left(\cos \frac{z}{l_o} - \sin \frac{z}{l_o} \right) - \frac{2M_o}{l_o} e^{-\frac{z}{l_o}} \sin \frac{z}{l_o}$$

$$\text{Line load} \quad p(z) = -Ky(z)$$

A Matlab program was written to plot these functions, as shown in Figure 18.24s.

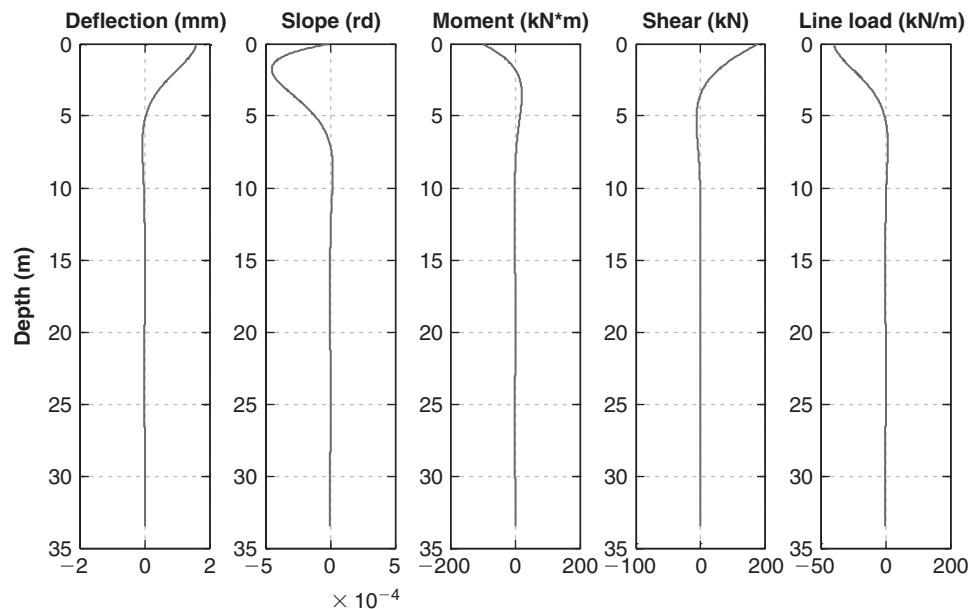


Figure 18.24s Deflection, slope, bending moment, shear, and line load in the fixed-head pile under a horizontal load H_o at the ground surface.